Karlsruhe Institute of Technology

Metal-Insulator Transition in 2D Disordered Bipartite Systems

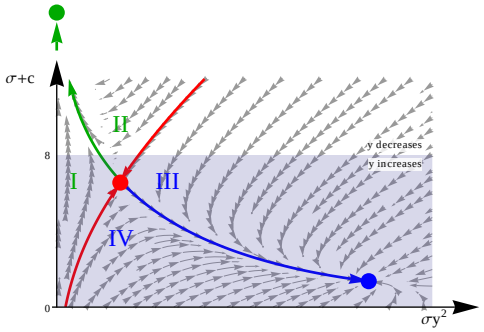

Metall-Isolator-Übergang in 2D ungeordneten bipartiten Systemen

Diploma Thesis by

Elio König

At the Department of Physics
Institut für Theorie der Kondensierten Materie

Reviewer:	Prof. Dr. Alexander Mirlin
Second reviewer:	Prof. Dr. Alexander Shnirman
Advisors:	Dr. Pavel Ostrovsky
	Dr. Ivan Protopopov

Duration: June, 15th 2010 – June, 14th 2011

Acknowledgements

First of all I would like to thank Professor Alexander Mirlin for giving me the opportunity to write my diploma thesis in his group, as well as for the fascinating research topic he proposed. Throughout the year he very actively assisted our work and, in addition, his warm and personal style creates an exceptionally pleasant working atmosphere.
I also would like to thank Professor Alexander Shnirman for accepting the second revision and his contribution to the agreeable ambiance in the institute.

I am infinitely indebted to my advisors, Doctors Pavel Ostrovsky and Ivan Protopopov, who with extraordinary patience and efforts made me understand what at all I was researching on. Apart from their inestimable professional support, the amicable, informal relationship to them is of great value for me.

Furthermore, I would like to thank my roommates Michael Schütt and Stéphane Ngo Dinh for interesting discussions on my research project, as well as Doctor Sam Carr for helping me with language problems. Otto Eberhardt and Ivan Protopopov corrected the first draft of this work, for which I am very grateful.

Eventually, I want to express my profound gratitude to Taya, who always patiently and affectionately supported me, independently of how late I returned from the institute. My parents, Claudia König and Andrea Sciola-König, and grandmothers, Agnes König and Lucia Sciola, gave me ideological, emotional, and financial assistance throughout my nearly six years of studies. It goes without saying that without their help this work could not exist and neither I was the happy person I claim to be.

"Ты наш человек..."
(My girlfriend's uncle after half a bottle of Cognac.)

Contents

Part I

Why?

Introduction

In the last decade, two experimental discoveries of extraordinary significance gave additional drive to research on disordered systems and Anderson transitions.
First, Novoselov, Geim and co-workers invented the ingeniously simple "scotch-tape-method" to produce graphene, a monoatomic layer of graphite [NGM+04]. More than that, they also immediately recognized the unique conduction properties this exceptional material displays. Among other stunning phenomena and in contrast to conventional metals, the minimal conductivity is nearly constant over an extended temperature window from room temperature down to ~ 1 K [NGM+05]. These "groundbreaking experiments"[1] convinced the Nobel committee to award the 2010 Nobel prize to Novoselov and Geim.
Second, new quantum Hall-like phases were observed both in two- and three-dimensional topological insulators [KWB+07] [HQW+08]. In such phases the matter is insulating in the interior and, paradoxically, at the same time conducting on the surface. Even more stupefying, the conducting surface states are extremely well protected against localizing disorder effects.
How can this happen? Why do these materials not obey Anderson's paradigm, which predicts localization as the kinetic energy is small in comparison to the disorder strength [And58]? And, eventually, which mechanisms suppress conductivity and why don't they work in graphene and topological insulators?
The recent experimental findings put these old questions into a modern context: since the seventies numerous condensed matter physicists have tried to understand disorder driven Anderson metal-insulator transitions. Many answers have been found, many more questions have arisen, and recent development shows that this research field still surprises with fascinating phenomena.

It is the declared goal of the present thesis to supply one tiny, but conceptionally new piece to the jigsaw puzzle of Anderson transitions. Only a certain family of materials shall be considered: the bipartite systems which form the chiral symmetry classes. According to the pioneering works by Gade and Wegner [GW91] [Gad93] and unlike the situation in usual metals, in the systems in question the conductivity is independent of external parameters such as temperature[2]. As a matter of fact, this remarkable property is supported by numerical tests [MDH02] [BC03], revealing also the appearance of a localized phase. But how can an insulator emerge, if, according to Gade and Wegner, the conductivity remains unchanged? The answer to this question is the main result of this work.

Apart from disordered metals, the investigation of chiral random systems is likewise of relevance for the low energy limit of QCD [VZ93]. In solid state physics, the most natural and charming realization is graphene. (However, depending on the type of disorder, it can fall into other symmetry classes as well.) There is also theoretical indication that topological insulators can exist in chiral classes. Experimental confirmation does not yet exist,

[1] From the Nobel Foundation announcement.
[2] This might recall the situation of graphene explained above. Even though the effect is similar, the theoretical reasons differ strongly.

but the extraordinary present-day efforts concerning the research on topological insulators might soon lead to a different result.
Whilst the work at hand provides new insights on how localization occurs in chiral classes, it also deepens the understanding on protected conducting states, which is more than ever a vibrant field of research.

Outline

This thesis is made up of four main parts, "Why?", "What:", "How:" and "Hence.". The first and the last (introduction and conclusion) are comparably shorter and constitute the framework for the two main sections in the middle.

The part "What:" is devoted to the well-established foundations which are necessary to understand the achievements of this work [3]. It consists of three chapters.
The first and longest among them reviews the physics of disordered metals. In the second chapter, two sorts of phase transitions in two dimensional systems are exposed: Anderson transitions and Berezinskii-Kosterlitz-Thouless transitions. The closing chapter is dedicated to chiral symmetry classes. Physical realizations are presented and the status quo of chiral systems is reviewed, the emphasis being on the controversy between Gade and Wegner's predictions on the one hand, and intuition and numerical works on the other.

The second main part, "How:", is mostly about the work performed within the year of duration of this project. Technical descriptions as well as explicit calculations are included; however, longer calculations were moved into the appendix.
In chapter four, the non-linear σ model is derived for Dirac electrons of chiral classes AIII and CII, for the latter including, in some sense, the $\mathbb{Z}_2$-topological term. Chapter five is about the derivation of the renormalized coupling constants within the background field formalism. Next to this, the well-known Gade-Wegner RG-equations are reobtained with this method. In order to exemplify the strength of Gade's and Wegner's argument, and also for the benefit of an exhaustive examination of topological effects in chiral symmetry classes, the (vanishing) influence of the Wess-Zumino-Novikov-Witten-term and the $\mathbb{Z}_2$-instanton on the conductivity are discussed in chapter six. The last two chapters are devoted to vortices: Their localizing effect is specifically demonstrated in chapter seven and the implied metal-insulator transition extensively discussed in chapter eight.

[3] It is obvious, that the most important readers of a diploma thesis, namely the reviewers, do not need such an introductory chapter. However, in order to best illustrate the newly acquired knowledge, the work targets a fictitious reader who is equipped with basic knowledge on (condensed matter) field theory and geometry. This exactly reflects the situation of the author one year ago.

Notation

- In order to simplify the reading, the reduced Planck constant as well as the unit of charge are set to unity $\hbar = 1 = e$. However, whenever a comparison to the observable conductivity is made, the units are restored.
- i denotes the imaginary unit throughout.
- For the Lie-algebra (denoted by Gothic lower case letters) as well as for the tangent space of the symmetric spaces, the "mathematical" convention is used, i.e. without the supplementary imaginary unit. For example, the Lie-algebra $\mathfrak{u}$ of the unitary group U consists of *anti*hermitian matrices A.
- If not specified otherwise, Einstein sums over repeated indices are to be understood.
- The following definition of Pauli matrices is employed

$$\sigma_x = \begin{pmatrix} 0 & 1 \\ 1 & 0 \end{pmatrix}, \ \sigma_y = \begin{pmatrix} 0 & -i \\ i & 0 \end{pmatrix}, \ \sigma_z = \begin{pmatrix} 1 & 0 \\ 0 & -1 \end{pmatrix}$$

Part II

What:

1. Anderson localization and disorder

1.1 What is Anderson localization?

In 1957, Philip Warren Anderson first realized that a quantum-mechanical particle subjected to a random potential might be localized, if the disorder strength is large enough [And58]. At first glance, this does not seem surprising: Also a classical particle which has sufficiently small energy, will be localized in the relatively deep valleys of a disordered potential landscape. But this is not the interesting point: The striking fact of Anderson's discovery is that the theorem predicts localization even where there is none expected classically. Furthermore, at given disorder strength, there do not exist energies at which both localized and delocalized states are present[1].
Finally, being all states either localized or all states delocalized, Anderson localization is a quantum-mechanical phenomenon with macroscopic effects. There exist two distinct phases (insulator and metal) and therefore at some point a phase transition occurs: The Anderson transition.

1.2 Scaling theory

Only about twenty years after Anderson's fundamental article a phenomenological scaling theory of this phase transition was developed. Following the ideas of Thouless and Wegner the "Gang of Four" (Abrahams, Anderson, Licciardello and Ramakrishnan) formulated a one parameter scaling theory for the dimensionless conductance g [AALR79]. Three main (physical) assumptions were made: First, $\frac{d\ln g}{d\ln L} = \beta_d\left(g\left(L\right)\right)$ does not explicitly depend on the system-size L for all values of g, second $\beta_d\left(g\right)$ is continuous and monotonously increasing and third the following asymptotics hold:

$$g\left(L\right) = \begin{cases} \sigma L^{d-2} & \text{Ohm's law for macroscopic transport for large } g \\ g_a e^{-\frac{L}{\xi}} & \text{Anderson localization for small } g \end{cases}$$

(σ denotes the conductivity, ξ the localization length and L^d the size of the d-dimensional hypercube.)
From these assumptions Abrahams *et al.* concluded that the β-function must qualitatively

[1] Mott's argument: Imagine the coexistence of the two. Then a small change in the disorder configuration would cause some extended states to be changed into extended states leaking into the region of a localized state, mix with it and therefore extend it. In this sense, localized states are not stable against extended states of the same energy. [Nay04], [AS10]

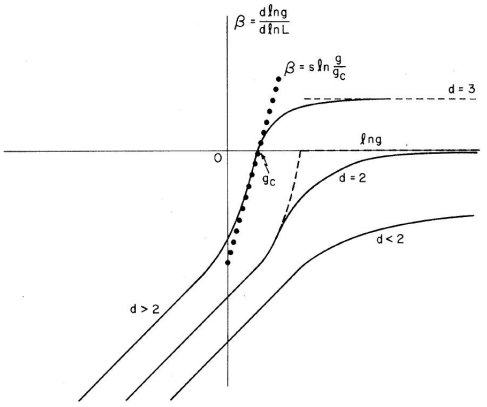

Figure 1.1: β-function for one, two and three dimensions. Original plot by [AALR79]

behave as given in figure (1.1)[2]. This implies the following consequences: First there is no metallic state at or below two dimensions. Second for $d > 2$ there exists a metallic phase and a metal-insulator-transition (MIT) point, at which the β- function vanishes for finite conductance $g = g_c$ and hence zero minimal conductivity $\sigma_c = g_c L^{2-d} \xrightarrow{L\to\infty} 0$. Third, at $2 + \epsilon$ dimension there exists a MIT (at $g \sim \frac{1}{\epsilon}$).
The "Gang of Four"-scaling theory was a milestone in the understanding of the Anderson phase transition. Its importance and implications will be wrapped up when a powerful, microscopically motivated theory will be introduced in (1.6). Instead, in the following sections, the focus will be spotted onto the role of very basic properties of the system: dimensionality and symmetry.

1.3 The role of dimensionality and weak-localization

The fundamental dependence on dimensionality can be understood qualitatively following arguments by A.I. Larkin and D.E. Khmel'nitskii [LK82][3]. They explain the impact on conductivity in the weak disorder limit as follows:

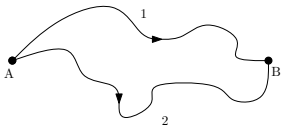

Figure 1.2: Two paths joining A to B.

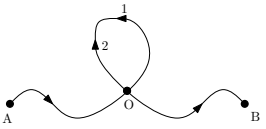

Figure 1.3: Self-intersecting paths with the opposite propagation through the loop.

An electron propagating from point A to point B in a dirty metal might take several different connecting paths. For a quantum-mechanical particle, the total probability for this propagation has to be calculated taking the sum of the amplitudes A_i corresponding to different trajectories and squaring afterwards: $W = |\sum_i A_i|^2 = \sum_i |A_i|^2 + \sum_{i\neq j} A_i A_j^*$. The second term describes the interference of amplitudes belonging to different paths.
The electron-propagation along different paths results in a phase difference of its wave function; e.g. along paths of the type 1 and 2 in figure (1.2). However, the effect of this

[2] A negative β function means decreasing conductance with increasing system size (i.e. decreasing temperature) and the converse. The asymptotical positive constant value $\beta_{d>2}|_{g\to\infty}$ correspond to increasing conductance but constant conductivity.
[3] ...which the author collected from textbooks in English language [Abr88], [Efe97].

phase difference vanishes as the average over the interference term $\langle \cos(\Delta\phi_j - \Delta\phi_i)\rangle$ is zero.
Nevertheless, there do exist paths where interference plays a crucial role: these are the self-intersecting trajectories, depicted in figure (1.3). For each of them there always exists a second path which is exactly the same up to the fact that the loop is taken the other way round. Still $\Delta\phi$ is the same for both and hence $W = |A_1 + A_2|^2 = 4|A_1|^2$. This is twice the classical value!
We see that quantum-interference enhances the impact of self-intersecting trajectories. Those suppress conductivity as the scattering probability increases[4]. But how does the crucial dependence on the dimension arise?
Classically, the probability for self-intersecting trajectories in phase space is zero, because they are "infinitesimally thin". However, quantum-mechanically, they have a finite thickness of order $\lambda_{deBroglie} = \frac{\hbar}{p_0}$. Therefore, the particle going to start its loop at point O in figure (1.3) "occupies" a finite volume element $\sim \lambda_{dB}^{d-1} v dt$ in the time-interval $[0, dt]$. In addition, within a certain time $t \in [\tau, \tau_\phi]$ [5] it might access any point within the volume $(Dt)^{\frac{d}{2}}$ (D is the classical diffusion coefficient). The probability of coming back to the initial point at time t is the fraction of these two volumes: $\sim \frac{v dt \lambda_{dB}^{d-1}}{(Dt)^{\frac{d}{2}}}$.
As the conductivity is decreased by the presence of self-intersecting trajectories, the interference induced relative correction to conductivity is

$$\frac{\Delta\sigma}{\sigma} \sim -\int_{\tau}^{\tau_\phi} \frac{\lambda_{dB}^{d-1} v dt}{(Dt)^{\frac{d}{2}}},$$

a quantity which diverges for $d \leq 2$ as $\tau_\phi \xrightarrow{T\to 0} \infty$. For $d = 3$ it depends on the ratio $\frac{\lambda}{l}$ and justifies classical treatment for the mean free path l much greater than the deBroglie wave-length λ.
In conclusion, the critical dimension $d_c = 2$ predicted by the "Gang of Four"-scaling can be explained qualitatively by Larkin's and Khmel'nitskii's arguments. This is the motivation for considering a spatial dimension of two (or nearby) within many works on Anderson localization and within this thesis.

1.4 The role of symmetries

In 1951, Eugene Wigner [Wig51] started to investigate heavy nuclei by their symmetries. This influenced Freeman Dyson: He developed the Random-Matrix-Theory of Hamiltonians, a theory which should be applied to nuclei in which "all shell structure is washed out and [that] no quantum numbers other than spin an parity remain good" [Dys62].
An electronic disordered system has very little symmetries (at least before averaging over disorder configurations). In this sense, here as well most quantum numbers are "washed out" and a classification analogous to Wigner's and Dyson's heavy nuclei is justified.

Time-reversal symmetry

The works concerning atomic nuclei were based on the investigation of time-reversal symmetry of the systems. Time reversion is realized by an antiunitary operator $T = UK$ (U unitary, K denotes complex conjugation) which might square to $+\mathbf{1}$ or $-\mathbf{1}$ depending on systems with even respectively odd total angular momentum. The transformed

[4] ...as already mentioned in Anderson's 1958 paper.
[5] i.e. a time longer than the (impurity-) scattering time τ but shorter than a timescale τ_ϕ where inelastic interaction destroys these arguments based on coherence.

Hamiltonian is

$$\mathcal{T} : H \to UH^TU^{-1}.$$

There is a total of three Wigner-Dyson classes: The time-reversal symmetry is absent, present and $T^2 = \mathbf{1}$, or present and $T^2 = -\mathbf{1}$.
As long as one requires the Hamiltonian to be invariant under energy shifts, these three classes are the only ones. Dropping this constraint one can extend the symmetry classification.

Particle-hole symmetry

Another rather illustrative concept of symmetry is charge conjugation (in other words particle-hole symmetry). As known, in quantum mechanics it is also represented by an antiunitary operator of the form $Q = VK$ (V unitary)[6]:

$$\mathcal{Q} : H \to -VH^TV^{-1}.$$

Particle hole symmetry again can be absent, present and $Q^2 = \mathbf{1}$, or present and $Q^2 = -\mathbf{1}$.

Collecting all combinations of time-reversal and particle-hole symmetry, one eventually obtains 9 different symmetry classes. However, the combined symmetry has also to be considered:

Chiral symmetry and the total number of symmetry classes

The chiral symmetry - it can be understood to be the combination of the upper two - is represented by a unitary operator W

$$\mathcal{C} : H \to -WHW^{-1}.$$

As chiral symmetry can either be present or absent in the absence of the two other symmetries, in total ten symmetry classes can be constructed[7].
Imposing chiral symmetry to the three Wigner-Dyson classes, three chiral classes are obtained.
Chiral systems have been known for a very long time, as for example the massless Dirac operator falls into this class. In this case, H anticommutes with the fifth Dirac matrix γ_5 and as a consequence all eigenvalues are paired $(\lambda, -\lambda)$ or zero. Such Hamiltonians play a fundamental role in high-energy physics. In the context of disordered electronic systems chiral systems were first considered by Gade and Wegner in the beginning of the nineties [GW91], [Gad93].
This thesis shall be about chiral systems, consequently the whole chapter 3 will be devoted to their importance, realizations and properties.

1.4.1 Classification by symmetries and completeness part I

As explained above, there exist

$$10 = 3|_{T^2=0,\pm\mathbf{1}} \times 3|_{Q^2=0,\pm\mathbf{1}} + 1|_{C=1,T=0,Q=0}$$

symmetry classes. Usually, they are grouped into three Wigner-Dyson classes, three chiral classes and the four other Bogoliubov-deGennes classes. The latter were only discovered in 1996 by Altland and Zirnbauer for certain superconducting systems [AZ97].
For this historical reason and as this work is mainly about chiral classes, the charge conjugation will be expressed by the combination of the two others: $\mathcal{Q} = \mathcal{C} \circ \mathcal{T}$.

[6] The unusual notation Q is used in order to keep C free for "chiral" and K for complex conjugation.
[7] This argumentation is taken from [SRFL08].

Physical arguments for the completeness of classes

The possibility of writing one of the symmetries as the product of the two other ones is a relict of the absence of further such symmetries: Any combination of symmetries of the three types exposed above will either commute with the Hamiltonian[8] or reproduce a symmetry falling into one of the three classes.

Mathematical expression of symmetries

In principle, any unitary matrices U, W are equally good to define the action of $\mathcal{T}$, $\mathcal{C}$ and $\mathcal{C} \circ \mathcal{T}$. However certain representations are common and appropriate [EM08]:
For example, for a Wigner-Dyson system with time-reversion invariance and $T^2 = \mathbf{1}$, $U = \mathbf{1}$ can be chosen and hence H is symmetric.
In the corresponding class where $T^2 = -\mathbf{1}$, $U = i\sigma_y$ is common, then $H = \sigma_y H^T \sigma_y$.
The chiral symmetry is usually realized by means of $W = \sigma_z$, therefore $\{H, \sigma_z\} = 0$ and H becomes block off-diagonal.
This way, the Matrix iH becomes an element of the tangent space of a certain symmetric space (see sec. 1.4.2) and a classification according to Cartan's table of symmetric spaces is appropriate. The classification table itself is given on the last page of the appendix.

1.4.2 What are symmetric spaces?

Symmetric spaces are the underlying mathematical concept for the classification of random matrices and (electronic) disordered systems. Furthermore, the effective field theories dealt with in the non-linear σ model approach also live on symmetric spaces. Finally, the topology-driven phenomena in disordered systems (like topological insulators, their prototype - the quantum Hall state - and the metal-insulator transition described in this work) rely on the topological properties of symmetric spaces.
Here a brief review is given, based on the lecture notes of a course given by Enrico Leuzinger [Leu10] and the standard textbook by Sigurdur Helgason [Hel78].

Symmetric spaces from the geometric point of view

A connected Riemannian manifold $M, \langle \cdot, \cdot \rangle$ is called symmetric space, if for all points $p \in M$ there exists an isometry s_p such that

1. p is fixed under s_p ($s_p(p) = p$) and

2. the differential mapping the tangent space T_pM onto itself has the property $ds_p|_p = -\mathrm{id}|_{T_pM}$.

As the operation s_p simply reflects all tangent vectors, it is called geodesic reflection: Any point on a geodesic will be mapped on the corresponding opposite point in the sense of figure 1.4.2.
It follows, that M is homogeneous with respect to group operations of the isometry group $\mathrm{Iso}(M)$. Accordingly, for any two points on M there is an isometry mapping the one onto the other: $\mathrm{Iso}(M)$ acts transitively on M. This mathematically reflects the equivalence of all points, which is of physical interest for the manifold of equivalent saddle points (see the non-linear σ model derivation in chapter 4).

[8] then diagonalization produces two Hamiltonians of a certain symmetry class

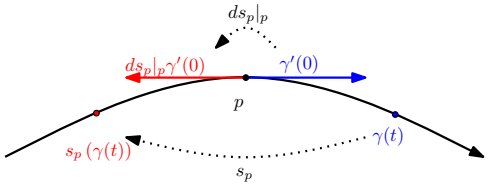

Figure 1.4: Geodesic reflection

Symmetric spaces from the group theoretical point of view

The geometric definition of a symmetric space can be brought to a group theoretical language:
Let M be a connected symmetric space. Denote the compact subgroup of $\mathrm{Iso}(M)$ by $G = \mathrm{Iso}^\circ(M)$ and pick out some base point x_0. Then the symmetric space is diffeomorphic to $\frac{G}{K}$ [9] where K is the compact stabilizer $K = \{g \in G | g \cdot x_0 = x_0\}$ [10].
The converse theorem also holds: Let G be a connected Lie Group, and K a compact subgroup of G[11]. Then $M = \frac{G}{K}$ is a symmetric space in the above given Riemannian/geometric sense with respect to any G-invariant Riemannian metric.

Symmetric spaces on the level of Lie-Algebras

Consider G,K as in the paragraph above. Be $\mathfrak{g}$, $\mathfrak{k}$ the corresponding Lie-Algebras and θ a non-trivial involutive Lie-Algebra automorphism of $\mathfrak{g}$, i.e. $\theta^2 = \mathrm{id}_\mathfrak{g}$ [12]. θ is usually called the Cartan-involution. Then

1. $\mathfrak{k} = \{X \in \mathfrak{g} | \theta(X) = X\}$,
2. $\mathfrak{p} = \{X \in \mathfrak{g} | \theta(X) = -X\}$,
3. $\mathfrak{g} = \mathfrak{k} \oplus \mathfrak{p}$ ("Cartan decomposition"), and
4. the following "Cartan-relations" hold: $[\mathfrak{k}, \mathfrak{k}] \subseteq \mathfrak{k}$, $[\mathfrak{k}, \mathfrak{p}] \subseteq \mathfrak{p}$, $[\mathfrak{p}, \mathfrak{p}] \subseteq \mathfrak{k}$.

In particular $\mathfrak{p}$ is the tangent space $T_\mathbf{1}\frac{G}{K}$.

1.4.3 Classification by symmetric spaces and completeness part II

The connection from the symmetry classification of Hamiltonians to symmetric spaces is carried out on this Lie-algebraic level: One simply checks in which tangent space $\mathfrak{p}$ the Hamiltonian multiplied by the imaginary unit (iH) lies.
The exemplary Hamiltonians given above[13] display one of the following symmetries: $H = H^T$, $H = \sigma_y H^T \sigma_y$ or $\{H, \sigma_z\} = 0$. Therefore iH lies in $\frac{\mathfrak{u}(N)}{\mathfrak{o}(N)}$, $\frac{\mathfrak{u}(2N)}{\mathfrak{sp}(2N)}$ or $\frac{\mathfrak{u}(p+q)}{\mathfrak{u}(p)\times\mathfrak{u}(q)}$ respectively.

[9] the quotient group is defined by the equivalence relation $g \sim h :\Leftrightarrow g \cdot x_0 = h \cdot x_0$ for $g, h \in G$.
[10] The geodesic reflection is incorporated into an involutive automorphism of G: $\sigma : g \mapsto sgs = sgs^{-1}$. The set $Fix(\sigma)$ of fix points of σ is a closed subgroup of G and $Fix^\circ(\sigma) \subseteq K \subseteq Fix(\sigma)$.
[11] Further an involutive map $\sigma \in \mathrm{Aut}G$ with $Fix^\circ(\sigma) \subseteq K \subseteq Fix(\sigma)$ has to be assumed. The geodesic reflection at a given base point $x_0 = eK$ is $s_{x_0}(gK) = \sigma(g)K$
[12] namely, θ is the differential map of the Lie Group involution σ, i.e. $\theta = d\sigma_e$.
[13] In paragraph "Mathematical expression of symmetries", sec. 1.4.1.

Mathematical arguments for the completeness of symmetry classes

In 1926, a complete classification of symmetric spaces was obtained by Elie Cartan. For the purpose of random-matrix theory and disordered systems, we will be interested in compact irreducible symmetric spaces, and the matrix groups have to be of arbitrary matrix size, i.e. we will not consider exceptional Lie groups (like E_8). Under these constraints, there exists a family of seven coset spaces of Lie groups (symmetric spaces of type I) and further four symmetric spaces of type II, which are simple, compact and connected Lie groups. However, within the last four, the orthogonal group in odd dimensions, class B, will not be taken into account: its physical realization would be a disordered superconductor, but the matrix size of Bogoliubov-Hamiltonians is even (it is a bilinear form of Nambu spinors which treat creator and *corresponding* annihilator within one spinor). Therefore a total of ten symmetry classes is obtained. This is a strong indication that the number of classes is complete, any other symmetry class would exceed the Cartan scheme. A rigorous proof has been given by Heinzner *et al.* in 2004 [HHZ05].

1.5 Effect of disorder

Unfortunately, for this section it will not be possible to outline how things evolved historically within a practical brevity. In the mid of the 1970s several authors were influenced by the analogy of the Anderson metal-insulator transition and thermodynamic phase transitions, especially magnetic phase transitions and spin-glasses[14]. Pars pro toto, the contributions by Thouless [Tho75], Aharony and Imry [AI77] and Cardy [Car78] are named. Note, that the conjecture of a (continuous) phase transition was qualitatively confirmed by the "gang of four"-scaling (see 1.2) shortly afterwards.
Much of the following summary is a condensed version of the pedagogic introduction in [AS10].

1.5.1 Techniques in averaging over disorder

The statistical nature of the impurity potential is often, and as well in this work, encoded in a spatially fluctuating potential landscape $V(\mathbf{x})$. It is assumed to have zero mean but non-vanishing second moment

$$\left\langle V(\mathbf{x})\, V\left(\mathbf{x}'\right)\right\rangle = \frac{1}{2\pi\nu\tau}\delta\left(\mathbf{x}-\mathbf{x}'\right). \tag{1.1}$$

Of course generalizations to this Gaussian white noise situation exist but will not be considered within this work.

Difficulties and remedies

Imagine one is interested in the quantum expectation value of a an observable O in a disordered system. In principle one could differentiate the logarithm of the (disorder potential dependent) generating functional with respect to the conjugated source-field J and afterwards average over disorder:

$$\langle O\rangle_{dis} = \left\langle \frac{-\frac{\delta}{\delta J}\big|_{J=0}\mathcal{Z}[J]}{\mathcal{Z}}\right\rangle_{dis}.$$

The evaluation of the disorder average is very problematic inasmuch as the disorder potential also enters the partition function in the denominator. Therefore techniques are

[14] in section 2.1 Anderson transitions will briefly be reviewed.

applied, where this denominator does not appear. These are the supersymmetric, Keldysh and replica methods.
The supersymmetric partition function is constructed such that for a quadratic action S the determinant of the bilinear form in S appears both in the numerator and in the denominator and cancels up to $\mathcal{Z} = 1$. The trick is that bosonic and fermionic variables are simultaneously (and supersymmetrically) treated.
In Keldysh technique the partition function is identically one because of the very construction of the Keldysh contour and the time evolution Operator $\hat{U}$.
Within this thesis replica technique will be used throughout. It is in principle only based on the following representation of the logarithm:

$$\langle O \rangle_{dis} = \left\langle -\frac{\delta}{\delta J}\bigg|_{J=0} \ln \mathcal{Z} \right\rangle_{dis} = -\frac{\delta}{\delta J}\bigg|_{J=0} \lim_{N\to 0} \frac{1}{N}\left(e^{N \ln \mathcal{Z}} - 1\right) = -\frac{\delta}{\delta J}\bigg|_{J=0} \lim_{N\to 0} \frac{\mathcal{Z}^N}{N}.$$

($\mathcal{Z} = \mathcal{Z}[J]$)
All physical quantities are first calculated for an arbitrary replica number N and afterwards the analytic continuation to $N \to 0$ is made.

Advantages and disadvantages of the different techniques

Probably replica is the most straightforward and mathematically "easy" approach. Nevertheless, the flaw of the analytic continuation to be carried out is not to be underestimated. Pioneers of the supersymmetric method, like Efetov, argue that because of this problem some results, like the level-level correlation function, can only be calculated with the supersymmetric technique. This one, in contrast, cannot be applied to interacting systems. The Keldysh technique is very powerful but unnecessarily complicated for the present work.
Even though supersymmetry would have been a good alternative, there are several reasons for treating the present problem in replica. In particular, Pruisken [Pru87b] [Pru87a] also used the replica technique in his works on the instanton-driven quantum Hall effect. Even though not related physically to the present work, it was often a reference and source of inspiration. Second, it seemed more convenient to handle only compact non-linear sigma model manifolds. In the supersymmetric treatment, the non-compact counterpart would also appear in the bosonic sector. This requires a useful parametrization of the σ model matrix, which is only known for AIII symmetry class. The lack of knowledge of useful parametrizations for BDI and CII, as well as the fact that each symmetry class should have been treated separately gave the third and final reason for replica instead of supersymmetry treatment.

1.5.2 Electronic Green's function

Consider the following fermionic replicated Matsubara action with a random potential in the sense of equation (1.1):

$$S\left[\bar{\psi}, \psi\right] = \sum_n \int d^d x \bar{\psi}_n^a(\mathbf{x}) \left(-i\omega_n - \frac{\nabla^2}{2m} - E_F - V(\mathbf{x})\right) \psi_n^a.$$

(a-summation is to be understood and refers to replicas $a = 1...N$. $\sum_n$ is the Matsubara sum.)

The system considered belongs to the Gaussian orthogonal class.
Now calculate the disorder averaged electron propagator in self-consistent Born approximation (SCBA) (see figures 1.5 and 1.6):

$$\langle G(\mathbf{p}) \rangle_{dis} = \frac{1}{i\omega_n + E_F - \frac{\mathbf{p}^2}{2m} + \frac{i}{2\tau} sgn(\omega_n)}.$$

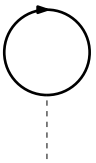

Figure 1.5: Hartree-type diagram

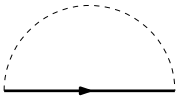

Figure 1.6: Fock-type diagram

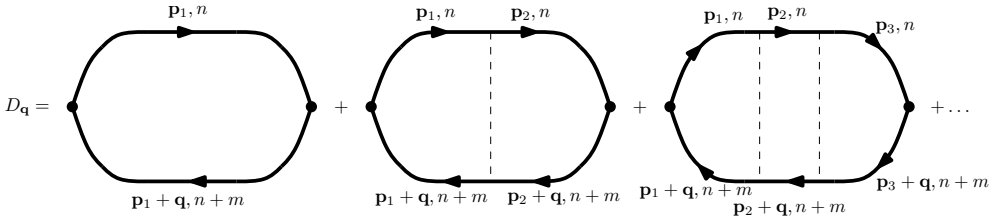

Figure 1.7: Series of diagrams contributing to the density density propagator

(Note that the Hartree-type diagram does not contribute in replica limit. The real part of the Fock-diagram is incorporated in a redefinition of E_F.)
It becomes apparent that the parameter τ^{-1}, which measures the strength of disorder, is responsible for the damping of the electron propagation. This is analogous to the fluctuation-dissipation theorem. τ^{-1} can be identified with the elastic impurity scattering rate.
The SCBA is valid for weak disorder $p_F \gg l^{-1}$, where the Fermi momentum is much larger than the inverse of the mean free path $l = v_F\tau$. Therefore diagrams with crossed impurity lines can be neglected.
Performing the summation over Matsubara frequencies and Fourier transforming back to real space obtain:

$$\langle G(\mathbf{x}, \mathbf{y}; \tilde{\tau})\rangle_{dis} = G_{clean}(\mathbf{x}, \mathbf{y}; \tilde{\tau})\, e^{-\frac{|\mathbf{x}-\mathbf{y}|}{2l}}. \tag{1.2}$$

($\tilde{\tau}$ is the imaginary time.)
Hence, even in the regime of weak disorder and extended states the electron correlation function decays exponentially on the scale of the mean free path. Some other modes will therefore be relevant for long-range correlations: diffusons and cooperons.

1.5.3 Diffusons and cooperons

Diffusive motion governs the relaxation process in a *classical* disordered system. This is the motivation to investigate the (*quantum mechanical*) density-density correlation function D on its long range behaviour.

Diffusons and Drude conductivity

Differentiating the logarithm of the partition function twice with respect to the source field $\mu(x) = \mu(\mathbf{x}, \tau)$ (a space and imaginary time dependent generalization of the chemical potential $\mu \sim E_F$) one obtains D in replica language

$$D(x) = \left\langle -T \left.\frac{\delta^2}{\delta\mu(x)\,\delta\mu(0)}\right|_{\mu(x)=\mu} \ln\mathcal{Z} \right\rangle_{dis} = \lim_{N\to 0} \frac{1}{N} \left\langle \bar{\psi}^a(x)\,\psi^a(x)\,\bar{\psi}^b(0)\,\psi^b(0) \right\rangle.$$

Neglecting again crossed impurity lines and assuming $x \gg l$ the density-density correlation $D_{\mathbf{q}}$ in momentum space can be represented as the series of ladder diagrams, see figure (1.7).

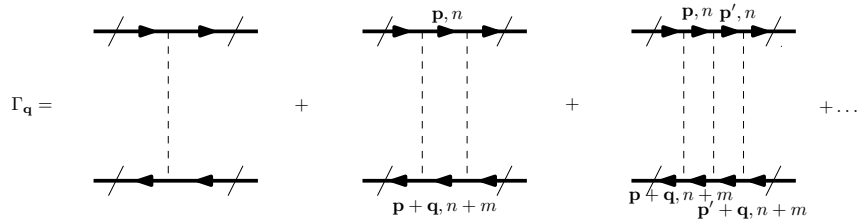

Figure 1.8: Diffuson mode: the particle-hole mode

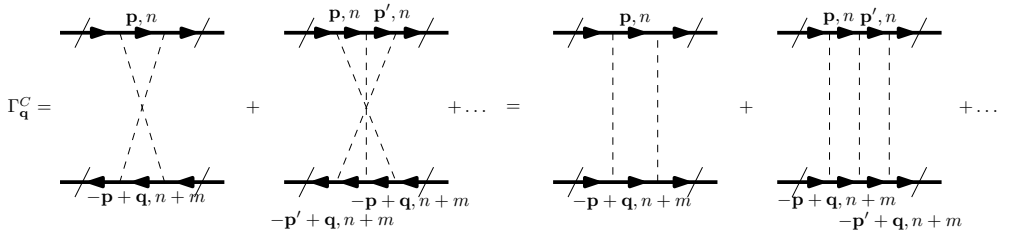

Figure 1.9: Cooperon mode: the particle-particle mode

Within this diagram an effective vertex $\Gamma_{\mathbf{q}}$ arises, it is depicted in figure (1.8). The calculation of this vertex yields

$$\Gamma_{\mathbf{q},m} = \frac{1}{2\pi n\tau^2 L^d}\frac{1}{\omega_m + Dq^2}, \tag{1.3}$$

($D = \frac{v_F l}{d}$ is the diffusion constant).
As the Fourier transform of (1.3) is proportional to the Green's function of the diffusion operator $\left(\partial_\tau - D\nabla^2\right)$, the corresponding mode is called *diffuson*. Hence the conjecture of diffusive motion is verified also for the quantum mechanical case. Furthermore the diffuson propagator is explicitly long-range and has a Goldstone-like form.
Inserting it into the density-density correlator a result again indicating the diffusive motion is obtained: $D_{\mathbf{q}} = \nu\frac{D\mathbf{q}^2}{|\omega_m| + D\mathbf{q}^2}$. From this and the continuity equation one can (re-)obtain the classic Drude conductivity.

Cooperons and Quantum corrections

Further one can consider the next order in $\frac{1}{p_F l}$. These are the maximally crossed diagrams, where the diffuson ladder-vertex (figure (1.8)) entering the density-density correlation (diagram (1.7)) is replaced by the vertex $\Gamma^C_{\mathbf{q}}$ [15] shown in figure (1.9). For analogy the single interaction line is included (first term in figure (1.8)), and Matsubara frequencies are assumed to be of opposite sign.
We can turn the lower line around and obtain a ladder (right hand side of diagram (1.9)), which is the same as diagram (1.8), except for the fact, that the lower momenta have been inversed. As long as $G_{\mathbf{p}} = G_{-\mathbf{p}}$, i.e. the system is invariant under time reversal symmetry, the calculation of $\Gamma^C_{\mathbf{q}}$ is analogous to $\Gamma_{\mathbf{q}}$ and the cooperon mode has the same diffusion pole structure:

$$\Gamma^C_{\mathbf{q},m} = \frac{1}{2\pi n\tau^2 L^d}\frac{1}{|\omega_m| + Dq^2}. \tag{1.4}$$

Still, if one breaks this symmetry explicitly, for example turning on a magnetic field, the mode will be exponentially decaying in space: In the denominator $\mathbf{q}$ will be replaced by

[15] In analogy to Cooper-pairs, this mode of two particles with nearly opposite momenta is called cooperon.

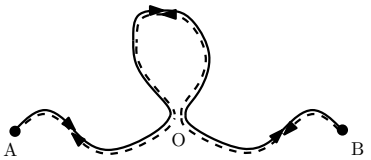

Figure 1.10: Redrawing of figure (1.3) with a diffuson mode

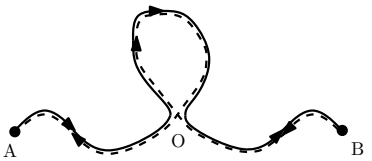

Figure 1.11: Redrawing of figure (1.3) with a cooperon mode

$\mathbf{q} \to (\mathbf{q} + 2\mathbf{A})$, the Goldstone propagator form is destroyed.
For the symmetry class considered (AI), the presence of the Cooperon mode will lead to weak localization. Note the crucial dependence on the symmetries of the problem. Indeed, it is known that only this symmetry class lacks a critical conductance in two dimensions [MEGO10].
The connection to Larkin's and Khmel'nitskii's argumentation of weak-localization is easily made: Replace the electronic Feynman paths depicted in (1.3) by a particle-hole propagator, which turns out to be the long range modes to be considered (see figure (1.10)). Then, considering the reversed propagation through the loop (1.11), the particle-particle propagation comes into play and weak localization occurs as predicted by Larkin and Khmel'nitskii and stated above.

1.6 Non-linear sigma models

Around 1980, the equivalence between the localization problem and non-linear sigma models (NLσMs) was understood. Starting from a microscopic description in terms of a single-particle Hamiltonian this effective field theory can directly be derived.
A brief technically summary is as follows: First the replicated partition function is averaged over disorder producing an effective four-fermion vertex. This vertex is decoupled by a Hubbard-Stratonovich transformation. Then the set of saddle-points corresponding to self-consistent Born approximation (section 1.5.2) is determined. Onto this set of saddle-points, which has the structure of a symmetric space, the (quantum-) fields are mapped. For one of the first historic examples see Hikami [Hik81]. In chapter 4 of this thesis an explicit derivation for chiral systems is presented.
Physically, the field living on the non-linear sigma model manifold $\mathcal{M}_\sigma$ describes the long range diffuson and cooperon modes. The two of them being related by time-reversal symmetry, it makes sense to describe them by a unified, symmetrized object. Depending on the symmetries of the system, different soft modes are present, and hence $\mathcal{M}_\sigma$ differs (see the table of symmetry classes, appendix I).
The sigma model therefore describes the disordered system in its metallic regime, and only as long as the conductivity is large (or the diffusive modes "slow").

1.6.1 An illustrative example

The most illustrative example of a NLσM is a system which is governed by a so called mexican hat potential. Within a mean-field approach such potentials arise (usually) below the critical temperature of a certain phase transition. The system spontaneously falling into a definite ground state out of the (degenerate) ground state manifold causes spontaneous symmetry breaking (SSB). By Goldstone's theorem, massless modes appear which describe the alteration of the ground state over spatial extension. All this happens within the ground state manifold, in the present example a circle, see figure (1.12). Furthermore, also massive modes appear, which describe changes perpendicular to the ground state manifold. In the NLσM treatment, the massive modes are neglected, as they are strongly suppressed by energetic reasons, see figure (1.13).

Physically, this example characterizes superfluid Helium-4 or any other system, where a spontaneous breaking of *global* U(1) symmetry appears. (Also s-wave superconductors exhibit such a potential structure, but here a *local* symmetry is broken.)

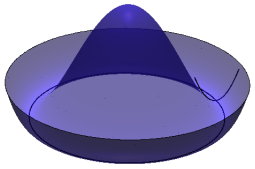

Figure 1.12: Mexican hat potential, massless and massive mode.

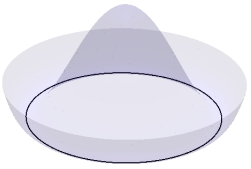

Figure 1.13: The simplest NLσM manifold: a circle.

If one calls the angle assigning a definite vacuum state ϕ, the NLσM action describing the system below the critical temperature is

$$S[\phi] = \int d^d x \frac{J}{2} (\nabla\phi)^2 . \tag{1.5}$$

Already in this simple example, also the role of topology becomes apparent: ϕ is a Goldstone mode and lives on a topologically non-trivial manifold: a circle. One implication of this fact, namely the Berezinskii-Kosterlitz-Thouless phase transition, is of fundamental importance for the present work and section 2.2 is devoted to it.

1.6.2 NLσM of disordered metals and renormalization group

In this work, we will be interested in two dimensional disordered metals. The circular NLσM arising due to SSB and the phase transition in a mean-field theory of superfluidity can be seen as a conceptional prototype.
For two-dimensional dirty metals, the NLσM looks like

$$S[Q] = \int d^2 x \frac{1}{t} \mathrm{tr} \left[\nabla Q \nabla Q^{-1}\right] . \tag{1.6}$$

Q is the field describing the low excitation modes and lives on some symmetric space (appendix I). The prefactor $\frac{1}{t}$ is proportional to the conductance.

Analogies and differences compared to the illustrative example

In the case of usual phase transitions (e.g. in superfluids or the Heisenberg ferromagnet) self-consistent average over the interaction term generates an effective mean-field "potential", for example the gap function or the magnetization. By symmetry arguments they are constrained to certain manifolds and the spontaneous symmetry breaking occurs, when the system falls into a definite ground state corresponding to a point on this manifold. Smooth variations of the order parameter, the Goldstone modes, are then described by non-linear σ models.
For disordered systems the situation is similar: The interaction with the disorder potential is also self-consistently (SCBA) averaged out, yielding an effective mean-field potential, namely the Hubbard-Stratonovich field. Analogously, there exists a mechanism of "symmetry breaking", namely when a saddle-point corresponding to SCBA is determined, as

well as a NLσM treating the fluctuations of the field.
However there are substantial differences: Most prominently the field Q does not play the role of an order parameter. In the replica limit, a phase of vanishing Q does not exist. This is due to the symmetry being broken both in the phase of extended and in the phase of localized states, as shall be explained below.
To this end consider the Goldstone propagator $\frac{1}{Dp^2+i\delta}$ [16]. Both for usual phase transitions and Anderson transitions, it is a manifestation of long-range correlations and there is no mass gap as the order parameter is responsive to infinitesimal perturbations of the order parameter. The propagator is divergent for $\mathbf{p} \to 0$ as $\delta \to 0$. For usual phase transitions, there is a phase of restored symmetry, yielding a mass term and hence the divergence is cured. However, for Anderson transitions this is not the case: at the transition from extended to localized states, the diffusion propagator changes from the Goldstone like form to $\frac{1}{\delta} e^{-\frac{\|\mathbf{x}-\mathbf{x}'\|}{\xi}}$, which is divergent in $\delta \to 0$ for any momentum (or real-space distance). In this sense, the spectrum is gapless in the localized regime as well, even though no long-wavelength excitations exist. This is, even though in an unconvential manner, a manifestation of Goldstone's theorem, which predicts this gapless spectrum as the symmetry is broken.[17]

The renormalization group

Now, in order to obtain information on the Anderson transition, perturbative renormalization group (RG) treatment is performed with the NLσM. Explicit examples are given below for chiral classes. There, an extra term appears during the RG procedure: the "Gade term" , see sec. 3.3.1.
The idea of RG is to collect the "fast" modes together, average them out, and incorporate the effect into slightly changed dynamics of the remaining "slow" fields. In this step approximations are made, and only the simplest of an infinite series of Feynman graphs might be kept. The division between "fast" and "slow" is somehow arbitrary, and hence in a next step, the faster part of the "slow" fields will be integrated out again and so fourth. Qualitatively, averaging "fast" modes (i.e. fluctuations with higher energy) out, reflects the lowering of temperature. Stated differently, we will experimentally be interested only in the very long-distance ($\sim$ sample size) behaviour of the diffusive modes, and therefore integrate out stepwise their small-scale fluctuations.

RG treatment of disorder NLσM's

If the scale-dependent corrections to the inverse conductivity t are calculated to one loop order, one will obtain a gradually lowered ("weak localization"), unchanged, or enhanced ("weak anti-localization") conductivity. There are also classes, the chiral classes, in which the β-function vanishes to all orders in perturbation theory. All this depends on the symmetry class, and for all of them the one loop correction is given in the table in appendix I. When the β-function is always negative (weak localization), there exists only the insulating state; the result exposed in section 1.5.3 is reproduced this way. On the contrary a positive β-function (weak anti-localization) in the perturbative regime (large conductivity) indicates the presence of a metallic phase. However, in most of the cases there is a localized phase for strong disorder and therefore also a transition point at which $\beta(g) = 0$.
The presence of weak anti-localization is physically related to the destructive interference

[16] Retarded and advanced Green's functions are defined $G^{R,A}(\mathbf{r}, \mathbf{r}') = \left(E - \hat{H} \pm \delta\right)^{-1}_{\mathbf{r},\mathbf{r}'}$. Then the diffusion propagator in the delocalized regime has the indicated Goldstone form.

[17] In order to describe Anderson transitions and the qualitative change of the Green's function in terms of spontaneous symmetry breaking, Zirnbauer [Zir86] first introduced the order parameter function $F(Q) = \int_{Q \neq Q(\mathbf{x}_0)} \mathcal{D}Q e^{-S_{\mathrm{NL}\sigma\mathrm{M}}}$.

of time-reversed paths for particles with spin $\frac{1}{2}$.
As a side remark, it should be mentioned that often the RG approach is taken slightly above the lower critical dimension $d_c = 2$ in order to study the transition point at $g \sim \frac{1}{\epsilon}$ (i.e. in the perturbative regime). In contrast, in the present work only two dimensional systems will be investigated.

1.7 Role of topology and connection to symmetries

In the sections above, the presence of both metallic and insulating phases, and consequently the presence of critical points was exposed for some of the ten symmetry classes. In all cases discussed, the appearance of a critical point was associated to the symmetries of the systems: weak anti-localization appears in fermionic systems (half-integer angular momentum) with time-reversion invariance, whereas the criticality in chiral systems explicitly depends on the chiral symmetry of the system (for a straightforward argument on the NLσM-level, see section 3.3.1). Here, it will be presented how within certain symmetry classes other mechanisms for criticality can emerge: those related to topology.
Topological terms arise often in the context of Dirac fermions. In this section, the *possible* appearance of topological terms is motivated from non-trivial homotopy groups. In section 3.2, the *definitive* emergence of certain topological terms is exposed for Dirac fermions (e.g. in graphene or topological insulators).

1.7.1 Topology of the σ-model and topological excitations

In the illustrative example of a NLσM (see sec. 1.6.1) arising in a mean-field theory, an interesting and relevant feature is already given: its non-trivial topology. Mathematically, the statement is that the first homotopy group of $U(1)$ is $\mathbb{Z}$.

Field theories and compactified base-manifold

The Q-fields map the physical space to the NLσM model manifold $\mathcal{M}_\sigma$:

$$Q : \mathbb{R}^d \to \mathcal{M}_\sigma.$$

However, in order to keep the action finite, a constraint has to be imposed on Q: namely $Q(\mathbf{x})|_{\|\mathbf{x}\|\to\infty} = \text{const.}$. Therefore, the more precise mapping is

$$Q : \mathbb{R}^d \cup \{\infty\} \simeq \mathbb{S}^d \to \mathcal{M}_\sigma,$$

where $\simeq$ denotes the homeomorphism, realized through stereographic projection.

Homotopy group

With the help of the homotopy group topologically different field configurations can be distinguished in a mathematically clean way:
Consider two field configurations $Q_i : \mathbb{S}^d \to \mathcal{M}_\sigma$ where $i = 1, 2$. Then an equivalence relation can be defined:

$$\begin{aligned} Q_1 \sim Q_2 \quad :\Leftrightarrow \quad & \exists \hat{Q} : \mathbb{S}^d \times [0,1] \to \mathcal{M}_\sigma \ , \ \hat{Q} \text{ continuous,} \\ & \text{such that } \hat{Q}(\mathbf{x}, 0) = Q_1(\mathbf{x}) \text{ and } \hat{Q}(\mathbf{x}, 1) = Q_2(\mathbf{x}). \end{aligned}$$

This simply states that two field configurations can continuously deformed one into the other. The set of equivalence classes forms the d-th homotopy group $\pi_d(\mathcal{M}_\sigma)$.

Figure 1.14: An $O(3)$-skyrmion as a prototype for instantons in disorder NLσMs

Non-trivial topology of σ-model manifolds

The homotopy groups of the Cartan symmetric spaces are well studied in mathematics and given in the table in appendix I. For the present work, the first, second and third homotopy group will be of interest.
Non-trivial topological properties can also be directly deduced from the Hamiltonians, as shown by Kitaev [Kit09][18]. In the past years, the most important interest when considering topological properties of disordered systems has been a classification scheme of topological insulators (see sec. 3.1.2). Both using Kitaev's and the σ-model homotopy group table, the same classification scheme can be obtained.
If one of the homotopy groups π_n, $n \leq d$, is non-trivial, then topological excitations, such as vortices or instantons (like in figure (1.14)), can appear. They always come along with a certain energy cost but on the other hand raise the entropy, as changing their position or orientation does not cost any further energy.
In many cases, the effect of the non-trivial homotopy group can be expressed via a locally defined topological term added to the action. Still, there not being a canonical recipe for constructing topological terms, in the present work we also encounter a case where such a topological term is not yet known.

In the remainder of this chapter, topological terms for two dimensional NLσMs will be exposed.

1.7.2 θ-terms

Three out of ten classes of disordered electronic two dimensional systems have a $\pi_2(\mathcal{M}_\sigma) = \mathbb{Z}$. For all of them the first homotopy group is trivial. They have broken time-reversal symmetry in common and differ in the presence or absence of particle-hole symmetry. The most prominent example among them, and maybe of all sigma models with a topological term, is Pruisken's action describing the integer quantum Hall effect (class A):

$$S[Q] = \frac{1}{8}\int d^2x \sigma_{xx} \mathrm{tr}\left[\nabla Q \nabla Q\right] - \sigma_{xy}\epsilon_{\mu\nu}\mathrm{tr}\left[Q\nabla_\mu Q \nabla_\nu Q\right].$$

The second term is the θ-term which counts how many times the mapping $Q : \mathbb{S}^2 \to \frac{U(2N)}{U(N)\times U(N)}$ covers the subgroup $\frac{U(2)}{U(1)\times U(1)} \simeq \mathbb{S}^2$.
The two other classes where a similar action occurs are C (spin quantum Hall effect) and D (thermal quantum Hall effect).

[18] Again, the homotopy groups are not obtained from the "direct" Hamiltonian symmetric space but from the symmetric space associated to "reduced Hamiltonians". They are obtained by replacing all eigenvalues by their sign and keeping the eigenvectors at the same time. An idea of how to deduce topological properties on Hamiltonian level is also given in sec. 3.1.2 based on Schnyder *et al.* [SRFL08].

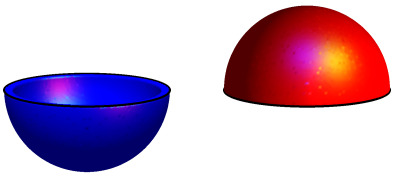

Figure 1.15: Extension of the base manifold to the lower (left) respectively upper (right) hemisphere. In the picture the physical space is a 1-sphere representing a 2-sphere, and the extension a 2-hemisphere representing the 3-hemisphere. The physical space is the boundary of the hemisphere, here depicted by a black line.

1.7.3 Wess-Zumino-Novikov-Witten terms

For the "principal chiral models", i.e. two-dimensional σ-models defined on a Lie group $U(N)$,$O(N)$ or $Sp(2N)$, the second homotopy group is trivial but $\pi_3(\mathcal{M}_\sigma) = \mathbb{Z}$. This allows for a Wess-Zumino-Novikov-Witten term (also WZW term). In the case of $U(N)$ it is

$$iS_{WZ} = \frac{ik}{12\pi}\int d^2x \int_0^1 ds\epsilon_{\mu\nu\lambda}\mathrm{tr}\left(Q^{-1}\partial_\mu Q\right)\left(Q^{-1}\partial_\nu Q\right)\left(Q^{-1}\partial_\lambda Q\right). \tag{1.7}$$

In order to write the WZW term in a manifestly invariant form, the field $Q : \mathbb{S}^2 \to U(N)$ has to be extended to

$$Q : \mathbb{S}^2 \times [0,1] \to U(N) \text{ such that } Q(\mathbf{x},0) = \mathbf{1}; Q(\mathbf{x},1) = Q(\mathbf{x}).$$

This is topologically equivalent to the base manifold being extended from a 2-sphere to a 3-hemisphere of which the the 2 -sphere is the boundary (see figure (1.15), left). $\pi_2(\mathcal{M}_\sigma) = 0$ is a necessary condition.
One could also imagine extensions in the other direction, i.e.

$$Q : \mathbb{S}^2 \times [1,2] \to U(N) \text{ s.th. } Q(\mathbf{x},1) = Q(\mathbf{x}); Q(\mathbf{x},2) = \mathbf{1},$$

and the base manifold is extended to the upper 3-hemisphere (see figure (1.15), right). In that case the WZW term (1.7) acquires an extra minus sign, as the orientation of the manifold is inversed.
The way of extending the base manifold does not matter,

$$iS_{WZ}^{s\in[0,1]} - iS_{WZ}^{s\in[1,2]} = \frac{ik}{12\pi}\int_{\mathbb{S}^3} d^2x ds\epsilon_{\mu\nu\lambda}\mathrm{tr}\left(Q^{-1}\partial_\mu Q\right)\left(Q^{-1}\partial_\nu Q\right)\left(Q^{-1}\partial_\lambda Q\right) = i2\pi k.$$

In this integral $Q : \mathbb{S}^3 \to U(N)$, see figure (1.16). The (integer) WZW-level k counts, how many times the $SU(2)$ subgroup of $U(N)$ is covered. This topological nature of the WZW term explains the stability of iS_{WZ} against different kinds of extensions.
It is important to stress that the WZW term itself is not quantized. Imagine a mapping of winding number $k = 1$. Then the integral in (1.7) measures the volume of the image of the lower ("blue") hemisphere on $U(N)$. It varies smoothly depending on the mapping and is not quantized. Only the sum of the "blue" and the "red" image gives an integer value, in this case $k = 1$. This will be of fundamental importance for the argumentation concerning the appearance of the $\mathbb{Z}_2$-topological term in class CII (sec. 4.5).

"Local" representation of the WZW term

There also exist another representation of the WZW term for which the Q-field is not extended. In order to understand its appearance, some notions from differential geometry

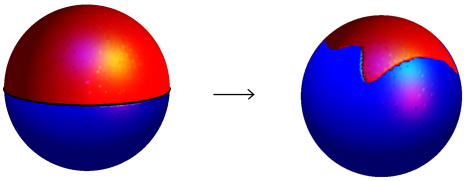

Figure 1.16: The mapping $Q : \mathbb{S}^3 \to \mathbb{S}^3 \subset U(N)$. The WZW-level k is the winding number of this mapping.

are used.
For any non-Abelian, simple group G (the target space) there exists a 3-form ω which is invariant under group rotations, closed ($d\omega = 0$) and locally exact $\omega = d\lambda$ (λ is hence a 2-form). Further let $\tilde{Q}$ be the field on the extended base manifold B and $\tilde{Q}^*$ denote the pullback of differential forms[19]. Using the commutativity of exterior derivative with the pullback and Stokes' theorem[20]

$$iS_{WZ} := i2\pi k \int_B \tilde{Q}^*\omega = i2\pi k \int_B \tilde{Q}^* d\lambda = i2\pi k \int_B d\left(\tilde{Q}^*\lambda\right) = i2\pi k \int_{\partial B = \mathbb{S}^2} Q^*\lambda.$$

With the help of coordinates ϕ_i on the target manifold, the formula is represented in a less abstract way

$$iS_{WZ} = i2\pi k \int d^2x \epsilon^{\mu\nu} \lambda_{ij}\left(\phi\left(\mathbf{x}\right)\right) \partial_\mu \phi^i \partial_\nu \phi^j. \tag{1.8}$$

($\lambda_{ij} = \lambda\left(\frac{\partial}{\partial\phi^i}, \frac{\partial}{\partial\phi^j}\right)$ is the coordinate representation of λ.)
It is of central importance to remark that the *local*[21] condition $\omega = d\lambda$ allows only for the *local* representation (1.8) (therefore the coordinate dependence).
A global[22] rotation of the Q-fields produces the following correction to λ_{ij} [Wit84]

$$\lambda_{ij} \to \lambda_{ij} + \frac{\partial\beta_j}{\partial\phi^i} - \frac{\partial\beta_i}{\partial\phi^j}. \tag{1.9}$$

(The $\beta\left(\phi\right)$ incorporate this rotation and are not explicitly space dependent (only ϕ is).)
The WZW term is corrected as well

$$\delta i S_{WZ} = i2\pi k \int d^2x \epsilon^{\mu\nu} \left(\frac{\partial\beta_j}{\partial\phi^i} - \frac{\partial\beta_i}{\partial\phi^j}\right) \partial_\mu\phi^i\partial_\nu\phi^j = i4\pi k \int d^2x \partial_\mu\left(\epsilon^{\mu\nu}\beta_j\partial_\nu\phi^j\right). \tag{1.10}$$

As the base manifold is compactified to a sphere, the integral vanishes and the WZW-model is invariant under group operations also in its "local" representation.

When do WZW terms occur?

WZW terms appear in the context of non-Abelian bosonization of massless Dirac-fermions [Wit84]. If the fermionic theory displays chiral anomaly[23], then the effect of the anomaly on the sigma model will be the WZW term.

[19] The pullback is defined $\left(\tilde{Q}^*\left(\omega\right)\right)\mathbf{v} = \omega\left(d\tilde{Q}\left(\mathbf{v}\right)\right)$ for any $\mathbf{v} \in \mathcal{V}B$.

[20] The first equals sign denotes the abstract definition of the WZW term. The normalization of ω is chosen such that the integral over upper and lower extension yields integer values.

[21] Local in the sense of the target manifold.

[22] Here global in the sense of the base manifold: The rotation is $\mathbf{x}$-independent.

[23] i.e. chiral symmetry is present in the classical action and equations of motion, but anomalously broken within (quantum-)perturbation theory

In solid state physics, the presence or absence of the chiral anomaly and the WZW depend on the underlying microscopic theory. For example, graphene with vacancies and a random vector potential falls into class AIII without WZW term, whereas the σ-model of graphene with dislocations and a random vector potential (also AIII) will include a WZW term [MEGO10].
More details can be found in section 3.2.

1.7.4 $\mathbb{Z}_2$-topological terms

$\mathbb{Z}_2$-topological terms arise for spin-$\frac{1}{2}$-particles with spin-orbit coupling and preserved time-reversal symmetry, and are related to Kramer's degeneracy (see also section 3.1.2). This is the case for the classes CII and AII. The following topological term is added to the action:

$$iS_{top} = i\pi N\left[Q\right] \ , \ N\left[Q\right] = 0, 1.$$

A local notion of this $\mathbb{Z}_2$-topological term is yet not known. However, for class CII, its appearance can be understood from the microscopic theory as a descendant of the AIII WZW term, see sec. 4.5. Some conjectures for its effect will be given as well in sections 6.2 and 7.5.

2. Some phase transitions in 2D

2.1 Anderson transitions

The mobility edge

Consider a weakly disordered metal, where the band structure is still present[1]. Then, due to their low kinetic energy, states at the bottom and top of the band will be localized. Conversely, states in the middle of the band are extended. It has already been stressed that extended and localized states cannot coexist at a certain energy and disorder strength (section 1.1). Consequently, a sharp energy E_c, called "mobility edge", will separate the localized from extended states in a certain band. As the Fermi energy is moved over the mobility edge, the phase transition occurs.

Critical exponents

The observables which exhibit a non-trivial behaviour nearby the Anderson transition are most importantly the localization length ξ on the insulating side and the DC-conductivity σ on the metallic side. The critical exponents will determine their scaling behaviour.
Let τ be the perturbation which most relevantly drives the system through the transition[2]. It scales as $\tau \to \tau b^{\frac{1}{\nu}}$ and changes sign at the transition from positive (extended) to negative (localized). Then the correlation length diverges as

$$\xi \propto |\tau|^{-\nu} \sim |E - E_c|^{-\nu}.$$

[1] This section is adapted from [Nay04]
[2] $\tau = \text{const.} \times (E - E_c)$ for a system homogeneous in energy.

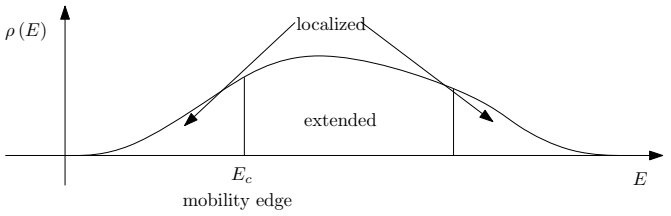

Figure 2.1: Graphical representation of mobility edge (adapted from [Nay04])

The scaling equation of the DC-conductivity is

$$\sigma(\tau) = b^{2-d}\,\sigma\left(\tau b^{\frac{1}{\nu}}\right).$$

From this Wegner [Weg76] first obtained the critical exponent for the vanishing conductivity

$$\sigma \propto \tau^{\nu(d-2)} \sim (E - E_c)^{\nu(d-2)} \ , \tau > 0.$$

The critical exponent ν can be expressed in terms of the β-function, which has been calculated, e.g., in perturbative RG of the NLσM (see section 1.6.2). The value for the Gaussian orthogonal class is for instance [Weg89]

$$\nu = -\frac{1}{\beta'(t_*)} = \frac{1}{d-2} - \frac{9}{4}\zeta(3)(d-2)^2 + \dots \ . \tag{2.1}$$

All this makes the Anderson transition look very similar to usual (SSB) phase transitions. We have a diverging correlation length, well defined critical exponents and the absence of a phase transition in two or less dimensions. However, the Anderson transition is *different* from usual thermodynamic phase transitions: The conductivity is the only thermodynamic quantity which changes, and only the propagator of the effective modes changes its form (the electronic propagator decays on both sides exponentially) [Nay04] [AI77]. In section 1.6.2 the impact on the different nature of the corresponding NLσM has already been discussed.

2.2 Berezinskii-Kosterlitz-Thouless phase transition

It is well-established that in two dimensions or less, no long-range ordered phase can occur (Mermin, Wagner, [MW66]). However, in the beginning of the seventies, Berezinskii [Ber70] and Kosterlitz and Thouless [KT73] established a theory which could explain two-dimensional phases of quasi-long range order.

A model with topological excitations

Let us consider again the simplest σ model stressed above, eq. (1.5), where the field ϕ is defined modulus 2π. J is often called spin-stiffness[3]. Its physical meaning varies in different systems, and is in many cases proportional to the inverse temperature.
If ϕ was living on a topologically trivial manifold, the theory would be Gaussian and no renormalization could occur. However, as $e^{i\phi} \in \mathbb{S}^1$, topological defects are allowed: Vortices, see figure (2.2), left.
Within the vortex core the σ-model description breaks down[4]: the mathematical singularity is regularized by some high core energy replacing the ϕ-field description. This energy is incorporated into the statistical weight $y_0 \ll 1$. Each vortex carries this weight, which is often called fugacity.
In principle and for completeness, vortices of any integer winding number have to be considered. However, it turns out that for the phase transition to be discussed below, those with winding number $n_i = \pm 1$ are the most relevant. All other kinds of vortices will be dropped.

[3] This terminology is due to the fact that (1.5) can be understood as the continuous version of the xy-model.

[4] A more precise technical description of what is going to follow will be given in 7.3, when the effect of vortices in the context of diffusive NLσMs is described.

Two distinct phases

What happens if one inserts N vortices into the action 1.5? Expressed in formulae, a vortex is a configuration where $\partial_\mu \phi = \mathrm{rot}_\mu n_i \ln \frac{\|\mathbf{x}-\mathbf{x}_i\|}{\gamma^{-1}}$ (γ^{-1} is the vortex core size)[5]. The contribution of the harmonic excitations, which decouple from the topological channel, will be neglected. Then the action of an overall neutral[6] N-vortex gas is

$$S_N = -2\pi J n_i n_j \sum_{i<j} \ln \frac{\|\mathbf{x}_i - \mathbf{x}_j\|}{\gamma^{-1}}.$$

As long as J is large (low temperature), the vortices are strongly bound in tiny dipoles $\|\mathbf{x}_i - \mathbf{x}_j\| \gtrsim \gamma^{-1}$. However, when J becomes small (high temperature), the dipole size might grow until, eventually, a plasma of charged isolated vortices is present.
A quantitative description of this phase transition follows.

RG from the low temperature side

In the present work the direct RG-calculation starting from the low-temperature phase is performed[7]. As mentioned above, here the vortices form a dilute gas of dipoles. The RG consists in integrating out the fastest (i.e. closest) dipole-pair $\|\mathbf{x}_i - \mathbf{x}_j\| \in \left[\gamma^{-1}, m^{-1}\right]$ and adding its effect into the renormalized stiffness J' and fugacity y'.
The corresponding RG-equations are well-established [JKKN77] and at the same time a special case of the calculations exposed in appendix H and sec. 7.3.4. For these reasons, only the result is given here:

$$\begin{aligned} -\frac{dJ}{d\ln m} &= -y^2 J^2, \\ -\frac{dy}{d\ln m} &= (2 - \pi J)\, y. \end{aligned}$$

(a prefactor of $\frac{\pi^2}{\gamma^2}$ has been incorporated into the definition of the fugacity.
At $J_c = \frac{2}{\pi}$ the β-function of the fugacity changes sign and vortices start to proliferate. In the vicinity of J_c the flow goes along hyperbolae $y = \sqrt{\frac{\pi}{4}(2-\pi J)^2 + \text{const.}}$ and a schematic plot is given in figure (2.2), right. The shaded region corresponds to the low-energy phase, where eventually, the fugacity vanishes and the stiffness assumes a finite value. The non-shaded region on the contrary, corresponds, to the high-temperature phase, where vanishing stiffness and large fugacity produce the vortex plasma[8].

Correlations and (absent) critical exponents

Above it is stressed that the phase transition distinguishes a phase of dipoles from a vortex plasma. However, this is rather abstract and one may ask, how more direct physical observables are affected. Is the low-temperature phase governed by long-range order, analogously to phase transitions in higher dimensions?
The Mermin-Wagner theorem rules long-range correlations out. Still, quasi-long-range correlations between elements of $U(1)$ can easily be shown:

$$\left\langle e^{i\phi(\mathbf{x})} e^{i\phi(0)} \right\rangle \approx \left(\frac{\gamma^{-1}}{\|\mathbf{x}\|} \right)^{\frac{1}{2\pi J_{eff}}}. \tag{2.2}$$

[5] The connection to the definition via a contour integral is given in sec. 7.2.
[6] Without imposing neutrality, a surface term diverging as $\ln L$ arises.
[7] One can also map the $U(1)$-problem onto a sine-Gordon model, the result being unchanged. The sine-Gordon-treatment might seem more rigorous, but is by far harder to generalize to the $U(N)$- NLσM of disordered systems.
[8] Note that the system flows towards a region where assuming small y is not anymore justified.

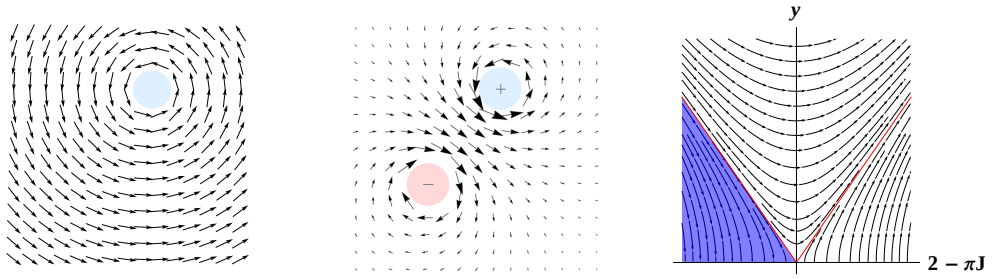

Figure 2.2: Left: A vortex in the field $e^{i\phi}$. Center: The gradient field $\nabla\phi$ visualizing the attractive vortex-antivortex interaction. Right: RG-flow in the vicinity of the critical (transition) point.

On the other side of the separatrix, in the high temperature phase, the correlations decay exponentially and the correlation length ξ can be defined as follows: Consider the system to be slightly above the transition point, i.e. in terms of temperature at $T - T_c$ and at small y_0. Then, the ξ is defined as the length scale, at which the fugacity has grown to $y \sim 1$ under RG. It diverges as

$$\xi \propto e^{C\sqrt{\frac{T_c}{T-T_c}}},$$

as it approaches T_c. Below, $\xi = \infty$ for the whole low temperature phase, as expected from the line of fixed points representing this phase.
From the scaling of ξ and the underlying RG-equations it is also evident that it is not possible to define the critical exponent associated to the correlation length (the same holds also for other exponents).
All this makes the Kosterlitz-Thouless-transition very peculiar and different from the standard phase transitions. It might be applied to different physical systems, such as two dimensional crystals, Josephson junction arrays, neutral superfluids[9] or the xy-model of interacting spin-systems.
The metal-insulator transition discovered in this work relies on a similar mechanism as the BKT-transition even though the implied critical behaviour differs (most likely) substantially. A discussion of analogies and differences is given in section 8.2.6.

[9]Note, that by Mermin-Wagner, there is no SSB in two dimensions and hence no superfluid and no $U(1)$-σ-model to start with. However, we assume small superfluid regions in the normal liquid, so the phase of the condensate function is defined *locally*.The discussion of the interaction of the phases of these flakes brings us back to the discussion above and the $U(1)$-σ-model.

3. Chiral classes and Dirac fermions

3.1 Physical realizations

3.1.1 Gade's original sublattice model

The first microscopic Hamiltonian describing a disordered chiral system was proposed by Renate Gade in 1993 [Gad93]. In full analogy to Anderson's original work, she considered a tight-binding model, but with an internal degree of freedom at each site (effective spin). Regular spin-flipping hopping is allowed between the sites whereas on the sites random spin-flipping occurs, see figure (3.1). The tight-binding Hamiltonian is manifestly invariant under chiral symmetry:

$$H = \sum_{\langle ij \rangle} \begin{pmatrix} c_\uparrow^+ & c_\downarrow^+ \end{pmatrix}_i \begin{pmatrix} 0 & t \\ t & 0 \end{pmatrix} \begin{pmatrix} c_\uparrow \\ c_\downarrow \end{pmatrix}_j + \sum_i \begin{pmatrix} c_\uparrow^+ & c_\downarrow^+ \end{pmatrix}_i \begin{pmatrix} 0 & \delta t_i \\ \delta t *_i & 0 \end{pmatrix} \begin{pmatrix} c_\uparrow \\ c_\downarrow \end{pmatrix}_i .$$

Instead of realizing the two sublattices as two different spin-orientations, any other bipartite lattice with symmetry-preserving randomness is equally chiral.
All this seems like an academic exercise, but there are indeed physical realizations of such a kind. The most prominent example of a bipartite lattice is graphene, see section 3.1.3.

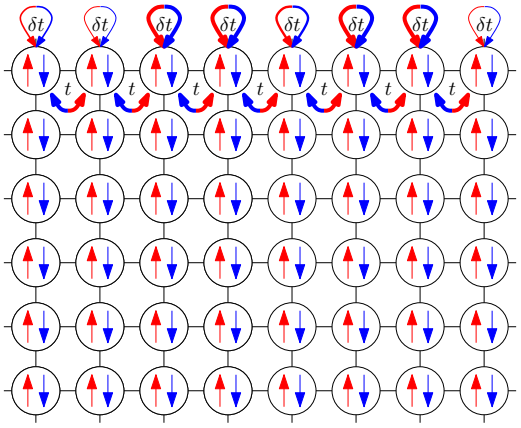

Figure 3.1: Gades original sublattice model: regular spin-flipping next neighbour hopping t and random on-site spin-flipping δt.

3.1.2 Topological Insulators

Topological insulators are one of the most active research areas in present-day solid state physics. Their bulk state is an insulator (gapped band structure) but in contrast to usual insulators this state is topologically non-trivial. The consequence are surface states which are stable against disorder.
The first known topological insulator was the quantum Hall state discovered by von Klitzing *et al.* in 1980 [KDP80]. The quantized σ_{xy}-plateaus arise in different topological phases between which at the steps a phase transition occurs.

Topology, Bloch's Theorem and connection to NLσM classification

Such topological phases can be explained using Bloch's theorem, as first stated by Thouless *et al.* [TKNdN82]. For example for the quantum Hall effect (Cartan class A) this works as follows [SRFL08]:
Assume the presence of (discrete) translational invariance [1], then for each reciprocal vector $\mathbf{k}$ there is a Bloch state $|u_{\hat{a}}(\mathbf{k})\rangle$ with energy $E_{\hat{a}}(\mathbf{k})$. Assume m (i.e. $E_{\hat{a}}(\mathbf{k}) < E_0$) filled and n ($E_{\hat{a}}(\mathbf{k}) > E_0$) empty Bloch states, where E_0 lies in the bulk gap. Define the $m+n$ matrix

$$Q_{Bloch} = \sum_{\hat{a},\text{filled}} |u_{\hat{a}}(\mathbf{k})\rangle\langle u_{\hat{a}}(\mathbf{k})| - \sum_{\hat{a},\text{empty}} |u_{\hat{a}}(\mathbf{k})\rangle\langle u_{\hat{a}}(\mathbf{k})|.$$

This matrix is involutive, unitary and invariant under $U(m)$ ($U(n)$) rotation of the filled (empty) states. Hence $Q_{Bloch} \in \frac{U(m+n)}{U(m)\times U(n)}$ and the Bloch states preserving the energy gap span a topologically non-trivial manifold! Its second homotopy group is $\mathbb{Z}$ which explains the appearance of topologically distinct ground states labeled by an integer k. (Recall that for the fermionic NLσM in class A $Q_{\text{NL}\sigma\text{M}} \in \frac{U(2N)}{U(N)\times U(N)}$.)

Gapless edge-states

At the interface between a topological insulator and an ordinary insulator (such as vacuum) the topological constant has to continuously change from an integer k to 0. But due to its very topological nature this is impossible: You cannot continuously undo such a "knot" tied in the manifold of Bloch states. Therefore, the only possibility is to broaden the manifold by closing the energy gap at the interface. The surface modes living in this region are gapless, in the case of 2D topological insulators chiral (i.e. one way propagating) and have a Dirac-particle like dispersion relation for 3D topological insulators (see figure (3.2)). As their appearance relies on the topological necessity of closing the gap they are robust against disorder ("topologically protected").

Classification and relation to chiral classes

The classification of topological insulators is very similar to the table of random Hamiltonians, appendix I. As stated in 1.7.1 the possible presence of topological insulators can equivalently be deduced from the homotopy groups of the reduced Hamiltonian spaces and NLσM-manifolds respectively. In the latter case the assignment is[2]

$$\text{d-dimensional TI of type} \left\{ \begin{array}{c} \mathbb{Z} \\ \mathbb{Z}_2 \end{array} \right\} \Leftrightarrow \left\{ \begin{array}{c} \pi_d(\mathcal{M}_\sigma) = \mathbb{Z} \\ \pi_{d-1}(\mathcal{M}_\sigma) = \mathbb{Z}_2 \end{array} \right\}. \tag{3.1}$$

The full classification is given in table 3.1. In particular, the chiral symplectic NLσM with a $\mathbb{Z}_2$ - topological term describes the surface states of a possible three dimensional

[1] Translational invariance in the presence of a vector potential can be achieved assuming rational numbers of flux quanta per unit cell.

[2] NLσMs with a WZW-term or a $\mathbb{Z}_2$ topological term can guarantee "non-localizable" boundary states, hence the connection.

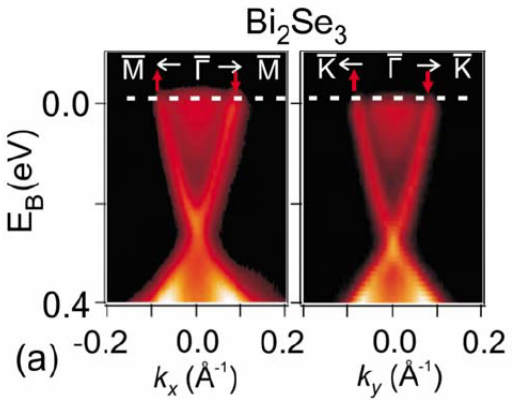

Figure 3.2: Experimental observation of the Dirac-like dispersion relation in the group of M.Z.Hasan [HK10].

Symmetry class	1D TI	2D TI	3D TI
AI	0	0	0
BDI	$\mathbb{Z}$	0	0
BD	$\mathbb{Z}_2$	$\mathbb{Z}$	0
DIII	$\mathbb{Z}_2$	$\mathbb{Z}_2$	$\mathbb{Z}$
AII	0	$\mathbb{Z}_2$	$\mathbb{Z}_2$
CII	$\mathbb{Z}$	0	$\mathbb{Z}_2$
C	0	$\mathbb{Z}$	0
CI	0	0	$\mathbb{Z}$
A	0	$\mathbb{Z}$	0
AIII	$\mathbb{Z}$	0	$\mathbb{Z}$

Table 3.1: Table of one-, two- and three-dimensional topological insulators.

topological insulator of class CII. Unfortunately such a topological insulator has not yet been realized experimentally.
All of the three chiral classes are $\mathbb{Z}$ topological insulators in one dimension. It is the very same topological property, that will be responsible for the metal-insulator transition in two dimensions.

3.1.3 Graphene

One of the most important experimental discoveries in the last decade was, without any doubt, graphene, first isolated by Noveselov, Geim, *et al.* in 2004 [NGM+04].
Graphene is a single layer of graphite. The sp^2-hybridized carbon atoms form a hexagonal lattice and their p_z-orbitals, oriented vertically to the lattice, allow for electronic mobility as they weakly overlap.
Graphene has fascinatingly good conduction properties and shows manifestations of the quantum Hall effect. This being of main interest for applications, graphene's beautiful theoretical description motivates also theorists' interest on it. These and more reasons convinced the Nobel prize committee to assign Novoselov and Geim the 2010 Nobel prize.

Tight-binding model and Dirac electrons

Graphene can be described by a tight-binding approach allowing next-neighbour hopping on a hexagonal lattice, see figure (3.3), left. The spectrum of such a tight-binding model

Figure 3.3: The hexagonal lattice of graphene and its spectrum.

Disorder	Class	Criticality
Vacancies, strong potential impurities	BDI	Gade
Vacancies and random magnetic field	AIII	Gade
$\sigma_3\tau_{1,2}$-disorder	CII	Gade
Dislocations	CI	WZW
Dislocations and random magnetic field	AIII	WZW
Ripples, random magnetic field	$2 \times$ AIII	WZW
Charged impurities	$2 \times$ AII	$\theta = \pi$
Random Dirac mass	$2 \times$ D	$\theta = \pi$
Charged impurities and random magnetic field	$2 \times$ A	$\theta = \pi$

Table 3.2: Types of disorder in graphene which lead to critical behaviour. Adapted from [MEGO10].

is plotted next to it. On account of the sublattice structure of the honeycomb lattice, the model is manifestly chiral similarly to Gade's Hamiltonian in sec. 3.1.1. Furthermore, the band structure of graphene includes two very peculiar points (K,K') per Brillouin zone, at which the conduction and valence band touch each other. In the vicinity of these points, the effective low energy Hamiltonian has Dirac-like form

$$H = v_0 \tau_3 \sigma \cdot \mathbf{k}. \tag{3.2}$$

(τ_3 is the third Pauli-matrix living in the $K - K'$-space and $\sigma = (\sigma_1, \sigma_2)$ the first and second Pauli matrix in the sublattice space.)

Symmetries of disorder in graphene

Depending on the type of disorder, all different symmetry classes can be obtained. Ostrovsky, Gornyi and Mirlin classified all possible kinds of disorder by symmetries of the clean Hamiltonian (3.2) [OGM06],[OGM07],[MEGO10]. All cases in which disorder leads to criticality are summarized in table (3.2). In particular, the shaded rows correspond to classes which are potentially relevant for the present work, as their NLσM allows for $\mathbb{Z}$-vortices. Differently stated, if the disorder in graphene is realized in one of these ways, the Anderson transition can occur as worked out within this diploma thesis.
The complete classification of 2D Dirac Hamiltonians reveals a subdivision of some of the ten Altland-Zirnbauer classes (Bernard and LeClair [BL02]). Why this is so and what the consequences are will be stated in the next section.

3.2 Dirac fermions and relation to topology

Graphene and topological insulators substantially differ from the Gade model: They come along with Dirac fermions (and hence a linear dispersion relation). In this section it will be reviewed, how Dirac fermions evoke topological phenomena in the NLσM.
As stated, Bernard and LeClair [BL02] classified all two-dimensional Dirac Hamiltonians with disorder potential and found a finer categorization than known within the usual Altland-Zirnbauer scheme. To be specific, each of the classes corresponding to the principle chiral models (AIII, DIII and CI) splits up. The authors conjectured that their classification scheme might distinguish systems whose NLσMs include the WZW term from those which do not.
If a WZW term is present in the NLσM of classes AIII and CI, there is an attractive fixed point at which $\sigma = \sigma^{clean} = \frac{4}{\pi}\frac{e^2}{h}$ (see sec. 6.1 and rows 3 to 5 of table (3.2)). This fixed point corresponds to the case, when the disorder in the underlying fermionic theory is of a certain type and therefore the theory exactly solvable. Ostrovsky, Gornyi and Mirlin [OGM06] showed how this occurs:
Consider a disordered system, the free theory being governed by the Hamiltonian (3.2), and the disorder preserving the $H = -\sigma_3 H \sigma_3$-symmetry. Further, because of the Dirac-structure of the Hamiltonian, the current operator follow $\sigma_3 j_x = -j_x \sigma_3 = i j_y$. Then, the Kubo formula for conductivity can be rewritten as

$$\begin{aligned}\sigma_{xx} &= -\frac{1}{\pi}\sum_{\alpha=x,y}\int d^2\left(r-r'\right)\mathrm{tr}\left[j_\alpha \mathcal{G}_R\left(0;\mathbf{r},\mathbf{r}'\right) j_\alpha \mathcal{G}_R\left(0;\mathbf{r}',\mathbf{r}\right)\right] \\ &\propto \left.\frac{\delta^2}{\delta A_\alpha \delta A_\alpha}\right|_{\mathbf{A}=0} \mathcal{Z}\left[\mathbf{A}\right] \propto \left.\frac{\delta}{\delta A_\alpha}\right|_{\mathbf{A}=0}\int \mathrm{tr} j_\alpha \mathcal{G}_R\left[\mathbf{A}\right].\end{aligned}$$

The right-hand side is proportional to the second derivative of the partition function with respect to a constant vector potential $\mathbf{A}$. As the partition function is gauge invariant, it should be independent of such a constant vector potential and $\sigma_{xx} = 0$. However, this argument does not hold for the clean conductivity bubble: $\int d^2k \mathrm{tr} j_\alpha \mathcal{G}_R^{clean}(\mathbf{k})$ is ultraviolet divergent, and a definite regularization scheme will bring the gauge-independence argument to collapse. For this reason, $\sigma = \sigma^{clean}$.
The outlined mechanism, which is responsible for the exactly solvable fermionic theory, is called chiral anomaly: The classical action is both chiral and gauge-invariant, but the quantized theory is not: Whichever regularization scheme one choses, either one preserves only chiral or only gauge symmetry[3].
Dirac fermions allow also for further topological phenomena. Systems which are described by a single-flavour Dirac Hamiltonian always display critical phenomena [MEGO10]. They occur in graphene, in which the disorder does not mix different valleys (long-range disorder). Both WZW-criticality as well as criticality corresponding to a $\theta = \pi$-topological term might appear. A more detailed review exceeds the purpose of this section, however, all cases of single-flavour Dirac fermions are listed in the last four rows of table (3.2).

3.3 The status quo of 2D chiral systems

3.3.1 Gade-Wegner criticality

The NLσM for chiral symmetry classes was first intensively studied by Renate Gade and Franz Wegner [GW91], [Gad93]. It has the following form

$$S\left[Q\right] = \int d^2x \left[\frac{\sigma}{8\pi} tr\left[\nabla Q^{-1}\nabla Q\right] - \frac{c}{8\pi}\left\{tr Q^{-1}\nabla Q\right\}^2\right]. \tag{3.3}$$

[3] ...or none of the two, but this is not a convenient choice.

$$(Q \in \begin{cases} U(N) \\ U(2N)/Sp(2N) \\ U(N)/O(N) \end{cases} \text{for classes} \begin{cases} AIII \\ BDI \\ CII \end{cases} \text{respectively.})$$

As stated above, in classes AIII and CII a WZW term respectively $\mathbb{Z}_2$-topological term might be added.
The first term in the action (3.3) is the kinetic term. $\sigma = \frac{\pi}{2}\sigma_{phys.}$ for class AIII and $\sigma = \frac{\pi}{4}\sigma_{phys.}$ for classes BDI and CII. $\sigma_{phys.}$ is the physical conductivity in units of the inverse Klitzing constant $\frac{e^2}{h}$, its bare value is the Drude conductivity (see also chapter 4). The second term, the "Gade term", appears only in the chiral classes, because the NLσM manifolds allow for traceful generators. Even though it usually does not appear in the direct NLσM derivation, it is generated within renormalization. The physical interpretation of the prefactor is not apparent, however, both the density of states and the scaling of the localization length depend on it [4].

Vanishing β function in perturbative RG: Gade's and Wegner's argument

Another pecularity of chiral systems is the absence of conductivity corrections in perturbative RG. Rewrite Q in (3.3) as $Q = e^{i\frac{\phi}{\sqrt{\mathrm{tr}\mathbf{1}}}}U$ (U is an element of the special submanifold of NLσM manifold and $detQ = e^{i\phi}$). As a functional of U and ϕ the action is

$$S[U,\phi] = \int d^2x \left[\frac{\sigma}{8\pi}\mathrm{tr}\left[\nabla U^{-1}\nabla U\right] + \left(\frac{\sigma + \mathrm{tr}\mathbf{1}c}{8\pi}\right)(\nabla\phi)^2\right]. \tag{3.4}$$

($\mathrm{tr}\mathbf{1} = N$ for classes AIII and CII and $\mathrm{tr}\mathbf{1} = 2N$ for BDI.)
Hence the theory is Gaussian in the phase ϕ and its prefactor is not renormalized.

$$\frac{d}{d\ln L}(\sigma + \mathrm{tr}\mathbf{1}c) = 0.$$

Using this and assuming non-singular β-functions β_σ and β_c in replica limit, it follows that the conductivity corrections vanish in every order of perturbation theory:

$$\begin{array}{lcccl} \frac{d\sigma}{d\ln L} & = & \beta_\sigma(N) = -\mathrm{tr}\mathbf{1}\beta_c(N) & \to & 0, \\ \frac{dc}{d\ln L} & = & \beta_c(N) & \to & \beta_c(0) < \infty. \end{array}$$

Hence, for any σ the system is critical: this is called the critical Gade phase.

3.3.2 Intuitive expectation of a phase transition

Wegner's argumentation and the Gade-Wegner criticality can be applied among others to graphene with vacancies (class BDI, see table (3.2)). Imagine a tight-binding model of graphene on the honeycomb lattice, from which sites are gradually removed, fig. (3.4). It is intuitive to expect two distinct phases: one in which only few vacancies occur (weak disorder, finite conductivity) and another one, where the disorder is strong, many sites removed and the conductivity zero. In between, a phase transition takes place. Numerical works (see section below) indicate that this transition is not the classical percolation transition but the Anderson transition. Gade-Wegner theory does not describe this phase transition.

[4] Due to the absence of conductivity corrections in chiral classes, the density of states and scaling of the localization length are calculated examining the crossover to usual Wigner-Dyson classes.

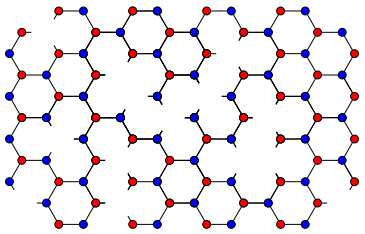

Figure 3.4: The hexagonal lattice of graphene with vacancies.

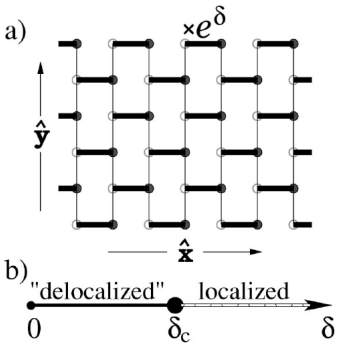

Figure 3.5: (a) The dimerized brickwall lattice. (b) The phase diagram of the system, $\delta_c \approx 1.432$. [MDH02]

3.3.3 Numerical works

Dimerization driving the system away from criticality

In the beginning of the last decade, Motrunich *et al.* [MDH02] examined chiral models with staggered hopping strength and demonstrated the appearance of a localized phase, in addition to confirming Gade's critical phase. [5]
One of the systems considered is the brick wall (honeycomb) lattice, where the random nearest neighbour hopping amplitudes are uniformly distributed in $[0, J_e]$. According to the background dimer pattern, some bonds (thick lines) are different (typically stronger) to others, see fig. (3.5). Here, this is realized taking $J_e = e^{\delta}$ for the thick bonds and $J_e = 1$ for all others. In particular it is argued that such a dimerized situation is a good description for the strong disorder limit.
The system is investigated using the transfer matrix analysis on a strip of width N. The inverse of the smallest, positive Lyapunov exponent of the random matrix product defines the largest localization length $\xi_{max}(N)$. Two qualitative distinct phases can be observed:

- $\xi_{max}(N)$ increases linearly with increasing N. This critical behaviour corresponds to the critical Gade-phase.
- $\xi_{max}(N \to \infty)$ saturates. This corresponds to the localized phase.

Motrunich *et al.* find that for weak dimerization $\delta < \delta_c = 1.432$ the system remains in the critical Gade-phase [6], whereas for larger $\delta > \delta_c$ the states are localized.

[5] There are chiral lattice models, such as the π-flux model and the honeycomb-lattice model with non-negative bonds, which allow for a direct mapping onto the random dimer model on the same lattice.
[6] For the purpose of better distinction, Motrunich *et al.* call the critical phase "delocalized".

Two phases in chiral network models

Marc Bocquet and John Chalker investigated chiral network models [BC03]. A brief review of their results concerning symmetry class AIII follows.
The AIII network model is constructed connecting two copies of the U(1) (class A) network model on their links in the following sense:

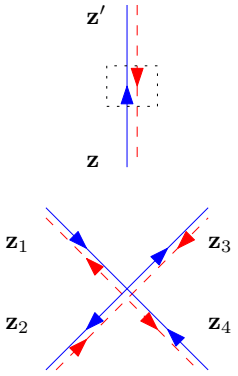

$$\mathbf{z}' = e^{i\phi} \begin{pmatrix} cosh\,(b) & sinh\,(b) \\ sinh\,(b) & cosh\,(b) \end{pmatrix} \mathbf{z}$$

$$\begin{pmatrix} \mathbf{z}_3 \\ \mathbf{z}_2 \end{pmatrix} = \mathbf{1}_2 \otimes \begin{pmatrix} cos\,(\alpha) & -sin\,(\alpha) \\ sin\,(\alpha) & cos\,(\alpha) \end{pmatrix} \begin{pmatrix} \mathbf{z}_1 \\ \mathbf{z}_4 \end{pmatrix}$$

Figure 3.6: Units of Bocquet's and Chalker's chiral network model.

Without mixing ($b = 0$) the two complex valued components of $\mathbf{z}$ describe the usual link amplitudes of two decoupled U(1)-network models.
Randomness is incorporated in the link-depending mixing variable b_l and into the independently random phase ϕ_l. b is Gaussian distributed with zero mean and variance g. The latter is parametrized by γ in the following way: $sin\,(\gamma) = tanh\sqrt{g}$.
The localization length ξ_M is again defined as the inverse of the smallest positive Lyapunov exponent. It was numerically calculated in a quasi one-dimensional system of fixed length L and given width M, node parameter $\alpha \in \left[0, \frac{\pi}{4}\right)$ and disorder strength $\gamma \in \left[0, \frac{\pi}{2}\right]$.
Again the two phases are distinguished analyzing the M-dependence of the ratio $\frac{\xi_M}{M}$. If it approaches a constant value for increasing M, the system is in the critical phase. If the ratio decreases, the states are localized. The phase diagram, fig. 3.7 (right), distinguishes

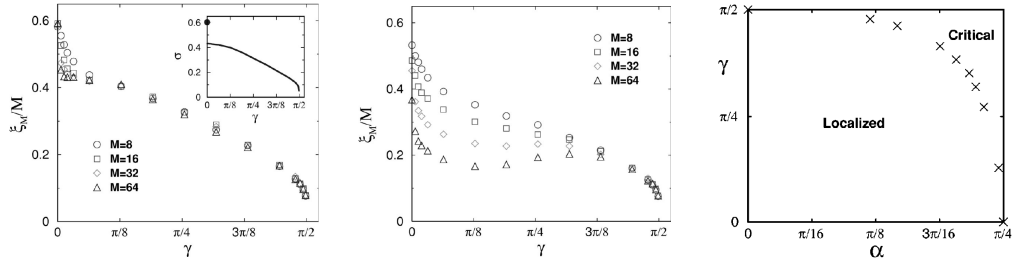

Figure 3.7: Left: $\frac{\xi_M}{M}$ at $\alpha = \frac{\pi}{4}$ as a function of γ. Also for very small γ the critical phase can be observed. Middle: $\frac{\xi_M}{M}$ at $\alpha = \frac{7\pi}{32}$ as a function of γ. The critical phase appears only at higher γ. Right: Phase diagram of the AIII network model in the (α, γ) plane [BC03].

these two phases. The line $\gamma = 0$ corresponds to the two decoupled U(1) submodels, in which the states are localized in the given range of α. In the region of small γ the localized phase can be understood as to be a relic from the A $\rightarrow$ AIII crossover. However, it is a remarkable result, that for any finite variance $g < \infty \Leftrightarrow \gamma < \frac{\pi}{2}$ a localized phase seems to exist. Note that this is well in the quantum regime and that in this model a percolation transition cannot take place. This phase was not described in Gade's and Wegner's NLσM approach.

3.3.4 Controversy

The results exposed in sec.s 3.3.1 - 3.3.3 suggest partly controversial behaviour:

- On the one hand, Gade's and Wegner's argument rules out any kind of conductivity corrections. Within the NLσM approach, there is no evidence suggesting the existence of an insulating phase.
- On the other hand, numerical simulations do predict the existence of a localized phase. This is also what one intuitively expects.

It is the aim of the present work, to resolve this apparent controversy.

Part III

How:

4. Derivation of chiral NLσMs and appearance of the $\mathbb{Z}_2$-topological term

In this chapter the non-linear sigma model for Dirac electrons will be derived. The classes to be considered are the chiral (AIII) and chiral symplectic (CII). Furthermore the crossover between the two is investigated and it will be explained, how within this crossover the WZW term in class AIII mutates to the $\mathbb{Z}_2$-term in class CII.

4.1 Dirac Hamiltonian of classes CII and AIII

The CII -Hamiltonian has to be invariant under the following transformations:

chiral symmetry	$\mathcal{C}: H$	$\rightarrow$	$-U^{-1}HU$		(U unitary),
time reversal	$\mathcal{T}: H$	$\rightarrow$	$V^{-1}H^*V$	$T^2=-\mathbf{1}$	(V unitary),
charge conjugation	$\mathcal{C}\circ\mathcal{T}: H$	$\rightarrow$	$-U^{-1}\left(V^{-1}H^*V\right)U$	$CT^2=-\mathbf{1}$	(U,V from above).

For AIII the latter two symmetries are absent. Following standard convention, $U=\sigma_z$ is chosen. The presence of time reversal and particle hole symmetry require the Hamiltonian to have a definite structure in a further subspace [1]. This substructure is determined by the matrix V, which in turn is constrained by the above symmetry operations. One possible choice is $V=\mathbf{1}_\sigma\otimes\tau_y$. Then,

$$H=\begin{pmatrix} 0 & 0 & p_-+A & V \\ 0 & 0 & -V^* & -p_++A^* \\ p_++A^\dagger & -V^T & 0 & 0 \\ V^\dagger & -p_-+A^T & 0 & 0 \end{pmatrix}. \tag{4.1}$$

(The potentials A,V incorporate the randomness, and an abbreviated notation for momentum operators is used: $p_\pm := p_x \pm ip_y$.)
H is diagonal in the space of the N replicas, whereas the disorder potentials mix the n fermionic flavours[2]. In contrast to usual Wigner-Dyson ensembles, in chiral classes it is not necessary to keep the advanced/retarded subspace: The Green's functions are related by chiral symmetry:

$$\mathcal{G}^A=-\sigma_z\mathcal{G}^R\sigma_z.$$

[1] U is diagonal in this subspace.

[2] In a minimal model of only one type of fermions, A and V are simple complex numbers, but in a more general ($n>1$) situation they are matrix-valued.

Connection to Cartan's symmetric space

Invariance under $\mathcal{T}$ requires $\tau_y (iH) + (iH)^T \tau_y = 0 \Leftrightarrow iH \in \mathfrak{sp}(4nN)$. Furthermore, chiral symmetry divides out the block diagonal generators $(\mathfrak{sp}(2nN) \times \mathfrak{sp}(2nN))$ and therefore

$$iH \in \frac{\mathfrak{sp}(4nN)}{\mathfrak{sp}(2nN) \times \mathfrak{sp}(2nN)}.$$

Fermionic action and crossover to AIII

Conveniently introducing the $8nN$ Grassmann-fields [3] allows to rewrite the zero-energy action as

$$\begin{aligned} S^{\mathrm{CII}} \equiv S &= -\int d^2x \begin{pmatrix} \bar{\Psi}^T_{I1} & \Psi^T_{I1} & -\bar{\Psi}^T_{II2} & -\Psi^T_{II2} \end{pmatrix} H \begin{pmatrix} \Psi_{I2} \\ -\bar{\Psi}_{I2} \\ -\Psi_{II1} \\ \bar{\Psi}_{II1} \end{pmatrix} \\ &= -\int d^2x \begin{pmatrix} \bar{\Psi}^T_I & \Psi^T_I \end{pmatrix} \begin{pmatrix} V & -p_- - A \\ -p_+ + A^* & V^* \end{pmatrix} \begin{pmatrix} \bar{\Psi}_{II} \\ \Psi_{II} \end{pmatrix}. \end{aligned} \tag{4.2}$$

In this step both manifest chirality and hermiticity were lost. Expression (4.2) will however be the starting point for the whole NLσM derivation.
Furthermore the crossover to AIII symmetry class is easily performed. Set $V = 0$, then

$$S^{\mathrm{AIII}} = S_{V=0} = -\int d^2x \, \bar{\Psi}^T \begin{pmatrix} 0 & -p_- - A \\ -p_+ - A^\dagger & 0 \end{pmatrix} \Psi. \tag{4.3}$$

This is the usual AIII-action for Dirac fermions subjected to a random vector potential (more precisely two copies of it, as $A = A \otimes \mathbf{1}_\tau$ in contrast to the usual case). Both chirality and hermiticity are restored.

Rotation of fermionic fields

S^{CII} and S^{AIII} are invariant under the following global rotations of Grassmann-fields :

$$\begin{aligned} \text{CII:} \quad & \begin{cases} \Psi \;\to\; \begin{pmatrix} U & 0 \\ 0 & U^{-T} \end{pmatrix} \Psi, \\ \bar{\Psi} \;\to\; \begin{pmatrix} U & 0 \\ 0 & U^{-T} \end{pmatrix} \bar{\Psi}, \end{cases} \\ \text{AIII:} \quad & \begin{cases} \Psi \;\to\; \begin{pmatrix} U & 0 \\ 0 & W \end{pmatrix} \Psi, \\ \bar{\Psi} \;\to\; \begin{pmatrix} W^{-T} & 0 \\ 0 & U^{-T} \end{pmatrix} \bar{\Psi}, \end{cases} \end{aligned} \qquad \text{with } U, W \in GL(2N). \tag{4.4}$$

Hence, the presence of the random potential V forces $W = U^{-T}$.

[3] The following notation is used: $\Psi^T = (\Psi^T_I, \Psi^T_{II}) = (\Psi^T_{I,1}, \Psi^T_{I,2}, \Psi^T_{II,1}, \Psi^T_{II,2})$ and equivalently for $\bar{\Psi}^T$. Roman indices $_{I,II}$ refer to the σ-space, Arabic numbers $_{1,2}$ to the τ-subspace of e.g. Ψ_I.

Randomness of potentials, SCBA and Drude conductivity

Gaussian white-noise statistics for each of the entries A, V of the quaternionic random potential is assumed:

$$\begin{aligned} \langle A\rangle = \langle A^*\rangle = \langle V\rangle = \langle V^*\rangle &= 0, \\ \langle A^\dagger_{\alpha\beta}(\mathbf{r})\, V_{\gamma\delta}(\mathbf{r}')\rangle = \langle A_{\alpha\beta}(\mathbf{r})\, V^\dagger_{\gamma\delta}(\mathbf{r}')\rangle = \langle A_{\alpha\beta}(\mathbf{r})\, V_{\gamma\delta}(\mathbf{r}')\rangle &= 0, \\ \langle A_{\alpha\beta}(\mathbf{r})\, A^\dagger_{\gamma\delta}(\mathbf{r}')\rangle = \langle A_{\alpha\beta}(\mathbf{r})\, A^*_{\delta\gamma}(\mathbf{r}')\rangle &= \frac{\pi\alpha}{n}\delta_{\alpha\delta}\delta_{\beta\gamma}\delta(\mathbf{r}-\mathbf{r}'), \\ \langle V_{\alpha\beta}(\mathbf{r})\, V^\dagger_{\gamma\delta}(\mathbf{r}')\rangle = \langle V_{\alpha\beta}(\mathbf{r})\, V^*_{\delta\gamma}(\mathbf{r}')\rangle &= \frac{\pi\beta}{n}\delta_{\alpha\delta}\delta_{\beta\gamma}\delta(\mathbf{r}-\mathbf{r}'). \end{aligned} \tag{4.5}$$

(Greek indices ($\alpha = 1, ..., n$) are used for flavour and $\langle ...\rangle$ denotes average in disorder.)
The crossover from CII to AIII, being performed as $V \to 0$, is equivalently taken as $\beta \to 0$. Consequently, soft modes which are connected via V-impurity lines disappear.

Self-consistent Born approximation

Self-consistent Born approximation (recall diagram (1.6) in sec. 1.5.2) leads to the following integral:

$$\begin{aligned} 1 &= \pi(\alpha+\beta)\int \frac{d^2p}{(2\pi)^2}\frac{1}{p^2+\gamma^2} \\ &\doteq \frac{\alpha+\beta}{2} ln\left(\frac{\Lambda}{\gamma}\right) \Leftrightarrow \gamma = \Lambda e^{-\frac{1}{\frac{\alpha+\beta}{2}}}. \end{aligned} \tag{4.6}$$

(Λ is the ultraviolet energy cut-off.)
For weak disorder, the imaginary self-energy γ is proportional to the scattering rate, i.e. to the inverse mean-free path.

Drude conductivity

The zero-temperature Kubo-formula for DC-conductivity is

$$\sigma_{xx} = -\frac{1}{2\pi}\int (\mathbf{dp})\,\mathrm{tr}\left(\hat{j}_x\left[\mathcal{G}^R(\mathbf{p}) - \mathcal{G}^A(\mathbf{p})\right]\right)^2,$$

and equivalently for σ_{yy}. $\hat{j}_\mu := \frac{\delta S}{\delta A_\mu}$ is the current operator (and A_μ is the vector potential introduced by minimal substitution).
The Drude conductivity is obtained calculating $\sigma_{xx} = \sigma_{yy} = \sigma$ on SCBA-level:

$$\begin{aligned} \sigma &= -\frac{1}{2\pi}\int (\mathbf{dp}) \sum_{\tau,\sigma,\text{flavour}} \frac{-4\gamma^2}{\mathbf{p}^2+\gamma^2} \\ &= \frac{2n}{\pi^2}. \end{aligned} \tag{4.7}$$

In the present system of units the elementary charge is set $e = 1$ as well as the reduced Planck's constant $\hbar = 1$. Restoring them yields the extra factor $\frac{e^2}{\hbar}$ in (4.7). Then, in units of the inverse Klitzing constant

$$\sigma = \frac{4n}{\pi}\frac{e^2}{h}. \tag{4.8}$$

For $n = 1$ the Hamiltonian (4.1) is a 4×4 matrix, describing Graphene for a certain kind of disorder (2 (spin) $\times$ 2 (valleys) = 4). In this case $\sigma = \frac{4}{\pi}\frac{e^2}{h}$ [4].

[4] This is in accordance to experiment and the theoretical works [OGM06] exposed in sec. 3.2.

4.2 Effective action and Hubbard-Stratonovich transformation

The potential part in (4.2) can be rewritten as

$$S^{dis} = \int d^2x \ \mathrm{tr}^{\sigma,\mathrm{flavour}} \begin{pmatrix} V & -p_- - A \\ -p_+ + A^* & V^* \end{pmatrix} \mathsf{M}, \tag{4.9}$$

where $\mathsf{M} = \sum_{\tau,\mathrm{replica}} \begin{pmatrix} \bar{\Psi}_{II} \\ \Psi_{II} \end{pmatrix} \begin{pmatrix} \bar{\Psi}_I^T & \Psi_I^T \end{pmatrix}$.

Average over disorder gives the effective four-point interaction

$$\begin{aligned} S^{(4)} &= -\frac{\pi}{n} \int d^2x \ \beta \ \mathrm{tr}^{\sigma,\mathrm{fl.}} \ \mathsf{M}_{11}\mathsf{M}_{22}^T - \alpha \ \mathrm{tr}^{\sigma,\mathrm{fl.}} \ \mathsf{M}_{21}\mathsf{M}_{12}^T \\ &= -\frac{\pi}{n} \int d^2x \ \beta \ \mathrm{tr}^{\tau,\mathrm{replica}} \ \mathsf{V}\mathsf{W}^T + \alpha \ \mathrm{tr}^{\tau,\mathrm{replica}} \ \mathsf{V}\mathsf{W} \end{aligned} \tag{4.10}$$

with $\mathsf{V}_{ab} := \sum_{flavour} \Psi_{II,a}\bar{\Psi}_{II,b}$ and $\mathsf{W}_{ab} := -\sum_{flavour} \Psi_{I,a}\bar{\Psi}_{I,b}$.
These last matrices are decoupled with four real Hubbard-Stratonovich matrix-fields $R_{1,2}, S_{1,2} \in \mathbb{R}^{2N\times 2N}$. It is convenient to use the definitions

$$\begin{aligned} Q_1^{\pm} &= S_1 \pm iR_1, \quad Q_2^+ = S_2^T + iR_2^T, \\ & \qquad\quad Q_2^- = S_2 - iR_2. \end{aligned}$$

Then the action, being quadratic in both Hubbard-Stratonovich fields and Grassmann fields allows to integrate out the fermions:

$$\begin{aligned} S^{HS} &= \int d^2x \ \frac{n\gamma^2}{\pi\beta} \ \mathrm{tr} \ Q_1^+ {Q_1^-}^T + \frac{n\gamma^2}{\pi\alpha} \ \mathrm{tr} \ Q_2^+Q_2^- \\ S^{(2)} &= \int d^2x \ \bar{\Psi}^T \begin{pmatrix} i\gamma\left(Q_1^+ + Q_2^+\right) & p_- \\ p_+ & i\gamma\left(Q_1^- + Q_2^-\right) \end{pmatrix} \Psi \\ &\to -n \int d^2x \ \mathrm{tr} \ \ln \begin{pmatrix} i\gamma\left(Q_1^+ + Q_2^+\right) & p_- \\ p_+ & i\gamma\left(Q_1^- + Q_2^-\right) \end{pmatrix}. \end{aligned} \tag{4.11}$$

Within the total action $S = S^{HS} + S^{(2)}$ the crossover from CII to AIII can be seen analogously to the fermionic actions (4.2) and (4.3). Sending the disorder potential $V \to 0$ implies sending its disorder strength $\beta \to 0$. Then the "mass" $\frac{n\gamma^2}{\pi\beta}$ of the fields $Q_1^{\pm}$ becomes infinite and their effect in (4.11) vanishes. Only the Hubbard-Stratonovich fields $Q_2^{\pm}$ are left: This corresponds to the AIII situation. It is worth to emphasize the structural difference between the massive terms $\frac{n\gamma^2}{\pi\beta}$ tr $Q_1^+{Q_1^-}^T$ and $\frac{n\gamma^2}{\pi\alpha}$ tr $Q_2^+Q_2^-$. The transposition operation in the $Q_1^{\pm}$-term will eventually constrain the fields to the smaller CII NLσM manifold.

4.3 Saddle point approximation

Variation of the total action yields the following saddle point equations for uniform fields $Q^{\pm}_{1,2}$:

$$\begin{aligned}
Q_1^{+T} &= \pi\beta \int (\mathbf{dp}) \frac{1}{\mathbf{p}^2 + \gamma^2 \left(Q_1^+ + Q_2^+\right)\left(Q_1^- + Q_2^-\right)} \left(Q_1^+ + Q_2^+\right), \\
Q_1^{-T} &= \pi\beta \int (\mathbf{dp}) \frac{1}{\mathbf{p}^2 + \gamma^2 \left(Q_1^- + Q_2^-\right)\left(Q_1^+ + Q_2^+\right)} \left(Q_1^- + Q_2^-\right), \\
Q_2^{+} &= \pi\alpha \int (\mathbf{dp}) \frac{1}{\mathbf{p}^2 + \gamma^2 \left(Q_1^+ + Q_2^+\right)\left(Q_1^- + Q_2^-\right)} \left(Q_1^+ + Q_2^+\right), \\
Q_2^{-} &= \pi\alpha \int (\mathbf{dp}) \frac{1}{\mathbf{p}^2 + \gamma^2 \left(Q_1^- + Q_2^-\right)\left(Q_1^+ + Q_2^+\right)} \left(Q_1^- + Q_2^-\right).
\end{aligned}$$

Manifold of equivalent saddle points

The saddle point equations are solved equivalently to SCBA by

$$\begin{aligned}
Q_1^{\pm}\big|_{\mathrm{SP}} &= \frac{\beta}{\alpha+\beta}\mathbf{1}_{\tau,N}, \\
Q_2^{\pm}\big|_{\mathrm{SP}} &= \frac{\alpha}{\alpha+\beta}\mathbf{1}_{\tau,N}.
\end{aligned}$$

However, invariance of the action under global rotations (4.4) implies that any of the following rotated saddle point matrices solves the equations just as well

$$\begin{aligned}
&\left.\begin{aligned} Q^+_{1,2}\Big|_{\mathrm{SP}} &\to U^T\, Q^+_{1,2}\Big|_{\mathrm{SP}}\, U \\ Q^-_{1,2}\Big|_{\mathrm{SP}} &\to U^{-1}\, Q^-_{1,2}\Big|_{\mathrm{SP}}\, U^{-T} \end{aligned}\right\} \quad \text{CII}, \\
&\left.\begin{aligned} Q^+_{1,2}\Big|_{\mathrm{SP}} &\to W^{-1}\, Q^+_{1,2}\Big|_{\mathrm{SP}}\, U \\ Q^-_{1,2}\Big|_{\mathrm{SP}} &\to U^{-1}\, Q^-_{1,2}\Big|_{\mathrm{SP}}\, W \end{aligned}\right\} \quad \text{AIII}.
\end{aligned} \tag{4.12}$$

(With $U, W \in GL\,(2N)$.)
As $Q^{\pm}_{1,2} \propto \mathbf{1}$ at the saddle point, rotations $U \in O\,(2N)$ for class CII and $U = W \in GL\,(2N)$ for AIII belong to the stabilizer. The generated manifold hence is $GL\,(2N)\,/O\,(2N)$ and $GL\,(2N) \times GL\,(2N)\,/GL\,(2N) \simeq GL\,(2N)$ for classes CII and AIII respectively. The convergence requirement restricts the saddle-point manifold to its maximal compact submanifold, on which the field theory of the NLσM is defined. It is

$$\begin{aligned}
&\frac{U\,(2N)}{O\,(2N)} \quad \text{for} \quad \text{CII}, \\
&U\,(2N) \quad \text{for} \quad \text{AIII}.
\end{aligned}$$

4.4 NLσM of class AIII and WZW term

At the saddle point, the action of Hubbard-Stratonovich fields has pure "trace-log"-form

$$S^{\mathrm{SP}} = -n \int d^2x \ \mathrm{tr} \ln \begin{pmatrix} i\gamma Q & p_- \\ p_+ & i\gamma Q^{-1} \end{pmatrix}, \tag{4.13}$$

where $Q \in U\,(2N)$ for class AIII.
It is known from non-abelian bosonization technique [Wit84] that the low-energy bosonic

theory corresponding to Dirac electrons includes a WZW term. The AIII NLσM of Dirac electrons in a random vector potential is also a bosonized theory which indeed includes a WZW term. Altland *et al.* obtained this WZW term from direct gradient expansion of the above action (4.13) with an appropriate regularization scheme [ASZ02]. The $U(2N)$-NLσM-action is

$$\begin{aligned} S[Q] &= \frac{\sigma}{32}\int d^2x\ \mathrm{tr}\nabla Q^{-1}\nabla Q - \frac{c}{32}\int d^2x\ \left[\mathrm{tr}\left(Q^{-1}\nabla Q\right)\right]^2 \\ &+ i\frac{k}{12\pi}\int d^2x\ \int_0^1 ds\ \epsilon_{\mu\nu\lambda}\mathrm{tr}\left(Q^{-1}\partial_\mu Q\right)\left(Q^{-1}\partial_\nu Q\right)\left(Q^{-1}\partial_\lambda Q\right). \end{aligned} \tag{4.14}$$

The second term ("Gade term") appears in RG or as a result of integrating out the massive modes.
The gradient expansion yields a prefactor $\frac{n}{8\pi} = \frac{\sigma}{32}$ and $\sigma = \frac{4n}{\pi}$ is the Drude conductivity of the present model in units of $\frac{e^2}{h}$. It is calculated in sec. 4.1, eq. (4.7)

WZW-level and number of flavours

The derivation of the WZW term in the work by Altland *et al.* was performed for one flavour. The outcome was a WZW term with WZW-level $k = 1$. For the above NLσM the whole action was multiplied by the number n of flavours, yielding the Drude conductivity as the prefactor of the kinetic term $\frac{n}{8\pi} = \frac{\sigma}{32}$. In particular, multiplying Altland's *et al.* WZW term with n, leads to eq. (4.14) with n instead of k. In this sense, the WZW-level k equals the number of flavours n ($k = n \in \mathbb{Z}$).
If the NLσM was derived for a $2n \times 2n$ Hamiltonian $H = -(p + A)_\mu \sigma_\mu$, the prefactor $\frac{n}{8\pi}$ of the kinetic term would be unchanged (but then $\sigma = \frac{2n}{\pi}$ and $Q \in U(N)$).
In particular, $\frac{n}{8\pi}$ is the correct prefactor displaying the fixed point $\sigma = \sigma^{clean}$ of the WZW-model, see sec.s 3.2 and 6.1.

4.5 NLσM of class CII and $\mathbb{Z}_2$-topological term

Again, at the saddle point, the action of Hubbard-Stratonovich fields has the form (4.13), with $Q \in \frac{U(2N)}{O(2N)}$ for class CII. Performing gradient expansion of the real part of the action yields the kinetic term:

$$S^{kin} = \int d^2x\ \frac{\sigma}{32}\mathrm{tr}\nabla Q^{-1}\nabla Q.$$

However, it is generally not known how and when the $\mathbb{Z}_2$-topological term arises and how a local form of it looks like.

AIII - CII crossover

In the following, it will be shown that for CII-Dirac electrons the $\mathbb{Z}_2$-topological term is present and it can be seen as a descendant of the AIII WZW term. To this end, a detour will be taken: The AIII-theory will be weakly perturbed by the disorder potential V (4.1). In this sense the $\frac{\pi\beta}{n}$-term in the effective fermionic four-point action (4.10) is evaluated at the AIII-saddle point where

$$\left\langle \Psi\bar{\Psi}^T \right\rangle = \frac{1}{\mathbf{p}^2 + \gamma^2}\begin{pmatrix} -i\gamma Q^{-1} & p_- \\ p_+ & -i\gamma Q \end{pmatrix} + \mathcal{O}(\nabla Q).$$

The matrix structure of the correlator reflects the spin-space, which will be denoted by Roman numbers I,II. Further, the Green's function is diagonal in flavour space (Greek letters $\alpha = 1, ..., n$) and its non-trivial structure in τ and replica space is incorporated in

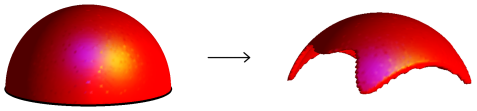

Figure 4.1: The image of the map from a 3-hemisphere onto $U(N)$ may have arbitrary (non-integer) volume (in units of the volume of $\mathbb{S}^3$).

$Q \in U(2N)$ (miniscule Latin letters).
Using Wick's theorem

$$\begin{aligned}\langle S_\beta \rangle &= -\frac{\pi\beta}{n}\int d^2x\ \left\langle \Psi_{II,a,\alpha}\bar{\Psi}_{II,b,\alpha}\bar{\Psi}_{I,b,\beta}\Psi_{I,a,\beta}\right\rangle \\ &= -\frac{\pi\beta}{n}\int d^2x\ \frac{\mathbf{p}^2 2Nn}{(\mathbf{p}^2+\gamma^2)^2} - n\frac{-i\gamma}{\mathbf{p}^2+\gamma^2}Q_{ab}\frac{-i\gamma}{\mathbf{p}^2+\gamma^2}Q^{-1}_{ab} \\ &\doteq \mu^2\int d^2x\ \mathrm{tr}\left[1-Q^TQ^{-1}\right].\end{aligned}$$

The symbol $\doteq$ denotes that a term $N\times$ const. was dropped, as well as all derivatives of Q. An effective mass has been introduced $\mu^2 := \frac{\sigma\pi^2\beta}{8n} \geq 0$ (equality for $\beta = 0$).
The AIII-WZW-action including the effective perturbation is

$$\begin{aligned}S[Q] &= \frac{\sigma}{32}\int d^2x\ \mathrm{tr}\nabla Q^{-1}\nabla Q - \frac{c}{32}\int d^2x\ \left[\mathrm{tr}\left(Q^{-1}\nabla Q\right)\right]^2 \\ &+ \mu^2\int d^2x\ \mathrm{tr}\left[1-Q^TQ^{-1}\right] \\ &+ i\frac{k}{12\pi}\int d^2x\ \int_0^1 ds\epsilon_{\mu\nu\lambda}\mathrm{tr}\left(Q^{-1}\partial_\mu Q\right)\left(Q^{-1}\partial_\nu Q\right)\left(Q^{-1}\partial_\lambda Q\right). \qquad (4.15)\end{aligned}$$

It is important to emphasize that

$$\mathrm{tr}\left[1-Q^TQ^{-1}\right] = \frac{1}{2}\mathrm{tr}\left[\left(Q-Q^T\right)\left(Q-Q^T\right)^\dagger\right] \geq 0.$$

Unitarity of Q was used. Here, equality is achieved if and only if $Q = Q^T$.
Accordingly, perturbing the AIII-theory with the (class CII)-potential V effectively assigns a mass to the antisymmetric modes in $U(2N)$. On large distance scales $d \gg \mu^{-1}$ (i.e. large β) only the symmetric $\frac{U(2N)}{O(2N)}$-fields will contribute and the model has become the CII-NLσM.

Mutation of WZW term to $\mathbb{Z}_2$-term

It has been stressed in the section on WZW terms 1.15, that the WZW term itself is not quantized as it measures the volume covered by the image of a hemisphere (figure 4.1). However, when the AIII NLσM is perturbed by the mass term $\mu^2\int d^2x\ \mathrm{tr}\left[1-Q^TQ^{-1}\right]$, the situation changes: On the boundary of the 3-hemisphere, i.e. on the physical space, only the unitary matrices which are symmetric are not suppressed. In the topologically relevant subgroup of $U(N)$ (this is $SU(2) \simeq \mathbb{S}^3$) the symmetric matrices form a hyperequator, a 2-sphere[5].

[5] $SU(2) \ni Q = a_0 + ia_\mu\sigma_\mu$ with $\sum_{\mu=0}^3 a_\mu^2 = 1$ and σ_μ are the Pauli matrices. Requiring symmetry sets $a_2 = 0$ (Q lies on an equator) and $a_0^2 + a_1^2 + a_3^2 = 1$, which is $\mathbb{S}^2$.

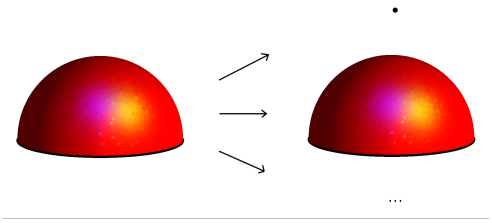

Figure 4.2: The mass term pushes the image of the boundary of the 3-hemisphere onto the equator of $SU(2)$. These mappings cover the 3-sphere a half-integer number of times.

The effect of the mass-term is incorporated into boundary conditions for the extended unitary Q-field:

$$Q(\mathbf{x}, 0) = \mathbf{1} \text{ and } Q(\mathbf{x}, 1) = Q(\mathbf{x}) = Q^T(\mathbf{x}).$$

Now, mappings where an arbitrary part of the 3-sphere is covered are not allowed anymore. As the boundary of the image of the hemisphere lies on the equator of $SU(N)$, the WZW term measures a volume which is a half integer times the volume of the 3-sphere (see fig. (4.2)). In this sense

$$i\, S_{WZ}|_{Q(\mathbf{x})=Q^T(\mathbf{x})} = i\pi N[Q] \text{ and } N \in \mathbb{Z}.$$

However, any $N[Q] + 2l$, $l \in \mathbb{Z}$ leads to the same result as $N[Q]$. Consequently, the AIII - WZW term becomes a $\mathbb{Z}_2$-topological term when the crossover from AIII to CII is taken. A mathematical proof for the topological quantization of the WZW-term with the indicated boundary conditions can be found in appendix A. There, an examplary $N[Q] = 1$ configuration is also discussed, completing the above argumentation.
The total CII NLσM-action is

$$S[Q] = \frac{\sigma}{32}\int d^2x\ \mathrm{tr}\nabla Q^{-1}\nabla Q - \frac{c}{32}\int d^2x\ \left[\mathrm{tr}\left(Q^{-1}\nabla Q\right)\right]^2 + i\pi N[Q]. \tag{4.16}$$

Again $\sigma = \frac{4n}{\pi}\frac{e^2}{h}$ is the Drude conductivity, the Gade term has already been introduced and $N[Q] = 0, 1$ reflects the $\mathbb{Z}_2$-topological term, which is present due to the arguments exposed above.

5. Quantum corrections to conductivity

The content of this chapter is twofold: First, it will be explained, how the renormalization procedure is precisely performed. Second, the perturbative RG-equations for the two parameter (σ,c)-scaling are rederived in accordance with [GW91].

5.1 Derivation of renormalized coupling constants

As has been exposed in sec.s 3.3.1 and 4, the bare chiral NLσM has the form

$$S_0[Q] = \int d^2x \left\{ \frac{\sigma_0}{8\pi} \mathrm{tr}\left[\nabla Q^{-1} \nabla Q\right] - \frac{c_0}{8\pi}\left[\mathrm{tr} Q^{-1}\nabla Q\right]^2 + \frac{\sigma_0}{8\pi}\frac{m^2}{4}\mathrm{tr}\left[Q - Q^{-1}\right]^2 \right\}. \quad (5.1)$$

In particular, σ_0 and c_0 are the bare coupling constants[1]. As stressed, their connection to the classical Drude conductivity is $\sigma_0 = \frac{\pi}{2}\sigma_{Drude}$ for class AIII and $\sigma_0 = \frac{\pi}{4}\sigma_{Drude}$ for classes BDI and CII (see sec. 3.3.1). It is the aim of renormalization group treatment to understand how the scale-dependence of the coupling constants is generated by the critical quantum fluctuations of $Q(\mathbf{x})$.
To this end, short-scale (i.e. fast) fluctuations will be averaged out and incorporated into the renormalized coupling constants. Within this work, the separation between fast and slow fields is achieved introducing the mass term in the action (5.1). The modes to be integrated out are subjected to this mass term and effectively, only those with momenta $m \lesssim |p| < \Lambda$ (i.e. $|p|$ "fast") contribute. m^{-1} hence plays the role of the running scale.

5.1.1 Technical description and renormalized coupling constants

The detailed derivation of the renormalized coupling constants is given in appendix C. Here only a summary is given as well as a motivation for this procedure, see next section 5.1.2.
As mentioned, the Q-field is divided into slow (background field) and fast contributions:

$$Q \to U^{-1}QV \ (Q \text{ fast}; U, V \text{ slow}). \quad (5.2)$$

For classes BDI and CII $V = \sigma_y U^{-T}\sigma_y$ and $V = U^{-T}$ respectively.
The action splits up into three parts: one for the slow fields, one for the fast ones and interaction terms. The exponent of the latter is expanded to second order in gradients of slow fields and reexponentiated into the renormalized action.
This way correction terms of the following types are obtained:

[1] Note the difference to the way the coupling constants were defined in ch. 4.

- "diamagnetic": $\int d^2x \left\langle \mathrm{tr}\left[Q^{-1}\left[\nabla\,(\mathrm{slow})\right]Q\left[\nabla\,(\mathrm{slow})\right]\right] - \left[\nabla\,(\mathrm{slow})\right]^2 \right\rangle$,
- "paramagnetic": $\int d^2x d^2x' \left\langle \mathrm{tr}\left[\left(Q^{-1}\nabla Q\right)\left[\nabla\,(\mathrm{slow})\right]\right]_x \mathrm{tr}\left[\left(Q^{-1}\nabla Q\right)\left[\nabla\,(\mathrm{slow})\right]\right]_{x'} \right\rangle$.

The renormalized coupling constants are calculated within background field formalism [Pol75], [Pru87a]. Within this approach, exponential parametrization is used for slow fields U, V. The Goldstone bosons associated to each of the generators are considered one by one and their gradient is assumed to be constant on the short length-scale of the fast fields.
This way the coupling constant of each Goldstone mode is renormalized. For the $U(1)$-Goldstone boson the coupling constant is $(\sigma + \mathrm{tr}1c)$, for all others σ. Now, the corrections to σ (which were obtained for all modes independently) are averaged over generators using the Fierz identities (see appendix B).
Eventually, the diamagnetic term is evaluated with the help of Ward Identities. These can be obtained considering the stabilizer modes, again one by one (see appendix C.2, eq. (C.4)). Averaging over generators of the stabilizer yields a relation that allows to replace the diamagnetic term.
The renormalized coupling constants are

$$\begin{aligned}\sigma &= \sigma_0 + \frac{1}{\mathrm{Vol}}\int d^2x d^2x' \, \frac{\sigma_0^2}{8\pi}\frac{1}{\mathrm{tr}\mathbf{1}\; dim\,[S\mathcal{M}]} \\ &\quad \left\{\mathrm{tr}\mathbf{1}\left\langle \mathrm{tr}\left[\left(Q^{-1}\nabla Q\right)_x\left(Q^{-1}\nabla Q\right)_{x'}\right]\right\rangle - \left\langle \mathrm{tr}\left[\left(Q^{-1}\nabla Q\right)_x\right]\mathrm{tr}\left[\left(Q^{-1}\nabla Q\right)_{x'}\right]\right\rangle\right\}, \end{aligned} \tag{5.3}$$

$$\begin{aligned} c &= c_0 + \frac{1}{\mathrm{Vol}}\int d^2x d^2x' \\ &\quad \frac{\sigma_0^2}{8\pi}\frac{-1}{\mathrm{tr}\mathbf{1}\; dim\,[S\mathcal{M}]}\left\langle \mathrm{tr}\left[\left(Q^{-1}\nabla Q\right)_x\left(Q^{-1}\nabla Q\right)_{x'}\right]\right\rangle \\ &\quad + \left[\frac{\sigma_0^2}{8\pi}\frac{dim\,[\mathcal{M}]}{(\mathrm{tr}\mathbf{1})^2\; dim\,[S\mathcal{M}]} + \frac{2\sigma_0 c_0}{\mathrm{tr}\mathbf{1}\; 8\pi} + \frac{c_0^2}{8\pi}\right]\left\langle \mathrm{tr}\left[\left(Q^{-1}\nabla Q\right)_x\right]\mathrm{tr}\left[\left(Q^{-1}\nabla Q\right)_{x'}\right]\right\rangle. \end{aligned} \tag{5.4}$$

$\mathcal{M}$ denotes the NLσM manifold and $S\mathcal{M}$ its special submanifold. The manifolds and their dimensions are

	$S\mathcal{M}$	$dim\,[S\mathcal{M}]$	$\mathrm{tr}\mathbf{1}$
AIII	$SU(N)$	N^2-1	N
BDI	$\frac{SU(2N)}{Sp(2N)}$	$2N^2-N-1$	$2N$
CII	$\frac{SU(N)}{O(N)}$	$\frac{N^2+N-2}{2}$	N

5.1.2 Why background field formalism and mass term regularization?

In the thesis at hand, renormalized coupling constants are derived using background-field formalism. As mentioned, this method was also applied by Pruisken in context of the field theory of the integer quantum Hall effect.

For class AIII the derivation of renormalized coupling constants was performed also in another way. Averaging over the gauge group $U(N)$ (on group level, not on generator level) the same renormalized coupling constants were derived.

Mass term regularization

The mass term introduced in eq. (5.1) is a way of regularizing the infrared singularity of the fast modes. Why was such a regularization introduced?
In many areas of physics, improper regularization methods come along with unwanted artefacts. For example, in high energy physics, cut-off regularization destroys gauge invariance. Therefore, dimensional regularization is widely used.
In the present work, something similar occurs: The RG-treatment of vortex-interactions produces a non-local term in the action if cut-off regularization is used. In particular, this non-local term couples also the smooth (i.e. non-vortex) parts of Q.
Using the Yukawa-like mass term regularization these terms do not appear.
How can the difference between regularization schemes be understood? The most natural infrared regularization for field theories describing a metal would be a finite sample with given boundary conditions and $m \to 0$. Taking now the thermodynamic limit means having interchanged $\lim_{TD}$ and $\lim_{m\to 0}$. Commutation of the two limits might have drastic effects, if the boundary conditions of the finite sample are not subtly chosen.
In this work, the boundary conditions allow the Q-field to vary only within a specific area $\mathcal{V}$ and require the trivial vacuum state $Q = \mathbf{1}$ outside this region. This is equivalent to mass term regularization [Pru87a].
The vortex-vortex correlations decay as a power-law. This slow decay eventually produces the non-local interaction of slow modes when an inappropriate regularization scheme is used. However, the mass term ensures vortex-vortex-correlations to decay exponentially on the length-scale of slow modes and locality is preserved.

Background field formalism

The background field formalism is a way to implicitly translate the Kubo formulae in NLσM language. During the year of working on the subject of this thesis, also different methods were applied. In particular, it has been tried to translate the fermionic Kubo formulae directly into Q-field language. The motivation was to have a more physical picture of how the conductivity σ is renormalized. These attempts failed. Chiral anomaly requested a very delicate treatment and it turned out that the background field method was a possibility to circumvent those problems.
In this approach the gradients of the Goldstone and stabilizer modes play the role of electromagnetic source terms. Their physical interpretation as slow fields might even be completely forgotten. In appendix C.4 the way the Kubo formulae translate is explicitly demonstrated. The sketch of the demonstration is as follows: Consider the quadratic fermionic action with Hubbard-Stratonovich fields living on the NLσM manifold. The replacement $Q \to U^{-1}QV$ is compensated by a slow rotation of fermionic degrees of freedom. For each Goldstone mode g_a (constant gradient) a supplementary term of the form $\bar{\Psi}\,(\nabla g_a)\cdot\mathbf{j}\,\sigma_z t^a \Psi$ enters the action. For each stabilizer mode s_a the additional term is $\bar{\Psi}\,(\nabla s_a)\cdot\mathbf{j}\,\tau^a\Psi$. In the appendix it is shown that twice differentiating with respect to stabilizer and Goldstone modes reproduces the (fermionic) Kubo formula for conductivity. In particular, when this differentiation is taken after gradient expansion and the above slow mode treatment (sec. 5.1.1), it reproduces

$$\sigma^{phys.} = \text{const.} \times (\text{eq.}(5.3)) \left[\frac{e^2}{\hbar}\right] = (\text{const.} \times \sigma_0 + \dots) \left[\frac{e^2}{\hbar}\right].$$

const. $= \frac{1}{\pi^2}$ for class AIII and const. $= \frac{2}{\pi^2}$ for classes BDI and CII are indeed the correct prefactors to reproduce the physical conductivity.

5.2 Perturbative RG: Gade-Wegner-criticality

The calculation of the perturbative coupling constants is performed using exponential coordinates for the fast fields

$$Q = e^{iW_a t^a},$$

where t^a are the generators of the special NLσM manifold. The mode of the U(1)-generator turns out not to contribute. The calculation itself is given in appendix D.
The propagators of W_a-fields are obtained expanding the fast action to quadratic order $\mathcal{O}\left(\nabla W_a^2\right)$. The corrections of the coupling constants are expanded to leading order in W_a (i.e. quartic order[2]). Again, the Fierz identities are used to obtain the logarithmically divergent result (eqs.(D.5) and (D.6)). Differentiating with respect to the mass:

$$\begin{aligned} -\tfrac{d\sigma}{d\ln m} &= -\mathrm{tr}\mathbf{1} \begin{cases} 1 & \text{AIII,} \\ \frac{1}{2} & \text{BDI,} \\ \frac{1}{2} & \text{CII,} \end{cases} \\ -\tfrac{dc}{d\ln m} &= \begin{cases} 1 & \text{AIII,} \\ \frac{1}{2} & \text{BDI,} \\ \frac{1}{2} & \text{CII.} \end{cases} \end{aligned}$$

Note the accordance with Gade's and Wegner's argument.
It has been stressed (sec. 3.3.1) that $\sigma = \frac{\pi}{2}\sigma_{phys.}$ for class AIII and $\sigma = \frac{\pi}{4}\sigma_{phys.}$ for classes BDI and CII. Therefore, the β-function of the physical conductivity is equal for all chiral classes even before replica limit.
Now replica limit is taken

$$\begin{aligned} -\tfrac{d\sigma}{d\ln m} &= 0, \\ -\tfrac{dc}{d\ln m} &= \begin{cases} 1 & & & \text{AIII,} \\ \frac{1}{2} & + & \mathcal{O}\left(\frac{1}{\sigma}\right) & \text{BDI,} \\ \frac{1}{2} & + & \mathcal{O}\left(\frac{1}{\sigma}\right) & \text{CII.} \end{cases} \end{aligned} \tag{5.5}$$

The results by Gade and Wegner are reproduced.
Note that the one-loop-RG is exact for class AIII, but not for classes BDI and CII. This is indicated by $+\mathcal{O}\left(\frac{1}{\sigma}\right)$.
The proof for exactness in class AIII is most easily seen in the supersymmetric approach and included in appendix E. In contrast, non-vanishing contributions from diagrams $\mathcal{O}\left(\frac{1}{\sigma}\right)$ in classes BDI and CII are known from works by Hikami and Wegner, which are summarized in [EM08].

[2]The quadratic order vanishes, because it corresponds to two integrals, each over one fast and slow field.

6. Influence of topological terms in chiral symmetry classes

This chapter is devoted to topology-induced corrections to conductivity, which arise due to other effects than vortices. In the first part the renormalization group flow of the WZW-model is reviewed. The second part is about the effect of the $\mathbb{Z}_2$-instanton in class CII. In particular, in both cases the RG flows according to Gade's and Wegner's arguments and there is no correction to conductivity in the replica limit.

6.1 AIII scaling with a WZW-term

The renormalization of the WZW-model is contained in Witten's original paper [Wit84] for the $O(N)$-NLσM and well-studied also for the $SU(N)$-NLσM. For $U(N)$ the flow obeys Gade's and Wegner's argument and can be found in textbooks, such as [AS10]:

$$-\frac{d\sigma}{d\ln m} = -N\left(1-\left(\frac{k}{\sigma}\right)^2\right),$$

$$-\frac{dc}{d\ln m} = \left(1-\left(\frac{k}{\sigma}\right)^2\right).$$

After replica limit, this is

$$-\frac{d\sigma}{d\ln m} = 0, \tag{6.1}$$

$$-\frac{dc}{d\ln m} = \left(1-\left(\frac{k}{\sigma}\right)^2\right). \tag{6.2}$$

In particular, there is a single true fixed point for $\sigma = k$ [1]. From direct derivation, sec. 4.4, it is known that the WZW-level is $k = n$ (n is the number of flavours). The critical

[1] This is a fixed point already before replica limit is taken, and hence also for the two other principle chiral models. For CI it is attractive and for DIII repulsive. AIII displays critical Gade scaling and by "single true fixed point" the vanishing β_c is meant.

value of conductivity is consequently the bare value $\sigma^* = \sigma_0 = n$ or in units of the Klitzing constant $\sigma^*_{phys.} = \sigma^{Drude}_{phys.} = \frac{2n}{\pi}\frac{e^2}{h}$ (sec. 3.3.1). As pointed out in sec. 3.2, for Dirac fermions the WZW-term translates the absence of conductivity corrections due to chiral anomaly into NLσM language.

6.2 Absence of conductivity correction in CII with $\mathbb{Z}_2$-term

In sec. 4.5 the $\mathbb{Z}_2$-term in class CII was derived as a descendant of the AIII-WZW-term. One can also look at it from the ($\mathbb{Z}$-)θ-term perspective. In the case of 2 replicas $\pi_2\left(\frac{U(N)}{O(N)}\Big|_{N=2}\right) = \mathbb{Z}$ as $\frac{U(2)}{O(2)} \simeq \mathbb{S}^2$. For higher N the homotopy group reduces to $\mathbb{Z}_2$ [2]. Even though the homotopy group is smaller, a single $\frac{U(2)}{O(2)}$-instanton still belongs to the topologically non-trivial sector. The effect of such an instanton will be considered in this section.

The $\mathbb{Z}_2$ instanton

The explicit calculations of the conductivity correction due to the instanton are given in appendix F. The topological excitation considered is

$$Q_{\mathbb{Z}_2} = \begin{pmatrix} a_3\mathbf{1}_2 + ia_2\sigma_x + ia_1\sigma_z & 0 \\ 0 & \mathbf{1} \end{pmatrix}.$$

Here, $\mathbf{a} = \frac{1}{\lambda^2+\|\mathbf{x}-\mathbf{x}_0\|}\left(2\lambda\left(x-x_0\right), 2\lambda\left(y-y_0\right), \|\mathbf{x}-\mathbf{x}_0\|^2-\lambda^2\right)^T$ is the skyrmion configuration of the $O(3)$-NLσM, it has size λ and position $\mathbf{x}_0$. This excitation was also considered by Pruisken [Pru87a].
The instanton configuration is weightened by[3] the action $S_{\mathbb{Z}_2} \equiv S\left[Q_{\mathbb{Z}_2}\right] = 2\sigma_0 + i\pi$.
Furthermore, the action is invariant under shifts and spatial rotations of the instanton, as well as under

$$Q_{\mathbb{Z}_2} \to O^T Q_{\mathbb{Z}_2} O \ , \ O \in \frac{O(N)}{\mathbb{Z}_2 \times O\left(N-2\right)}. \tag{6.3}$$

Any transformed instanton is therefore equivalent to $Q_{\mathbb{Z}_2}$, which results in an overall prefactor

$$2\pi \mathrm{Vol}_{space} \mathrm{Vol}\frac{O(N)}{\mathbb{Z}_2 \times O\left(N-2\right)} = 4\pi \mathrm{Vol}_{space}\frac{\pi^{N-\frac{1}{2}}}{\Gamma\left(\frac{N}{2}\right)\Gamma\left(\frac{N-1}{2}\right)}. \tag{6.4}$$

There is one more degree of freedom of the instanton: its size λ. The integral over it produces the logarithmic divergence, as

$$\frac{\mathcal{Z}_{inst.}}{\mathcal{Z}_0} \propto \int \frac{d\lambda}{\lambda^3},$$

and

$$\int d^2x d^2x' \left\langle \mathrm{tr}\left[\left(Q^{-1}\nabla Q\right)_x \left(Q^{-1}\nabla Q\right)_{x'}\right]\right\rangle_{\mathbb{Z}_2} = -16\pi^2\lambda^2$$

(see [Pru87b], [Pru87a]). Note that the expectation value of the two-trace term in the "Q-field Kubo formulae", eqs. (5.3),(5.4) vanishes. The ratio of partition functions for the instanton and topologically trivial sector $\frac{\mathcal{Z}_{inst.}}{\mathcal{Z}_0}$ contains also the above mentioned prefactor (6.4).
The corrections to the coupling constants due to the instanton are given in eqs. (F.3),

[2] An illustrative explanation: Insert two instantons in the $\frac{U(2)}{O(2)}$ submanifold of $\frac{U(N)}{O(N)}$. Then one of the two can be rotated on the whole manifold and back to its original replicas $\frac{U(2)}{O(2)}$ such that the configuration becomes a (topological trivial) instanton-antiinstanton configuration.
[3] ... the inverse of the exponent of...

(F.4). Combining them with the quantum correction from sec. 5.2, the β-function of the coupling constants are

$$\begin{aligned} -\frac{d\sigma}{d\ln m} &= -N\left(\frac{1}{2} - 2\pi\sigma^2 e^{-2\sigma}\frac{2\pi^{N+\frac{1}{2}}}{(N+2)\,\Gamma\left(\frac{N}{2}+1\right)\Gamma\left(\frac{N+1}{2}\right)}\right), \\ -\frac{dc}{d\ln m} &= \frac{1}{2} - 2\pi\sigma^2 e^{-2\sigma}\frac{2\pi^{N+\frac{1}{2}}}{(N+2)\,\Gamma\left(\frac{N}{2}+1\right)\Gamma\left(\frac{N+1}{2}\right)}. \end{aligned}$$

In particular, as the corrections obey Gade's and Wegner's argument, in replica limit the β-function of conductivity vanishes:

$$\begin{aligned} -\frac{d\sigma}{d\ln m} &= 0, \\ -\frac{dc}{d\ln m} &= \frac{1}{2} - 2\pi\sigma^2 e^{-2\sigma}. \end{aligned} \tag{6.5}$$

Similarly to class AIII with a WZW-term, "true" fixed points arise for definite (small) values of conductivity ($\sigma \approx 0.436$ and $\sigma \approx 1.915$). However, in class CII the perturbative β_c function is not exact and these fixed points are far beyond the controllable region where $\frac{1}{\sigma}$ is small.
In the large conductivity limit, the instanton corrections to β_c are exponentially small with respect to the quantum corrections. This justifies neglecting them.

7. Influence of vortex excitations in chiral symmetry classes

In this chapter the most important results of this work are exposed: Taking vortex excitations into consideration, localization effects and consequently (traces of) the metal-insulator transition in two-dimensional bipartite systems are demonstrated.

7.1 How to circumvent Gade's and Wegner's argument

A brief review of what has been explained up to now follows:

- Gade's and Wegner's argument, sec. 3.3.1, states that $\beta_\sigma = -\mathrm{tr}\mathbf{1}\beta_c \to 0$ because of the Gaussian nature of $S[\phi] = \int d^2x \ \left(\frac{\sigma+\mathrm{tr}\mathbf{1}c}{8\pi}\right)(\nabla\phi)^2$.
- The perturbative β-functions follow this argument (sec. 5.2) ...
- ... as well the β-functions for the NLσMs which include topological terms (ch. 6).

Summing up, it looks as if Gade's and Wegner's argument prevented any kind of metal-insulator transition. Still a loophole exists: as $\phi \in \mathbb{S}^1$ lives on a topologically non-trivial manifold, $S[\phi]$ is not really Gaussian. Topological excitations, namely vortices, are allowed. Their logarithmical interaction will produce logarithmic corrections to the coupling constants under RG. All this is to some extent similar to the Berezinskii-Kosterlitz-Thouless transition (sec. 2.2).

7.2 Generalities on vortex excitations

In which field do vortices appear?

In Gade's and Wegner's argument the following notation of the Q-field was assumed: $Q = e^{i\frac{\phi}{\sqrt{\mathrm{tr}\mathbf{1}}}}U$ with $detU = 1$ and $detQ = e^{i\phi} \in U(1)$. This notation has to be treated with care, both for physical and mathematical reasons:
The non-trivial first homotopy group of the chiral NLσM manifolds arises due to its $U(1)$ determinant. It seems natural to assume vortex excitations in ϕ. However, this is very questionable, as it would be equivalent to replica dependent, fractal vortex excitations $e^{i\frac{\phi}{\sqrt{\mathrm{tr}\mathbf{1}}}}$ in the Q-fields.
Mathematically, these problematics arise due to the fact that the unitary group is not the

direct product of its subgroups $U(N) \neq U(1) \times SU(N)$. This is related to the extension problem of $U(1)$ by $SU(N)$, which yields the so-called semi-direct product [Bac67], [Isa08]. Vortices are hence not introduced into the overall phase-factor but into the phase of a single replica. The topologically trivial saddle-point, which served as a base point for the NLσM manifold, is replaced by a vortex configuration

$$Q_{SP} = \mathbf{1} \to Q_{SP(\text{vortex})} = \begin{pmatrix} e^{i\phi(\mathbf{x})} & 0 \\ 0 & \mathbf{1} \end{pmatrix},$$

where

$$\oint d\mathbf{s}\cdot\nabla\phi = 2\pi. \tag{7.1}$$

($\oint$ integrates over a path enclosing the center of the vortex.)[1] [2]
The vortex solution is then rotated by the appropriate soft modes of classes AIII, BDI and CII respectively (see sec. 7.3.3). It is worth to remark that for any such rotated matrix $detQ_{\text{vortex}} = e^{i\psi+i\phi} \in U(1)$ (ψ is the contribution from the soft modes). The determinant of the Q-field hence acquired the vorticity, in accordance to its $\mathbb{S}^1$-topology.
Inserting the vortex excitations into distinct replica's is in complete analogy to how Pruisken [Pru87b] introduced the instantons into the NLσM describing the integer quantum Hall effect.

7.2.1 Estimate of the vortex size

The following estimate will be performed for an AIII-model with Dirac fermions. In particular, the disorder is supposed to be of the kind not to imply a WZW-model (e.g. vacancies and random magnetic field).
Even though a particular model is considered, the conclusions are valid for any other chiral NLσM which allows for vortices.
The action in terms of Hubbard-Stratonovich fields is (analogously eq. (4.11), $Q_2^{\pm}$ have been renamed Q and P)

$$S[Q,P] = \int d^2x \, \frac{n\gamma^2}{\pi\alpha} \operatorname{tr} QP - n \int d^2x \operatorname{tr} \ln \begin{pmatrix} i\gamma Q & p_- \\ p_+ & i\gamma P \end{pmatrix}. \tag{7.2}$$

As a vortex excitation of the kind of eq. (7.1) has a diverging action in the center of the vortex, the NLσM treatment is not valid within a certain region around this point. This region will be called "core" of the vortex and its extension shall be estimated. To this end the following ansatz is made:

$$Q = \operatorname{diag}\left(A(r)\, e^{i\phi}, 1, 1, .., 1\right) \text{ and } P = \operatorname{diag}\left(A(r)\, e^{-i\phi}, 1, 1, .., 1\right). \tag{7.3}$$

($r = \|\mathbf{x}\|$ and ϕ is the vortex field in the sense of eq. (7.1). For $A(r) \to 1$ the fields obey the saddle-point constraint $Q = P^{-1}$.)

[1] For BDI $Q_{SP(\text{vortex})} = \begin{pmatrix} e^{i\phi(\mathbf{x})}\mathbf{1}_2 & 0 \\ 0 & \mathbf{1} \end{pmatrix}$

[2] For the semidirect product $U(N) = U(1) \rtimes SU(N)$ the $U(1)$-subgroup is realized by $\operatorname{diag}\left(e^{i\phi}, 1, 1, .., 1\right) =: e^{i\phi}\hat{\Pi}$ (or equivalently). The semidirect product comes along with the following multiplication:

$$\begin{aligned} * : (U(1) \rtimes SU(N)) \times (U(1) \rtimes SU(N)) \quad &\to \quad U(1) \rtimes SU(N), \\ &\left(e^{i\phi}\hat{\Pi}, U\right) * \left(e^{i\psi}\hat{\Pi}, V\right) := \left(e^{i\phi}\hat{\Pi}Ue^{i\psi}\hat{\Pi}U^{-1}, UV\right), \end{aligned}$$

which is nothing but the usual matrix multiplication. A very good presentation can also be found on www.en.wikipedia.org → "Unitary Group" (Version of May, 19th, 2011).

Inserting the Q and P field into the saddle-point equation leads to the following operator equality

$$\frac{1}{\pi\alpha} = \left[\mathbf{p}^2 + 2\mathbf{B}' \cdot \mathbf{p} + \gamma^2 A^2(r)\right]^{-1}_{\mathbf{xx}}, \tag{7.4}$$

($\mathbf{B}' = \frac{e^{-i\phi}}{2}\begin{pmatrix} -i \\ 1 \end{pmatrix}\left(\frac{1}{r} - \frac{\partial_r A(r)}{A(r)}\right)$.)
This recalls the structure of the Green's function of a particle subjected to a "vector-potential" $\mathbf{B}'$. Hermitizing the corresponding Hamiltonian by a non-unitary "gauge"-transformation[3] $H \to e^{-\phi(\mathbf{x})} H e^{\phi(\mathbf{x})}$ yields the Hamiltonian

$$H = \gamma^2 \left(\left(\frac{\mathbf{p}}{\gamma} + \mathbf{B}(r) \right)^2 + V(r) \right),$$

($\mathbf{B}(r) = \frac{1}{2}\begin{pmatrix} -sin\phi \\ cos\phi \end{pmatrix}\left(\frac{1}{\gamma r} - \frac{A'(\gamma r)}{A(\gamma r)}\right)$ and $V(r) = A^2(\gamma r) - \frac{1}{\gamma r}\partial_{\gamma r}\left(\frac{\gamma r A'(\gamma r)}{A(\gamma r)}\right)$. $A'(\gamma r) = \partial_{\gamma r} A(\gamma r)$.)
For large distances from the vortex center ($\gamma r \gg 1$) the SCBA solution $A(\gamma r) = 1$ solves also equation (7.4). In contrast, in the vicinity of the center of the vortex ($\gamma r \ll 1$) the divergence of $\frac{1}{\gamma r}$ requests $A(\gamma r) = \text{const.} \times \gamma r$ (otherwise the effective d potential $\mathbf{B}$ diverges).
In this sense the mean free path γ^{-1} sets the length-scale, which distinguishes between inside and outside the vortex core. Taking this estimate as a basis, the amplitude $A(r)$ of the vortex fields is approximated by the step function,

$$A(r) \approx \theta\left(r - \gamma^{-1}\right).$$

7.2.2 Estimate of the core energy

In the section above, the vanishing amplitude $A(r)$ was introduced to regularize the divergence of the action inside the vortex core. In this section an estimate for the regularized core energy shall be given.
The action per unit volume ($s = S[Q]/\text{Vol}$) inside the vortex is larger than outside. The difference multiplied by the inner volume is approximately the core energy:

$$S_{\text{core}} \approx V_{\text{inside}}\left(s_{inside} - s_{outside}\right). \tag{7.5}$$

In this rough estimate, the kinetic contribution of the vortex field is not taken into consideration. The Hubbard-Stratonovich-fields inserted into eq. (7.2) are $Q = P = \text{diag}\left(\begin{Bmatrix} 0 \\ 1 \end{Bmatrix}, 1, 1, 1, ..., 1\right)$ for the calculation of $\begin{Bmatrix} s_{\text{inside}} \\ s_{\text{outside}} \end{Bmatrix}$.
The explicit calculation of the core energy is straightforward but somewhat lengthy. For this reason it has been relegated to appendix G. The final result is

$$S_{\text{core}} \approx \frac{n}{4} = \frac{\sigma_0}{4}. \tag{7.6}$$

("$\approx$" reflects only the estimate in the definition of S_{core}, eq. (7.5). The calculation itself is exact.)
σ_0 is the bare coupling constant in the Gade-Wegner NLσM (eq. (3.3)) and related to the Drude conductivity via $\sigma_0 = \frac{\pi}{2}\sigma^{Drude}$ for class AIII and $\sigma_0 = \frac{\pi}{4}\sigma^{Drude}$ for classes BDI and CII.

[3] Note that the Green's function is evaluated at coincident points.

7.2.3 Mathematical description of a vortex

Summarizing the estimates from the last two sections, in our model, vortices have a spatial extension of the order of the mean-free path and are energetically suppressed by a factor $e^{-S_{\text{core}}} = e^{-\frac{\sigma_0}{4}} =: y_0$. The last quantity, y_0, is called bare fugacity and describes the statistical weight for each vortex.
Vortices of charge $n_i = \pm 1$[4] and position $\mathbf{x}_i$ are introduced only in the first replica (first pair of replicas for BDI) in the following sense:

$$Q_{\text{Vortex}} = e^{in_i\phi_{\mathbf{x}_i}(\mathbf{x})}\hat{P} + \left(\mathbf{1} - \hat{P}\right). \tag{7.7}$$

($\hat{P}$ denotes the projector on the first replica for classes AIII and CII and on the first pair of replicas for BDI.)
The vorticity is encoded in the analytical property

$$\nabla_\mu \phi_{\mathbf{x}_i}(\mathbf{x}) = \text{rot}_\mu \ln \frac{\|\mathbf{x} - \mathbf{x}_i\|}{\gamma^{-1}}. \tag{7.8}$$

Using Stokes' theorem the correspondence between this local definition and the integral definition in eq. (7.1) becomes apparent.

7.3 Explanation of RG-procedure

The idea behind the RG-procedure, which describes the corrections to the coupling constants, is similar to the concept for the BKT-transition exposed in sec. 2.2. As explained, the stiffness J is replaced by $\text{tr}\hat{P}\frac{\sigma_0 + \text{tr}\hat{P}c_0}{4\pi}$. Therefore, the low temperature phase (J large), where dipoles are tiny, corresponds to the metallic regime. The small stiffness phase, which describes the plasma of unbound charged vortices, appears here for small $\sigma_0 + \text{tr}\hat{P}c_0$.
As the NLσM describes the metallic regime, the RG-procedure is taken from the large stiffness side, analogously to the usual BKT-transition. A dilute gas of tiny vortex dipoles is therefore assumed, and, as explained, the smallest of these dipole pairs is explicitly integrated out. Its effect is incorporated into the renormalized coupling constants.
It is of central relevance to state that keeping a single dipole corresponds to expanding the vortex-corrected coupling constants to leading order in fugacity, i.e. to order $\mathcal{O}\left(y^2\right)$[5].
As mentioned, vortices are introduced in the first replica(s) and can be seen as an additional saddle-point solution. The following approximation is used: only slow soft-mode rotations of this saddle-point are assumed. Differently stated, the fast Q-field (see eq. (5.2)) contains only the topological excitations. In particular, this implies that vortex dipoles are each in the same replica[6].

7.3.1 The calculation of vortex-induced corrections

A vortex-antivortex pair at positions $\mathbf{x}_1$, $\mathbf{x}_2$ is introduced in the Q-field according to eq.(7.7). Then, the action for such a configuration is

$$S_{V-AV} = 2S_{core} + \text{tr}\hat{P}\frac{\sigma_0 + \text{tr}\hat{P}c_0}{2}\ln\frac{\|\mathbf{x}_1 - \mathbf{x}_2\|}{\gamma^{-1}} + S_m. \tag{7.9}$$

[4] Vortices with higher winding number are less relevant for the phase transition and therefore neglected.
[5] Any further vortex pair is suppressed by additional y^2. Note that overall neutrality of the vortex gas is imposed, otherwise a surface term diverging as $\ln L$ arises in the action.
[6] The configuration of two vortices close to each other but situated in different replicas is the same as a pair in the same replica which was rotated by fast fields.

The first term is the core energy, estimated in sec. 7.2.2. The last term is the mass term regularization and approximately $e^{-S_m} \approx \theta\left(m^{-1} - \|\mathbf{x}_1 - \mathbf{x}_2\|\right)$. The logarithmic term in the middle reflects the Coulomb-like interaction between vortex and antivortex, it eventually provides the logarithmic corrections.
The explicit calculation of the current-current-correlators renormalizing σ and c (eqs. (5.3) and (5.4)) can be found in appendix H. In particular, considering vortices, *both* the single trace *and* two trace term of the "Kubo formulae" contribute. This is how Gade's and Wegner's argument is circumvented by vortices.

$$\begin{aligned} \frac{1}{\mathrm{tr}\hat{P}} \int d^2x d^2x' \left\langle \mathrm{tr}\left[\left(Q^{-1}\nabla Q\right)_x \left(Q^{-1}\nabla Q\right)_{x'}\right]\right\rangle &= \\ \frac{1}{\left(\mathrm{tr}\hat{P}\right)^2} \int d^2x d^2x' \left\langle \mathrm{tr}\left[\left(Q^{-1}\nabla Q\right)_x\right] \mathrm{tr}\left[\left(Q^{-1}\nabla Q\right)_{x'}\right]\right\rangle &\sim \\ - \quad \mathrm{Vol}_{\hat{P}} \quad \mathrm{Vol}\, \frac{\gamma^4\pi^2 y_0^2}{2}\, \mathrm{I}_\xi. \end{aligned} \tag{7.10}$$

$\xi = \|\mathbf{x}_1 - \mathbf{x}_2\|$ denotes the relative distance of vortex and antivortex. This result is obtained in leading order expansion in small[7] ξ and includes the following integral (which is divergent for small stiffness):

$$\mathrm{I}_\xi = 2\pi \int_{\frac{1}{\gamma}} d\xi\, \xi^3 e^{-\mathrm{tr}\hat{P}\frac{\sigma_0 + \mathrm{tr}\hat{P}c_0}{2}\ln\frac{\xi}{\gamma^{-1}}}. \tag{7.11}$$

7.3.2 Renormalization group procedure

The renormalization group procedure follows the method first exposed by José, Kadanoff, Kirkpatrick and Nelson [JKKN77].
The integral (7.11) appears whenever the effect of a vortex pair is incorporated into the coupling constants. For the smallest vortex pair ($\gamma^{-1} < \xi < m^{-1}$)[8] the integral yields

$$\mathrm{I}_\xi^{\mathrm{fast}} \approx \frac{2\pi}{\gamma^4}\ln\frac{\gamma}{m} + \mathcal{O}\left(\left(\ln\frac{\gamma}{m}\right)^2\right). \tag{7.12}$$

The coupling constants σ_0, c_0 are renormalized. Assume to perform another RG step where a dipole of size $m^{-1} < \xi$ is integrated out, producing the same integral I_ξ (eq. (7.11)), this time with lower bound m^{-1}. It can be rescaled to the original integral:

$$\begin{aligned} \mathrm{I}_\xi^{\mathrm{slow}} &= 2\pi \int_{\frac{1}{m}} d\xi\, \xi^3 e^{-\mathrm{tr}\hat{P}\frac{\sigma + \mathrm{tr}\hat{P}c}{2}\ln\frac{\xi}{\gamma^{-1}}} \\ &= \left(\frac{\gamma}{m}\right)^{4 - \mathrm{tr}\hat{P}\frac{\sigma + \mathrm{tr}\hat{P}c}{2}} \mathrm{I}_\xi. \end{aligned} \tag{7.13}$$

At the new scale determined by m, y_0^2 is replaced by $y_0^2\left(\frac{\gamma}{m}\right)^{4 - \mathrm{tr}\hat{P}\frac{\sigma + \mathrm{tr}\hat{P}c}{2}}$ (see eq. (7.10)). Hence, all of the bare constants σ_0, c_0 and y_0 have to be replaced by their renormalized values.

[7] With respect to the slow-mode length scale $\|\mathbf{x} - \mathbf{x}'\|$.
[8] More rigorously, the integral has a lower bound $2\gamma^{-1}$, which is twice the vortex core radius. However, this is beyond the accuracy of the estimate of sec. 7.2.1 and neither changes the RG-equations (7.15), in which a prefactor is included into a redefined fugacity y anyhow.

7.3.3 Volume of space of possible projections

Similarly to the case of the $\mathbb{Z}_2$ instanton in class CII, the vortex-antivortex pair has several degrees of freedom which do not alter the value of the action (7.9): It might be shifted, rotated around its center in the two-dimensional plane or rotated in replica space. There is one degree of freedom of the dipole which does not leave the action invariant, namely changing the extension of the dipole. This is the reason why the logarithmic correction to the coupling constants is provided by $\xi = \|\mathbf{x}_1 - \mathbf{x}_2\|$. (In the case of the $\mathbb{Z}_2$ instanton, the argumentation is completely analogous regarding the size of the instanton λ instead of the dipole size.)
In the derivation of the renormalized coupling constants σ_0 and c_0, eq. (7.10), the formula already included the integration over all dipole positions and dipole orientations in the physical space. What is left, is to integrate the result over possible projection in replica space. The infrared boundary condition $Q(\mathbf{x}) \xrightarrow{x\to\infty} \mathbf{1}$, as well as the structure of $\hat{P}$ constricts the space of possible projections to compact manifolds: these are the complex, quaternionic and real projective space (CP^{N-1}, HP^{N-1} and RP^{N-1}) for classes AIII, BDI and CII respectively (see appendix H). Their volume is

$$\mathrm{Vol}_{\hat{P}} = \begin{cases} \frac{\mathbb{S}^{2N-1}}{\mathbb{S}^1} &= \frac{\pi^N}{\pi\Gamma(N)} & \text{AIII,} \\ \frac{\mathbb{S}^{4N-1}}{\mathbb{S}^3} &= \frac{\pi^{2N}}{\pi^2\Gamma(2N)} & \text{BDI,} \\ \frac{\mathbb{S}^{N-1}}{\mathbb{S}^0} &= \frac{\pi^{\frac{N}{2}}}{\Gamma\left(\frac{N}{2}\right)} & \text{CII.} \end{cases} \tag{7.14}$$

7.3.4 Vortex-induced corrections to the coupling constants

In this subsection the vortex-induced corrections to the coupling constants for arbitrary number replicas N shall be given. For the benefit of a better overview, the perturbative corrections from the topologically trivial sector will be left apart for the moment. The RG-equations obtained from the interplay of both vortex and quantum corrections are exposed in the next section 7.4.
Using the above calculated expectation values of current-current correlators (7.10), the RG treatment from sec. 7.3.2 and the calculated volume of possible projections (7.14) to renormalize the coupling constants according to eqs. (5.3) and (5.4) yields the result (adapted from appendix H, eq. (H.7)):

$$\begin{array}{ll} & \left\{ \begin{array}{rcl} -\frac{d\sigma}{d\ln m}\big|_V &=& -\frac{\pi^N}{\Gamma(N+2)}\sigma^2 y^2, \\ -\frac{dc}{d\ln m}\big|_V &=& -\left[\sigma^2\frac{\pi^N}{\Gamma(N+2)} + 2\sigma c\frac{\pi^N}{\Gamma(N+1)} + c^2\frac{\pi^N}{\Gamma(N)}\right] y^2, \\ -\frac{dy}{d\ln m}\Big|_V &=& \left[2 - \frac{\sigma+c}{4}\right] y, \end{array} \right. \quad \text{AIII} \\ & \left\{ \begin{array}{rcl} -\frac{d\sigma}{d\ln m}\big|_V &=& -\frac{\pi^{2N}}{\Gamma(2N+2)}\sigma^2 y^2, \\ -\frac{dc}{d\ln m}\big|_V &=& -\left[\sigma^2\frac{\pi^{2N}}{\Gamma(2N+2)} + 2\sigma c\frac{\pi^{2N}}{\Gamma(2N+1)} + c^2\frac{\pi^{2N}}{\Gamma(2N)}\right] y^2, \\ -\frac{dy}{d\ln m}\Big|_V &=& \left[2 - \frac{\sigma+2c}{2}\right] y, \end{array} \right. \quad \text{BDI} \\ & \left\{ \begin{array}{rcl} -\frac{d\sigma}{d\ln m}\big|_V &=& -\frac{2\pi^{\frac{N}{2}}}{(N+2)\Gamma\left(\frac{N}{2}+1\right)}\sigma^2 y^2, \\ -\frac{dc}{d\ln m}\big|_V &=& -\left[\sigma^2\frac{\pi^{\frac{N}{2}}}{(N+2)\Gamma\left(\frac{N}{2}+1\right)} + 2\sigma c\frac{\pi^{\frac{N}{2}}}{\Gamma\left(\frac{N}{2}+1\right)} + 2c^2\frac{\pi^{\frac{N}{2}}}{\Gamma\left(\frac{N}{2}\right)}\right] y^2, \\ -\frac{dy}{d\ln m}\Big|_V &=& \left[2 - \frac{\sigma+c}{4}\right] y. \end{array} \right. \quad \text{CII} \end{array} \tag{7.15}$$

For the different symmetry classes, different prefactors have been incorporated into y, see appendix H.

The case $N = 1$ of eqs. (7.15) reproduces, as to be expected, the well-studied usual RG-equations of the BKT-transition exposed in sec. 2.2 for any of the symmetry classes.

7.4 RG including vortex and perturbative corrections

The main results of this diploma thesis are exposed in this section. These are the $N \to 0$ RG-equations of the the three chiral symmetry classes under the influence of both perturbative and vortex-induced corrections. In particular, in all three symmetry classes localization effects are demonstrated.
The perturbative corrections are exact for class AIII and leading order corrections for BDI and CII, which is denoted by $+\mathcal{O}\left(\frac{1}{\sigma}\right)$. For all of the three classes, the RG-equations are obtained in the limit of small fugacity y (which is not further marked).

$$
\begin{array}{ll}
\text{AIII} & \left\{\begin{array}{rcrl}
-\frac{d\sigma}{d\ln m} &=& - & \sigma^2 y^2, \\
-\frac{dc}{d\ln m} &=& 1 - & \left[\sigma^2 + 2\sigma c\right] y^2, \\
-\frac{dy}{d\ln m} &=& & \left[2 - \frac{\sigma + c}{4}\right] y,
\end{array}\right. \\
\text{BDI} & \left\{\begin{array}{rcrl}
-\frac{d\sigma}{d\ln m} &=& - & \sigma^2 y^2, \\
-\frac{dc}{d\ln m} &=& \frac{1}{2} - & \left[\sigma^2 + 2\sigma c\right] y^2 + \mathcal{O}\left(\frac{1}{\sigma}\right), \\
-\frac{dy}{d\ln m} &=& & \left[2 - \frac{\sigma + 2c}{2}\right] y,
\end{array}\right. \\
\text{CII} & \left\{\begin{array}{rcrl}
-\frac{d\sigma}{d\ln m} &=& - & \sigma^2 y^2, \\
-\frac{dc}{d\ln m} &=& \frac{1}{2} - & \left[\frac{1}{2}\sigma^2 + 2\sigma c\right] y^2 + \mathcal{O}\left(\frac{1}{\sigma}\right), \\
-\frac{dy}{d\ln m} &=& & \left[2 - \frac{\sigma + c}{4}\right] y.
\end{array}\right.
\end{array}
\tag{7.16}
$$

(One last time it is recalled that σ is related to the physical conductivity in units of $\frac{e^2}{h}$ via $\sigma = \frac{\pi}{2}\sigma_{phys.}$ for class AIII and $\sigma = \frac{\pi}{4}\sigma_{phys.}$ in classes BDI and CII.)

7.5 Vortices and topological terms

In section 1.7 the possible appearance of a WZW term or $\mathbb{Z}_2$-topological term in classes AIII and CII respectively has been exposed. In particular, for Dirac fermions with a certain kind of disorder, these terms were explicitly derived (sec.s 4.4 and 4.5). In both cases, the physical meaning was associated to the absence of localization corrections: The WZW term is the NLσM expression which reflects that due to the form of the current operators and to chiral anomaly only the clean conductivity bubble contributes, see sec. 3.2. The class CII-NLσM with $\mathbb{Z}_2$-term describes the surface states of a three-dimensional topological insulator, which are protected against localization.
How can the absence of localization be understood if vortices (which drive the system into the localized phase, see above 7.4) are present? There is no definite answer to this question, but a very strong conjecture. Consider first the model with the WZW term, the $\mathbb{Z}_2$ term can be understood as its descendant afterwards. The manifestly U(N)-invariant definition of the WZW relies on the extension of the base manifold from a 2-sphere to a 3-hemisphere. This way of defining the WZW term is, however, not opportune in the presence of vortices. Inside the vortex core the theory is not defined, or more sloppily said, there are holes in the base manifold. Expanding into the third dimension, the base manifold is continuously shrunk to a point and it is not clear how to unambiguously do

that when the vortex holes are present.
Therefore, it is more convenient to consider the "local" expression of the WZW term, eq. (1.8). It is constructed without the extended base manifold but is tied to a certain coordinate representation ϕ^i. It was exposed in section 1.7.3 that a global rotation of Q-fields (represented by $\beta_k\left(\phi^i\right)$) produces the following correction to the WZW term

$$i\delta S_{WZ} = i4\pi k \int d^2x \partial_\mu \left(\epsilon^{\mu\nu}\beta_j \partial_\nu \phi^j\right).$$

As long as vortices are absent, this integral vanishes due to the compactified base-manifold $\mathbb{S}^2$, and the theory is $U(N)$ invariant. On the contrary, when vortices are present, this term does not vanish: The theory is only defined outside the vortex core, which yields a boundary contribution for each vortex

$$i\delta S_{WZ} = i4\pi k \oint_{\text{Vortex}} d\mathbf{s} \cdot \left(\beta_j \nabla \phi^j\right) =: i\phi\left(\beta\right).$$

By definition, the Q-field acquires a phase of 2π on the path around the vortex core[9]. This phase does also enter the non-Abelian part of Q (see sec. 7.2) and consequently the above integral. Depending on the values of β, the total action acquires a phase $i\phi\left(\beta\right)$.
Following the above argumentation, the action seems to lose its $U(N)$-invariance as soon as both a vortex and the WZW term are present. However, the $U(N)$-invariance is a strict symmetry from the underlying fermionic theory. Reexpressing the theory in terms of the NLσM should not destroy this basic property. How can this happen?
It has been stressed that inside the vortex core the NLσM description breaks down and it was replaced by a hole in the sample. This brute approximation is obviously not physical. Inside the core, there exists another theory describing the physics which is not known. The energy associated to it is estimated by S_{core} and, in order to restore the $U(N)$ symmetry, it must have boundary conditions such that it produces a term $-i\phi\left(\beta\right)$ under the above mentioned transformation.
With these requirements to the extended theory inside the vortex core, the WZW term is well defined. So are the vortices, which now carry a complex core energy

$$S_{core} + i\phi,$$

ϕ transforms in the way to keep the theory $U(N)$-symmetric. The vortices acquired an extra degree of freedom ϕ, over which the vortex-induced corrections have to be averaged. This average over a phase, however, eventually destroys the effect of the vortices.
For class CII with the $\mathbb{Z}_2$-topological term the argumentation is similar. The phase $\phi\left(\beta\right)$ can only acquire values $0, \pi$ and so can the imaginary part of the core energy. Still, the average over this degree of freedom cancels the vortex contributions.

7.6 $\mathbb{Z}_2$ vortices

In total, five symmetry classes display a non-trivial first homotopy group. The three chiral classes AIII, BDI and CII have $\pi_1\left(\mathcal{M}_\sigma\right) = \mathbb{Z}$ and were considered in the main part of this work. For two more classes (AII and DIII) $\pi_1\left(\mathcal{M}_\sigma\right) = \mathcal{Z}_2$. This also allows for ($\mathbb{Z}_2$-)vortex excitations. Some of these vortices are known from studies of the B-phase of superfluid He^3 (class DIII), and rely on the topology of $SO(3)$, which is homeomorphic to a ball with opposite points on the boundary identified, see fig.s (7.1) and (7.2). In particular, such $\mathbb{Z}_2$ vortices are their own antivortices.

[9] $\phi^j \equiv \phi^j\left(Q\left(\mathbf{x}\right)\right) = \mathrm{tr}|j\rangle\langle j|Q$ is the Q matrix projected onto a certain coordinate. One can formally rewrite $\sum_j \beta_j \nabla \langle j|Q|j\rangle = \mathrm{tr} B\nabla Q$ for $B = \sum_j \beta_j |j\rangle\langle j|$ to see that the vorticity of the Q matrix enters whatever coordinate representation is chosen.

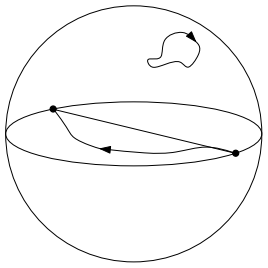

Figure 7.1: Two distinct paths in $SO(3)$.

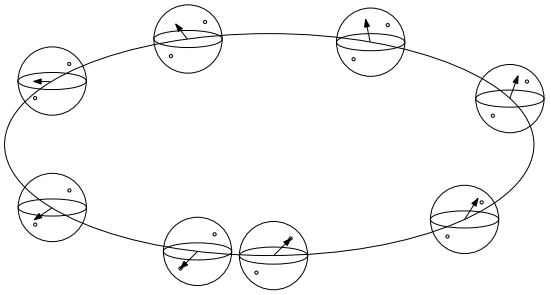

Figure 7.2: A $\mathbb{Z}_2$ vortex in $SO(3)$.

No explicit calculation has been performed for these kind of excitations. In contrast to chiral classes, the effect is expected to be less relevant for classes AII and DIII: Vortex corrections are of order $\sigma^2 y^2 \sim \sigma^2 e^{-2\sigma}$ and hence exponentially suppressed with respect to the weak antilocalization corrections. Still, y scales itself and, if the RG-equations are similar to eq.s (7.16) a new kind of fixed point might appear[10].
Conclusively, a closer investigation might lead to interesting results, but could not be done within the diploma thesis.

[10]For example, if also $\mathbb{Z}_2$ vortices have a localizing effect, the following RG-equations are conceivable: $\dot{\sigma} = 1 - \sigma^2 y^2$, $\dot{y} = (2 - \sigma)\, y$. This implies an unstable fixed point at $\sigma = 2$, $y = \frac{1}{2}$.

8. Analysis of the renormalization flow

8.1 Discussion of approximations

The main result, the RG-equations (7.16), was obtained making certain approximations:

- The size of the vortex core as well as the bare fugacity y_0 could only be roughly estimated (sec.s 7.2.1 and 7.2.2).
- The calculation was performed in the region of small fugacity y.
- Quantum fluctuations around the vortex solutions were not considered.
- For classes BDI and CII the perturbative β_c-function is valid only deep in the metallic regime where σ is large (sec. 5.2).

The precise estimate of the vortex size and energy does not influence the RG-equations (7.16). The size enters only the lower limit of the integral I_ξ, eq. (7.11). The differentiation is taken with respect to the upper limit m, the lower bound does not matter. The bare value of the fugacity neither is of crucial importance. It has been stressed that in eq.s (7.16) a prefactor $\mathcal{O}(1)$ has been included into its definition. Hence, the bare value of the fugacity is not related directly to the bare conductivity. Depending on the disorder strength it might take any value within a certain diffuse region of the parameter space.
In any case it is legitimate to assume the bare fugacity to be small in the metallic regime, which justifies the calculation to order $\mathcal{O}\left(y^2\right)$. This has to be taken into account when the RG-equations are evaluated.
The influence of quantum fluctuations around the vortex solution is not clear. Being corrections of higher orders $\left(\frac{1}{\sigma}\right)$ to the vortex-induced term, at least in the high conductivity regime it is reasonable to drop them.
If there do not exist any quantum-corrections to the vortex sector, for class AIII the RG-equations (7.16) are exact in σ and c and valid for small y. For classes BDI and CII, the high conductivity assumption has to be taken in any case.

8.2 Metal-insulator transition

In this section it shall be demonstrated that eq.s (7.16) indeed allow for a metallic and an insulating phase. First, assuming the RG-equations to be valid in the whole parameter space, the points of "stationary" flow will be derived. Afterwards, examining in particular class AIII more precisely, the regions of validity and accessibility are determined. Finally some remarks concerning the nature of the phase transition are made.

8.2.1 Class AIII: transformed RG-equations and "fixed" points

For class AIII it is possible to rearrange the RG-equations such to decouple the equation for the fugacity from the two others.
Define

$$K = \sigma + c \text{ and } \Sigma = \sigma y^2, \tag{8.1}$$

then

$$\begin{aligned} -\tfrac{d\Sigma}{d\ln m} &= -\Sigma^2 + \left[4 - \tfrac{K}{2}\right]\Sigma, \\ -\tfrac{dK}{d\ln m} &= 1 - 2\Sigma K, \\ -\tfrac{dy}{d\ln m} &= \left[2 - \tfrac{K}{4}\right] y. \end{aligned} \tag{8.2}$$

The two upper equations are now decoupled and allow for three "stationary" points[1]

$$\begin{pmatrix} \sigma y^2 \\ \sigma + c \\ y \end{pmatrix}^* \in \left\{ \begin{pmatrix} 0 \\ \infty \\ 0 \end{pmatrix}, \begin{pmatrix} 2 - \frac{\sqrt{15}}{2} \\ 4 + \sqrt{15} \\ \infty, 0 \end{pmatrix}, \begin{pmatrix} 2 + \frac{\sqrt{15}}{2} \\ 4 - \sqrt{15} \\ \infty, 0 \end{pmatrix} \right\}. \tag{8.3}$$

The first out of the three fixed points describes the "metallic" phase. It corresponds to the Gade-Wegner critical phase, where $c^* \to \infty$ because $K^* \to \infty$ and $y^* = 0$. Translating back to the original RG-equations, as $y^* = 0$, $\beta_\sigma = 0$ for any finite σ yielding the "usual" line of fixed points.
The middle one is "the" Metal-insulator transition point. More precisely, there are two "fixed" points: both are unstable in the (σy^2)-$(\sigma + c)$-plane and differ only by the value of y^*. Among them, the first is attractive in y-direction and $\sigma^* = 0$ as $(\sigma y^2)^*$ is finite and $y^* \to \infty$. The physical meaning of the second (it is unstable also in y-direction) is questionable: $(\sigma, c, y)^* = (\infty, -\infty, 0)$ even though vortices of weight y are responsible for its formation.
Also the last fixed point, it is attractive in the (σy^2)-$(\sigma + c)$-plane, appears doubled. The first, being attractive in all directions, corresponds to the insulating phase: again $y^* \to \infty$ while $(\sigma y^2)^*$ is finite, hence $\sigma^* \to 0$. As with the transition point there also exists an unstable fixed point at $y = 0$.

Before the flow towards these fixed points is discussed (see sec. 8.2.3 and fig. (8.1)) the attention will first be spotted onto the two other symmetry classes.

8.2.2 "Fixed" points in classes BDI and CII

Even though it is not known how to transform the RG-equations of classes BDI and CII into relations of the form (8.2), also for these classes fixed points analogous to (8.3) can be obtained.

Class BDI

As for all chiral classes there exists a metallic fixed point corresponding to the Gade fixed point(s) at $y^* = 0$ and $c^* \to \infty$ for any value of σ^*. For the two other fixed points $\beta_c = 0$ and therefore $(\sigma + 2c)^* = \frac{1}{2(\sigma y^2)^*}$. Then the beta function for $\Sigma = \sigma y^2$ depends only on

[1] Similarly to the usual Gade-Wegner RG-equations, it is not always possible to have all three β-functions vanishing. The symbol ∞ indicates the one out of the three β-functions which remains positive at the "fixed" point.

the variable itself yielding a quadratic expression. Solving this equation and summarizing gives

$$\begin{pmatrix} \sigma y^2 \\ c \\ y \end{pmatrix}^* \in \left\{ \begin{pmatrix} 0 \\ \infty \\ 0 \end{pmatrix}, \begin{pmatrix} 2 - \frac{\sqrt{14}}{2} \\ 1 + \frac{\sqrt{14}}{4} \\ \infty, 0 \end{pmatrix}, \begin{pmatrix} 2 + \frac{\sqrt{14}}{2} \\ 1 - \frac{\sqrt{14}}{4} \\ \infty, 0 \end{pmatrix} \right\}. \tag{8.4}$$

The interpretation of the fixed points is in complete analogy to the case of class AIII, sec. 8.2.1.

Class CII

In order to obtain the fixed points for class CII the same procedure as for class BDI is applied. To gather the connection $\sigma y^2 \leftrightarrow \sigma + c$, the β-function of $\frac{3\sigma}{2} + c$ is set to zero. As it turns out that $\sigma = 0$ at these fixed points anyhow, the arbitrariness of the definition is irrelevant. The stationary points are

$$\begin{pmatrix} \sigma y^2 \\ \frac{3\sigma}{2} + c \\ y \end{pmatrix}^* \in \left\{ \begin{pmatrix} 0 \\ \infty \\ 0 \end{pmatrix}, \begin{pmatrix} 2 - \sqrt{\frac{31}{8}} \\ 4 + \sqrt{\frac{31}{2}} \\ \infty, 0 \end{pmatrix}, \begin{pmatrix} 2 + \sqrt{\frac{31}{8}} \\ 4 - \sqrt{\frac{31}{2}} \\ \infty, 0 \end{pmatrix} \right\}. \tag{8.5}$$

Again, the interpretation is akin to the other two chiral classes. The c-value of the fixed points was derived for the combination $\sigma + c$ but for the Gade-like fixed point(s) the σ-value is irrelevant, and for the two others it vanishes.

8.2.3 Phase diagram class AIII

For class AIII, the RG-flow in the $(\sigma y^2, \sigma + c)$-plane is depicted in figure (8.1), right. In order to better visualize the flow diagram, a schematic plot is given as well ((8.1), left)[2]. As the RG-equation for the fugacity decouples from the others, the flow diagram is the same for any value of y (however, for large values of y the equations are not correct). The shaded (white) region indicates that y grows (shrinks)[3]. The flow diagram is at the same time the phase diagram for the AIII disordered metal: The red line separates the curves which flow towards the "metallic" fixed point(s) (green dot, $\sigma + c \to \infty$) from those which flow towards the insulating fixed point (blue dot). The unstable fixed point is marked by a red dot. The region, where the curves are directed to the metallic fixed point is denoted by green roman numbers I,II and the areas where the flow points to the insulating fixed point are labeled by blue roman numbers III, IV.

8.2.4 Validity

As mentioned, in the gray shaded region of the phase diagram (8.1) the fugacity y increases. If the system, which evolves according to the curves in the $(\sigma^2 y, \sigma + c)$-plane, stays in this region for too long, y will have increased too much and the small fugacity expansion is no more valid. In particular, this also happens in the vicinity of the unstable metal-insulator transition point. The flow within the plane slows down while y grows (nearly) constantly. As all points which lie on the red separating curve or very close nearby will eventually flow close to the unstable fix point the theory can neither be applied to them. The same is

[2] The RG equation of K has been modified (the number 8 has been added). This does not change the qualitative RG flow.

[3] For $y > 0$.

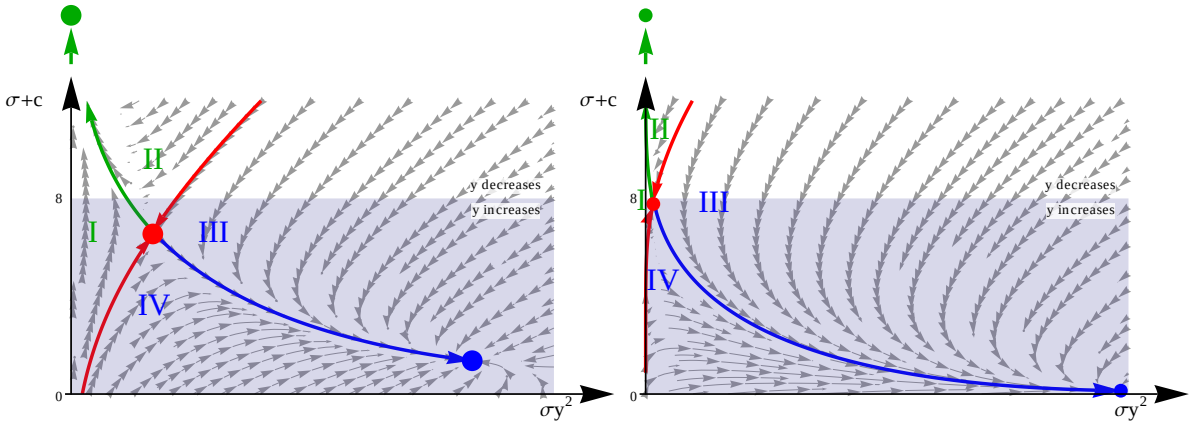

Figure 8.1: RG flow for class AIII in the $(\sigma y^2, \sigma + c)$-plane. Left: Schematic RG-flow. Right: Flow according to equations (8.2). The flow in the $(\sigma y^2, \sigma + c)$-plane is the same for any value of y. The white/shaded region, $\sigma + c \gtrless 8$, indicates the y decreases/increases.

true for the insulating fixed point. Consequently, vortices provide a mechanism producing an insulating state, the corresponding stable and unstable fixed points are however out of the range of applicability of the theory.
Furthermore, in classes BDI and CII, the perturbative RG-equations are valid for large conductivity σ only. In all three chiral classes higher terms in $\frac{1}{\sigma}$ might multiply the vortex-induced terms due to quantum fluctuations around the vortex solutions.
It has been stressed, that the flow in the $(\sigma^2 y, \sigma + c)$-plane is valid for any value of y and in particular for $y = 0$. The physical meaning is doubtful but mathematically all of the $y^* = 0$ fixed points lie in the controllable region. Consequently, criticality might be studied at the transition point for $y = 0$, keeping always in mind that eventually only other technical approaches (e.g. simulations) might clarify its meaning.

8.2.5 Region of possible bare values

The fugacity y which enters the RG-equations (7.16), even though rescaled, falls exponentially with increasing bare conductivity:

$$y_0 \sim e^{-\sigma_0}.$$

The region where σ_0 is large is the upper left part of phase diagram (8.1), flowing towards the Gade fixed points and hence confirming expectation.
Even though the rough estimate of the fugacity, section 7.2.2, yields a disorder strength independent value, corrections to this estimate can depend on the concentration of impurities. It is intuitive to expect stronger disorder to eventually drive the system towards the right hand side of the flow diagram, hence to the insulator.
In particular, assuming the NLσM description itself to be appropriate for any non-vanishing bare conductivity[4], the whole $(\sigma^2 y, \sigma + c)$-plane might be covered by the initial values of the type $(\sigma_0 = n, c_0, \text{disorder strength})$[5] ($n$ is the number of flavours). Among the regions where the theory is applicable, all of the regions I, II, III and IV are accessible by the set of bare values.

[4] For class AIII the exact perturbative RG justifies this assumption.
[5] It has been mentioned in sec. 4.4 that the Gade term can also be introduced by integrating massive modes out. For class AIII with Dirac fermions, this yields a bare value $c_0 \approx 0.18$ [Ost07].

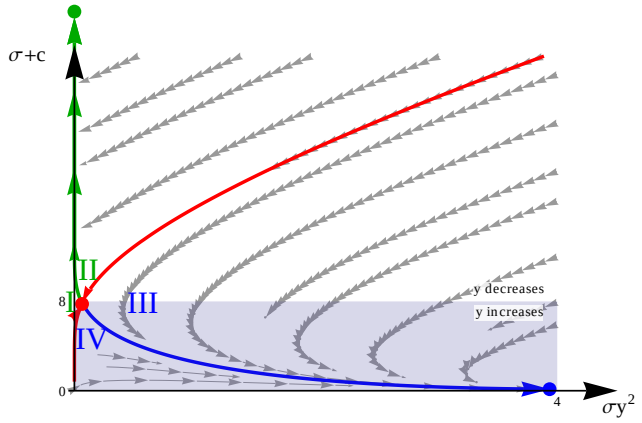

Figure 8.2: RG flow for class AIII in a larger set of the parameter space in the $(\sigma y^2, \sigma + c)$-plane.

8.2.6 Conjectures on the phase transition

It has been stressed that the applicability of the present theory breaks down at the metal-insulator transition point and the separating red curve (plane). For this reason it is not possible to study the nature of the phase transition within the given context. Nonetheless some indications can be deduced from the phase diagram.
The theory is not valid on the transition line (plane) but it definitely distinguishes the critical phase from the insulator. In particular, for a given bare conductivity there exists most likely a definite critical disorder strength above which the red line is crossed and the system flows into the insulating state. The other way round, for a given disorder strength there is probably a finite minimal bare conductivity for which the system still flows into the Gade-phase, and below which the system is insulating. They can be determined by intersecting the red line with the family of curves

$$\left(\sigma y^2, \sigma + c\right) \sim \left(\sigma_0 e^{-2\sigma_0 + f(\text{disorder})}, \sigma_0 + c_0\right) \tag{8.6}$$

for given disorder strength, bare conductivity and bare value of c. The further the intersection point is away from the critical point, the better is the accuracy for the obtained value.
Consequently, as expected by Motrunich *et al.* [MDH02], for given disorder strength there is a critical conductivity which separates the insulating from the Gade phase. But this point in parameter space is not the end point of a line of fixed points in the sense of the BKT-transition. It is simply the intersection of the curve (8.6) with the red separatrix, which is however not necessarily accessible to the theory.
In particular, as the theory fails to describe the unstable fixed point, there is no information of the nature of the phase transition. Formally, the theory allows for the calculation of (finite) critical exponents but the result is not at all reliable. It might also be that in the inaccessible region close to the critical point further phase transitions occur. In spite of the little information about the unstable fixed point, the RG-flow indicates the phase transition to be possibly of the Anderson-type rather then of the Kosterlitz-Thouless type.

Part IV

Hence.

Conclusion

The main achievement of this work is the demonstration of localization effects in chiral classes, induced by vortices in the NLσM fields. A more distinctive summary of the results follows.
In chapter 4, an explicit mathematical proof for the presence of a $\mathbb{Z}_2$-topological term in the CII NLσM for Dirac fermions is given. Concretely, the term can be expressed as a class AIII Wess-Zumino-Novikov-Witten term with additional boundary conditions. In the present case, these are imposed by the natural appearance of a mass term within the AIII-CII crossover.
Having a system with the definite appearance of the $\mathbb{Z}_2$-term at hand, microscopic examples for each of the chiral NLσMs (with and without topological term) are known. With regard to this, the RG-equations for chiral symmetry classes are (re-)derived. Quantum-fluctuations as well as all conceivable topological corrections are taken into account. In this sense, the results are complete.
Chapter 5 is devoted to the technical description of the procedure - especially to the background field formalism - and the Gade-Wegner RG-equations are recalculated. Next, the influence of topological terms is investigated. In particular, as these topological properties are inherited from the special submanifold, Gade's and Wegner's argument takes effect and conductivity is not renormalized.
Eventually, vortex-like excitations are examined. Starting from general argumentation estimates for the bare vortex size and core energy are given. Thereafter the explicit calculation of the renormalization of the N-replica NLσM coupling constants is presented. For $N = 1$ the results reproduce the $U(1)$-Berezinskii-Kosterlitz-Thouless-transition, whereas in the replica limit they yield suppression of conductivity. Also, the interplay of topological terms with vortices is discussed: it eventually results in vanishing localization effects. Finally some conjectures are made concerning $\mathbb{Z}_2$-vortices.
The main part of the thesis ends with an extensive discussion of the obtained results. The three parameter scaling, its fixed points and limits of validity are examined, as well as the region of possible bare values. Most strikingly, the appearance of an insulating phase next to the critical phase is shown, the two of them being within the domain of both applicability and accessibility. Ultimately, some remarks concerning the Anderson-like nature of the phase transition conclude the main part.

Altogether, a novel localizing mechanism was added to the variety of critical phenomena in two-dimensional disordered systems. This is the announced newly inserted piece into the Anderson jigsaw puzzle. The apparent controversy between the observed localized phase in numerical tests [MDH02] [BC03] and the Gade-Wegner scaling is resolved. In particular, the results of this work are in full agreement with the simulations.
Notwithstanding, there are still issues open for investigation. Above all, numerical simulations directly attached to the exposed mechanism are expected to allow a more detailed understanding of the phase transition. They possibly provide a link to experimental research, too.
Furthermore, direct follow-up analyses also remain. A more rigorous statement concerning

the neglected quantum-fluctuations around the vortex-saddle point, as well as regarding the vanishing effect of vortices in the presence of topological terms are desirable. Besides, analogous consideration of classes AII and DIII will help to elucidate the (presumably antagonistic) interplay of weak-antilocalization and $\mathbb{Z}_2$-vortices. Both classes have NLσM with topological terms, and extraordinary experimental realizations. Notably, the B-phase of superfluid He^3 falls into class DIII and, even more topical, (most) experimentally realized three-dimensional topological insulators are of class AII, and so is graphene with charged impurities.

The open questions eventually bring us back to the beginning of this diploma thesis. Graphene and topological insulators, apart from displaying amazing experimental properties, provide a fascinating arena for the research on Anderson transitions. Their promising future technical applications, as well as the natural realization of abstract concepts from fundamental physics illuminate the immense scientific richness implicated by the 1958 discovery of P.W. Anderson.

Deutsche Zusammenfassung

Zwei außerordentliche experimentelle Entdeckungen des noch jungen einundzwandzigsten Jahrhunderts gaben der Forschung an ungeordneten Systemen und Anderson-Lokalisierung zusätzlichen Schwung.
Zum einen erfanden Novoselov, Geim und Mitarbeiter die genial einfache "Tesafilm - Methode", mit der Graphen, eine einatomige Graphitschicht, effektiv produziert werden kann [NGM$^+$04]. Sie erkannten darüber hinaus unmittelbar die einzigartigen elektrischen Eigenschaften dieses Materials. Unter anderem ist, im Gegensatz zu gewöhlichen Metallen, die Leitfähigkeit über ein beträchtliches Temperaturfenster (von Raumtemperatur bis $\sim 1K$) hinweg nahezu konstant [NGM$^+$05]. Diese "bahnbrechenden Experimente" [6] veranlassten das Nobelkomitee, den Nobelpreis 2010 Novoselov und Geim zu verleihen.
Zum anderen wurden neuartige, Quanten-Hall-artige Phasen in zwei- und dreidimensionalen topologischen Isolatoren beobachtet [KWB$^+$07] [HQW$^+$08]. In diesen Phasen ist Materie isolierend im Inneren und, paradoxerweise, gleichzeitig auf der Oberfläche leitend. Noch erstaunlicher ist, dass die leitenden Oberflächenzustände extrem gut gegen lokalisierende Unordnungseffekte geschützt sind.
Wie kann das passieren? Wieso gehorchen diese Materialen nicht Andersons Satz, welcher Lokalisierung vorhersagt, falls die kinetische Energie klein im Vergleich zur Unordungsstärke ist [And58]? Welche Mechanismen unterdrücken die Leitfähigkeit und warum greifen sie nicht in den genannten Beispielen?
Graphen und topologische Isolatoren setzen diese alten Fragen in einen modernen Kontext: Seit den siebziger Jahren versuchen zahlreiche Festkörperphysiker die unordnungsgetriebenen Andersonübergänge zu verstehen. Viele Antworten wurden gefunden, noch mehr Fragen aufgeworfen doch die jüngsten Entwicklungen bestätigen, dass dieses Forschungsfeld noch immer mit faszinierend überraschenden Phänomenen aufwarten kann.

Das ausgesprochene Ziel dieser Arbeit ist es, ein winziges, aber konzeptionell doch neues Stück dem Puzzle der Andersonübergänge hinzuzufügen. Nur eine bestimmte Sorte Materialien soll betrachtet werden, nämlich die sogenannten bipartiten Systeme, die die chiralen Symmetrieklassen bilden. Gemäß den Pionierarbeiten von Gade und Wegner [GW91] [Gad93] und im Gegensatz zur Situation in gewöhnlichen Metallen ist die Leitfähigkeit der betroffenen Systeme unabhängig von externen Parametern wie Temperatur[7]. Tatsächlich ist diese bemerkenswerte Eigenschaft durch numerische Tests bestätigt worden [MDH02] [BC03], allerdings entlarvten diese auch eine zusätzliche lokalisierte Phase. Wie kann ein Isolator entstehen, wenn, nach Gade und Wegner, die Leitfähigkeit unverändert bleibt? Die Antwort zu dieser Frage ist das wichtigste Ergebnis dieser Arbeit.

Abgesehen von ungeordneten Metallen ist die Untersuchung chiraler zufälliger Systeme ebenfalls für den Grenzwert kleiner Energien in der Quantenchromodynamik relevant [VZ93]. In der Festkörperphysik ist die natürlichste und charmanteste Verwirklichung Gra-

[6] Aus der Preisankündigung der Alfred Nobel Stiftung.

[7] Das erinnert womöglich an die Situation von Graphen, die weiter ober geschildert wurde. Obwohl der Effekt ähnlich ist unterscheiden sich die theoretischen Gründe deutlich.

phen. (Je nach Art der Unordnung, kann Graphen allerdings auch in andere Symmetrieklassen fallen.) Es gibt des weiteren theoretische Hinweise darauf, dass auch topologische Isolotoren chiraler Symmetrieklassen existieren. Bis jetzt steht der experimentelle Nachweis noch aus, die außergewöhnlichen Anstrengungen, die heutzutage in der Forschung an topologischen Isolatoren unternommen werden, können jedoch unter Umständen schon bald zu einem anderen Ergebnis führen.
Indem die vorliegende Arbeit neue Einsichten darüber gewährt, wie Lokalisierung in chiralen Klassen auftritt, vertieft sie gleichzeitig das Verständnis geschützter Zustände, die mehr denn je ein lebhaftes Forschungsfeld darstellen.

Anderson-Lokalisierung

1957 machte Philip Warren Anderson die Entdeckung, dass ein quantenmechanisches Teilchen in einem ungeordneten Potential lokalisiert wird, falls die Unordnungsstärke im Vergleich zur kinetischen Energie groß genug ist. Das Besondere daran ist, dass die Anderson-Lokalisierung auch dann stattfindet, wenn man sie klassisch nicht erwartet. Ferner sind bei gegebener Unordungsstärke und Energie entweder alle Zustände lokalisiert oder alle delokalisiert. Es gibt also eine bestimmte Energie oder Unordungsstärke, bei der ein Phasenübergang stattfindet: der Andersonübergang.
Frühen Arbeiten von Wigner [Wig51] folgend entwickelte Freeman Dyson die sogenannte Zufallsmatrixtheorie um die Physik schwerer Atomkerne zu beschreiben, in denen "jegliche Schalenstruktur ausgewaschen und keine Quantenzahlen außer Spin und Parität gut sind" [Dys62].
Elektronische ungeordnete Systeme haben sehr wenige Symmetrien (zumindest, bevor über Unordnung gemittelt wird). In diesem Sinn sind auch hier die meisten Quantenzahlen "ausgewaschen" und eine Klassifizierung ähnlich derer von Wigner und Dyson ist angebracht. Auf diese Art und Weise wurde nach und nach eine Liste von zehn unterschiedlichen Symmetrieklassen erstellt. Aufgrund physikalischer Argumente, aber auch mathematischer Beweise [HHZ05] kann diese Liste als vollständig angenommen werden. Sie ist im Anhang I widergegeben.
Die zehn Symmetrieklassen spalten sich in drei Wigner-Dyson-, drei chirale und vier Bogoliubov-deGennes-Klassen auf. Für die vorliegende Arbeit sind nur die drei chiralen Klassen AIII, BDI und CII von Belang.
In ungeordneten Metallen fällt die elektronische Green's Funktion auf der Längenskala der mittleren freien Weglänge ab. Es gibt jedoch auch Moden, Diffusonen und Cooperonen, die langreichweitig sind. In Störungstheorie und mit Hilfe des Replicatricks [8] lässt sich deren korrigierender Effekt auf die klassische Drudeleitfähigkeit berechnen.
Anfang der achtziger Jahre wurde man sich dessen gewahr, dass diese perturbative Renormierung exakt der Renormierung nichtlinearer Sigmamodelle (NLσM) entspricht. Es konnte gezeigt werden, dass ausgehend von einer mikroskopischen Theorie diese niederenergetischen effektiven Theorien direkt hergeleitet werden können. Abhängig von den ursprünglichen Symmetrien des Systems bilden die Q-Felder des NLσM auf unterschiedliche Zielmannigfaltigkeiten ab.

Chirale Symmetrieklassen

Für chirale Symmetrieklassen sind die Zielmannigfaltigkeiten die unitäre Gruppe oder deren Quotientengruppen. Da die Moden, die mit der Determinante des Feldes assoziert sind, eine Gauß'sche Theorie bilden, ist ihr Vorfaktor nicht renormiert. Dies führt letztlich zum Verschwinden der Korrekturen zur Leitfähigkeit. Dieses Argument von Gade und Wegner wird bestätigt durch die perturbative Renormierung des NLσMs [GW91] [Gad93]. Auch topologische Terme, wie der Wess-Zumino-Witten-Term in AIII und der $\mathbb{Z}_2$ topologische

[8] Auch die supersymmetrische Methode und die Keldysh-Technik sind weit verbreitet.

Term in CII (dessen Auftreten in dieser Arbeit für ein bestimmtes System bewiesen wird) ändern nichts am Gade-Wegner-Skalenverhalten.
Allerdings gibt es in Gades und Wegners Argument ein Schlupfloch, das schließlich lokalisierende Effekte hervorruft: die "Gauß'sche" Theorie der Fluktuationen der Determinante kann Wirbelanregungen enthalten, da sie auf einer einem Kreis homöomorphen Mannigfaltigkeit definiert ist ($\det(U(N)) = U(1)$). Diese Wirbelanregungen entsprechen Punktdefekten, die coulombartig, das heißt logarithmisch, miteinander wechselwirken. Zunächst wird das Ausmaß und statistische Gewicht (Fugazität) dieser Anregungen abgeschätzt. Die nackte (nicht renormierte) Fugazität ist das Inverse des Exponenten der Drudeleitfähigkeit. Anschließend kann die explizite Berechnung der Renormierung des N-replica NLσM durchgeführt werden. Für $N = 1$ reproduzieren die Ergebnisse den wohlbekannten Berezinskii-Kosterlitz-Thouless-Phasenübergang [Ber70] [KT73]. Im Replicalimes N$\to$ 0 ergeben sie eine Unterdrückung der Leitfähigkeit:

$$
\begin{array}{ll}
\text{AIII} & \begin{cases} -\frac{d\sigma}{d\ln m} &= \quad - \quad \sigma^2 y^2, \\ -\frac{dc}{d\ln m} &= 1 - \left[\sigma^2 + 2\sigma c\right] y^2, \\ -\frac{dy}{d\ln m} &= \quad \left[2 - \frac{\sigma + c}{4}\right] y, \end{cases} \\
\text{BDI} & \begin{cases} -\frac{d\sigma}{d\ln m} &= \quad - \quad \sigma^2 y^2, \\ -\frac{dc}{d\ln m} &= \frac{1}{2} - \left[\sigma^2 + 2\sigma c\right] y^2 + \mathcal{O}\left(\frac{1}{\sigma}\right), \\ -\frac{dy}{d\ln m} &= \quad \left[2 - \frac{\sigma + 2c}{2}\right] y, \end{cases} \\
\text{CII} & \begin{cases} -\frac{d\sigma}{d\ln m} &= \quad - \quad \sigma^2 y^2, \\ -\frac{dc}{d\ln m} &= \frac{1}{2} - \left[\frac{1}{2}\sigma^2 + 2\sigma c\right] y^2 + \mathcal{O}\left(\frac{1}{\sigma}\right), \\ -\frac{dy}{d\ln m} &= \quad \left[2 - \frac{\sigma + c}{4}\right] y. \end{cases}
\end{array}
$$

(σ ist proportional zur Leitfähigkeit, c der Vorfaktor des sogenannten Gadeterms und y die Fugazität.)
Die Analyse des Renormierungsflusses, der den Wirbeln Rechnung trägt, lässt auf drei "stationäre" Punkte schließen. Diese entsprechen der Gade-Wegner-Phase, der isolierenden Phase und einem instabilen Metall-Isolator-Übergangspunkt. Insbesondere zeigt die Diskussion der möglichen Anfangswerte und der Grenzen der Anwendbarkeit der Theorie, dass sowohl die isolierende, als auch die "metallische" Phase im Parameterraum zugänglich sind.

Résumé und Ausblick

Alles in allem wurde ein neuer lokalisierender Mechanismus der Vielfalt kritischer Phänomene in zweidimensionalen ungeordneten Systemen hinzugefügt. Das ist das genannte neu in das Puzzlespiel der Anderson-Lokalisierung eingesetzte Stück. Der scheinbare Widerspruch zwischen der in numerischen Tests beobachteten lokalisierten Phase [MDH02] [BC03] und dem Gade-Wegner Skalenverhalten ist gelöst. Insbesondere stehen die Ergebnisse dieser Arbeit in vollem Einklang mit den Simulationen.
Dennoch sind noch einige Probleme ungelöst. Vor allem von numerischen Simulationen, die direkt an den dargestellten Mechanismus anknüpfen, wird ein tieferes Verständnis des Phasenübergangs erwartet. Auf diese Art und Weise könnte ebenfalls eine Verbindung zu experimentellen Untersuchungen hergestellt werden.
Desweiteren bleiben auch direkt anschließende Fragen zurück. Tiefergehende Argumente

bezüglich des Vernachlässigens von Quantenkorrekturen um den Wirbel-Sattelpunkt und auch für das Verschwinden der wirbelinduzierten Effekte in der Gegenwart topologischer Terme sind wünschenswert. Im Übrigen können gleichartige Betrachtungen der Symmetrieklassen AII und DIII helfen, das (vermutlich gegensätzliche) Wechselspiel von schwacher Antilokalisierung mit $\mathbb{Z}_2$-Wirbeln aufzuklären. Beide Symmetrieklassen erlauben topologisch nichttriviale nichtlineare Sigmamodelle; darüber hinaus gibt es außergewöhnliche experimentelle Realisierungen. So fällt beispielsweise die B-Phase supraflüssigen 3-Heliums in DIII. Noch aktuelleren Bezug gibt es zu AII: die meisten dreidimensionalen topologischen Isolatoren und auch Graphen mit geladenen Störstellen gehören in diese Symmetrieklasse. Die offenen Fragen bringen uns schließlich zurück zum Ausgangspunkt dieser Zusammenfassung. Graphen und topologische Isolotoren bilden, neben ihrer erstaunlichen experimentellen Eigenschaften, einen faszinierenden Schauplatz für die Forschung an Andersonübergängen. Ihre vielversprechenden technischen Anwendungen, aber auch die natürliche Verwirklichung abstrakter Konzepte aus der fundamentalen Physk erhellen den immensen wissenschaftlichen Reichtum, den wir dank P.W. Andersons Entdeckung aus dem Jahre 1958 erforschen dürfen.

Bibliography

[AALR79] E. Abrahams, P. W. Anderson, D. C. Licciardello, and T. V. Ramakrishnan, "Scaling theory of localization: Absence of quantum diffusion in two dimensions," *Phys. Rev. Lett.*, vol. 42, no. 10, pp. 673–676, Mar 1979.

[Abr88] A. A. Abrikosov, *Fundamentals of the Theory of Metals.* North-Holland, 1988.

[AI77] A. Aharony and Y. Imry, "The mobility edge as a spin-glass problem," *Journal of Physics C: Solid State Physics*, vol. 10, no. 17, p. L487, 1977. [Online]. Available: http://stacks.iop.org/0022-3719/10/i=17/a=005

[And58] P. W. Anderson, "Absence of diffusion in certain random lattices," *Phys. Rev.*, vol. 109, no. 5, pp. 1492–1505, Mar 1958.

[AS10] A. Altland and B. S. Simons, *Condensed Matter Field Theory*, 2nd ed. Cambridge University Press, 2010.

[ASZ02] A. Altland, B. D. Simons, and M. R. Zirnbauer, "Theories of low-energy quasi-particle states in disordered d-wave superconductors," *Physics Reports*, vol. 359, no. 4, pp. 283 – 354, 2002. [Online]. Available: http://www.sciencedirect.com/science/article/B6TVP-44W6DBS-1/2/84658c164b7bcdc0c2ecca19eef44dc7

[AZ97] A. Altland and M. R. Zirnbauer, "Nonstandard symmetry classes in mesoscopic normal-superconducting hybrid structures," *Phys. Rev. B*, vol. 55, no. 2, pp. 1142–1161, Jan 1997.

[Bac67] H. Bacry, *Leçons sur la théorie des groupes et les symétries des particules élémentaires*, ser. Cours et documents de mathḿatiques et de physique. Gordon and Breach, 1967.

[BC03] M. Bocquet and J. T. Chalker, "Network models for localization problems belonging to the chiral symmetry classes," *Phys. Rev. B*, vol. 67, no. 5, p. 054204, Feb 2003.

[Ber70] V. L. Berezinksii, *Sov.Phys.-JETP*, vol. 32, pp. 493–500, 1970.

[BL02] D. Bernard and A. LeClair, "A classification of 2d random dirac fermions," *Journal of Physics A: Mathematical and General*, vol. 35, no. 11, p. 2555, 2002. [Online]. Available: http://stacks.iop.org/0305-4470/35/i=11/a=303

[Car78] J. L. Cardy, "Electron localisation in disordered systems and classical solutions in ginzburg-landau field theory," *Journal of Physics C: Solid State Physics*, vol. 11, no. 8, p. L321, 1978. [Online]. Available: http://stacks.iop.org/0022-3719/11/i=8/a=006

[Dys62] F. J. Dyson, "Statistical theory of the energy levels of complex systems. i," *Journal of Mathematical Physics*, vol. 3, no. 1, pp. 140–156, 1962. [Online]. Available: http://link.aip.org/link/?JMP/3/140/1

[Efe97] K. Efetov, *Supersymmetry in disorder and chaos.* Cambridge University Press, 1997.

[EM08] F. Evers and A. D. Mirlin, "Anderson transitions," *Rev. Mod. Phys.*, vol. 80, no. 4, pp. 1355–1417, Oct 2008.

[Gad93] R. Gade, "Anderson localization for sublattice models," *Nuclear Physics B*, vol. 398, no. 3, pp. 499 – 515, 1993. [Online]. Available: http://www.sciencedirect.com/science/article/B6TVC-472T7Y7-2XT/2/72182679fcfcc053483840d256da28eb

[GW91] R. Gade and F. Wegner, "The n = 0 replica limit of u(n) and models," *Nuclear Physics B*, vol. 360, no. 2-3, pp. 213 – 218, 1991. [Online]. Available: http://www.sciencedirect.com/science/article/B6TVC-470F3HY-2W/2/951780029c1047a05aafbf8a5cd978bb

[Hel78] S. Helgason, *Differential Geometry, Lie Groups, and Symmetric Spaces.* American Mathematical Society, 1978.

[HHZ05] P. Heinzner, A. Huckleberry, and M. Zirnbauer, "Symmetry classes of disordered fermions," *Communications in Mathematical Physics*, vol. 257, pp. 725–771, 2005, 10.1007/s00220-005-1330-9. [Online]. Available: http://dx.doi.org/10.1007/s00220-005-1330-9

[Hik81] S. Hikami, "Anderson localization in a nonlinear-σ-model representation," *Phys. Rev. B*, vol. 24, no. 5, pp. 2671–2679, Sep 1981.

[HK10] M. Z. Hasan and C. L. Kane, "Colloquium: Topological insulators," *Rev. Mod. Phys.*, vol. 82, no. 4, pp. 3045–3067, Nov 2010.

[HQW+08] D. Hsieh, D. Qian, L. Wray, Y. Xia, Y. S. Hor, and M. Z. Cava, R. J. Hasan, "A topological dirac insulator in a quantum spin hall phase," *Nature*, vol. 452, pp. 970–974, Apr 2008. [Online]. Available: http://www.nature.com/nature/journal/v452/n7190/suppinfo/nature06843_S1.html

[Isa08] I. Isaacs, *Finite group theory*, ser. Graduate studies in mathematics. American Mathematical Society, 2008.

[JKKN77] J. V. José, L. P. Kadanoff, S. Kirkpatrick, and D. R. Nelson, "Renormalization, vortices, and symmetry-breaking perturbations in the two-dimensional planar model," *Phys. Rev. B*, vol. 16, no. 3, pp. 1217–1241, Aug 1977.

[KDP80] K. v. Klitzing, G. Dorda, and M. Pepper, "New method for high-accuracy determination of the fine-structure constant based on quantized hall resistance," *Phys. Rev. Lett.*, vol. 45, no. 6, pp. 494–497, Aug 1980.

[Kit09] A. Kitaev, "Periodic table for topological insulators and superconductors," *AIP Conference Proceedings*, vol. 1134, no. 1, pp. 22–30, 2009. [Online]. Available: http://link.aip.org/link/?APC/1134/22/1

[KT73] J. M. Kosterlitz and D. J. Thouless, "Ordering, metastability and phase transitions in two-dimensional systems," *Journal of Physics C: Solid State Physics*, vol. 6, no. 7, p. 1181, 1973. [Online]. Available: http://stacks.iop.org/0022-3719/6/i=7/a=010

[KWB+07] M. König, S. Wiedmann, C. Brüne, A. Roth, H. Buhmann, L. W. Molenkamp, X.-L. Qi, and S.-C. Zhang, "Quantum spin hall insulator state in hgte quantum wells," *Science*, vol. 318, no. 5851, pp. 766–770, 2007. [Online]. Available: http://www.sciencemag.org/content/318/5851/766.abstract

[Leu10] E. Leuzinger, "Homogeneous and symmetric spaces, lecture notes," 2010, online lecture notes password saved. [Online]. Available: https://ilias.rz.uni-karlsruhe.de/goto_rz-uka_crs_62102.html

[LK82] A. I. Larkin and D. E. Khmel'nitskii, "Andersonovskaya lokalizatsiya i anomal'noe magnetosoprotivlenie pri nizkikh temperaturakh," *Uspekhi Fizicheskikh Nauk*, vol. 136, no. 3, pp. 536–538, 1982. [Online]. Available: http://ufn.ru/ru/articles/1982/3/i/

[MDH02] O. Motrunich, K. Damle, and D. A. Huse, "Particle-hole symmetric localization in two dimensions," *Phys. Rev. B*, vol. 65, no. 6, p. 064206, Jan 2002.

[MEGO10] A. D. Mirlin, F. Evers, I. V. Gornyi, and P. M. Ostrovsky, "Anderson transitions: Criticality, symmetries and topologies," in *50 years of Anderson Localization*, E. Abrahams, Ed. World scientific, 2010.

[MW66] N. D. Mermin and H. Wagner, "Absence of ferromagnetism or antiferromagnetism in one- or two-dimensional isotropic heisenberg models," *Phys. Rev. Lett.*, vol. 17, no. 22, pp. 1133–1136, Nov 1966.

[Nay04] C. Nayak, "Quantum condensed matter physics, lecture notes," 2004. [Online]. Available: http://www.physics.ucla.edu/~nayak/many_body.pdf

[NGM+04] K. S. Novoselov, A. K. Geim, S. V. Morozov, D. Jiang, Y. Zhang, S. V. Dubonos, I. V. Grigorieva, and A. A. Firsov, "Electric field effect in atomically thin carbon films," *Science*, vol. 306, no. 5696, pp. 666–669, 2004. [Online]. Available: http://www.sciencemag.org/content/306/5696/666.abstract

[NGM+05] K. S. Novoselov, A. K. Geim, S. V. Morozov, D. Jiang, M. I. Katsnelson, I. V. Grigorieva, S. V. Dubonos, and A. A. Firsov, "Two-dimensional gas of massless dirac fermions in graphene," *Nature*, vol. 438, pp. 197–200, 2005.

[OGM06] P. M. Ostrovsky, I. V. Gornyi, and A. D. Mirlin, "Electron transport in disordered graphene," *Phys. Rev. B*, vol. 74, no. 23, p. 235443, Dec 2006.

[OGM07] ——, "Conductivity of disordered graphene at half filling," *The European Physical Journal - Special Topics*, vol. 148, pp. 63–72, 2007, 10.1140/epjst/e2007-00226-4. [Online]. Available: http://dx.doi.org/10.1140/epjst/e2007-00226-4

[Ost07] P. Ostrovsky, 2007, unpublished.

[Pol75] A. M. Polyakov, "Interaction of goldstone particles in two dimensions. applications to ferromagnets and massive yang-mills fields," *Physics Letters B*, vol. 59, no. 1, pp. 79 – 81, 1975. [Online]. Available: http://www.sciencedirect.com/science/article/pii/0370269375901616

[Pru87a] A. M. M. Pruisken, "Quasi particles in the theory of the integral quantum hall effect : (ii). renormalization of the hall conductance or instanton angle theta," *Nuclear Physics B*, vol. 290, pp. 61 – 86, 1987. [Online]. Available: http://www.sciencedirect.com/science/article/B6TVC-4719S7Y-26G/2/be24214d392b80aa933ac7ae462979f9

[Pru87b] ——, "Quasiparticles in the theory of the integral quantum hall effect (i)," *Nuclear Physics B*, vol. 285, pp. 719 – 759, 1987. [Online]. Available: http://www.sciencedirect.com/science/article/B6TVC-47316PP-G5/2/51caca1b88266fb675cdab2f3573cf20

[SRFL08] A. P. Schnyder, S. Ryu, A. Furusaki, and A. W. W. Ludwig, "Classification of topological insulators and superconductors in three spatial dimensions," *Phys. Rev. B*, vol. 78, no. 19, p. 195125, Nov 2008.

[Tho75] D. J. Thouless, "Phase transitions for the one-dimensional landau-ginzburg system and their relation to the theory of polymers and of electrons in a random potential," *Journal of Physics C: Solid*

State Physics, vol. 8, no. 12, p. 1803, 1975. [Online]. Available: http://stacks.iop.org/0022-3719/8/i=12/a=004

[TKNdN82] D. J. Thouless, M. Kohmoto, M. P. Nightingale, and M. den Nijs, "Quantized hall conductance in a two-dimensional periodic potential," *Phys. Rev. Lett.*, vol. 49, no. 6, pp. 405–408, Aug 1982.

[VZ93] J. J. M. Verbaarschot and I. Zahed, "Spectral density of the qcd dirac operator near zero virtuality," *Phys. Rev. Lett.*, vol. 70, no. 25, pp. 3852–3855, Jun 1993.

[Weg76] F. J. Wegner, "Electrons in disordered systems. scaling near the mobility edge," *Zeitschrift für Physik B Condensed Matter*, vol. 25, pp. 327–337, 1976, 10.1007/BF01315248. [Online]. Available: http://dx.doi.org/10.1007/BF01315248

[Weg89] F. Wegner, "Four-loop-order [beta]-function of nonlinear [sigma]-models in symmetric spaces," *Nuclear Physics B*, vol. 316, no. 3, pp. 663 – 678, 1989. [Online]. Available: http://www.sciencedirect.com/science/article/B6TVC-471997C-5W/2/40baa290bb940fd43a8b313fac467aca

[Wig51] E. P. Wigner, "On the statistical distribution of the widths and spacings of nuclear resonance levels," *Mathematical Proceedings of the Cambridge Philosophical Society*, vol. 47, pp. 790–798, 1951.

[Wit84] E. Witten, "Non-abelian bosonization in two dimensions," *Communications in Mathematical Physics*, vol. 92, pp. 455–472, 1984, 10.1007/BF01215276. [Online]. Available: http://dx.doi.org/10.1007/BF01215276

[Zir86] M. R. Zirnbauer, "Localization transition on the bethe lattice," *Phys. Rev. B*, vol. 34, no. 9, pp. 6394–6408, Nov 1986.

Appendix

A $\mathbb{Z}_2$ topological term from the WZW perspective

This section is supplementary to the discussion in section 4.5. There it is argued that the WZW term with boundary conditions $Q(\mathbf{x}, s=0) = Q^T(\mathbf{x}, s=0)$ is a $\mathbb{Z}_2$ topological term, acquiring only values in $\{0, i\pi\}$ (mod $2\pi i$).

A.1 Topological quantization

Here, a proof is presented, that the WZW term with the boundary conditions has only quantized values. To this end, consider small and slow fluctuations changing the extended Q-field:

$$Q \to e^{iV} Q e^{iW} \approx (\mathbf{1} + iV)\, Q\, (\mathbf{1} + iW)\,.$$

The symmetry condition on the boundary imposes $V(\mathbf{x}, s=0) = W^T(\mathbf{x}, s=0)$. With these assumptions, the variation of the WZW-term vanishes:

$$\begin{aligned}
i\delta S_{WZ} &= \tfrac{ik}{4\pi}\textstyle\int d^2x ds & &\epsilon_{\mu\nu\lambda}\mathrm{tr}\left(Q^{-1}i\partial_\mu V Q\right)\left(Q^{-1}\partial_\nu Q\right)\left(Q^{-1}\partial_\lambda Q\right)\\
&& &+\epsilon_{\mu\nu\lambda}\mathrm{tr}\left(i\partial_\mu W\right)\left(Q^{-1}\partial_\nu Q\right)\left(Q^{-1}\partial_\lambda Q\right)\\
&= \tfrac{ik}{4\pi}\textstyle\int d^2x ds & &\partial_\mu\left\{-i\epsilon_{\mu\nu\lambda}\left(\mathrm{tr}\left[V\partial_\nu Q\partial_\lambda Q^{-1}\right]+\mathrm{tr}\left[W\partial_\nu Q^{-1}\partial_\lambda Q\right]\right)\right\}\\
&= \tfrac{ik}{4\pi}\textstyle\int_{\mathbb{S}^2} d^2x & &\left\{-i\epsilon_{\nu\lambda}\left(\mathrm{tr}\left[V\partial_\nu Q\partial_\lambda Q^{-1}\right]+\mathrm{tr}\left[W\partial_\nu Q^{-1}\partial_\lambda Q\right]\right)\right\}\\
&\overset{\text{boundary cond.}}{=} \tfrac{ik}{4\pi}\textstyle\int_{\mathbb{S}^2} d^2x & &\left\{-i\epsilon_{\nu\lambda}\mathrm{tr}\left[V\left(\partial_\nu Q\partial_\lambda Q^{-1}+\left(\partial_\nu Q^{-1}\partial_\lambda Q\right)^T\right)\right]\right\}\\
&= 0.
\end{aligned}$$

A.2 An exemplary $\mathbb{Z}_2$ instanton

In this section an example for an instanton yielding the non-trivial value

$$i\, S_{WZ}|_{Q(\mathbf{x})=Q^T(\mathbf{x})} = i\pi$$

is exposed. This eventually demonstrates that the interpretation of the WZW term as $\mathbb{Z}_2$ topological term is meaningful.
It is sufficient to restrict oneself to the $SU(2)$ subgroup of the NLσM manifold. The extended fields are defined the following way:

$$Q : \left(\mathbb{R}^2 \times [0,\infty)\right) \cup \{\infty\} \to SU(2) \subset U(2N),$$

hence the boundary $s=0$ is the physical space and $Q(\mathbf{x}, 0) = Q^T(\mathbf{x}, 0)$. Notably, $SU(2)$ is parametrized in the "quaternionic" way

$$Q = a_\mu \tilde{\sigma}_\mu \text{ where } \tilde{\sigma}_\mu = \begin{cases} \mathbf{1}, & \mu = 0, \\ i\sigma_m, & \mu = m \in \{1,2,3\}\,. \end{cases}$$

Now the WZW term is rewritten in terms of the real fields a_μ:

$$\begin{aligned}
iS_{WZ} &= i\tfrac{k}{12\pi}\int d^2x ds\ \epsilon_{\mu\nu\lambda}\ \mathrm{tr}\left(Q^{-1}\partial_\mu Q\right)\left(Q^{-1}\partial_\nu Q\right)\left(Q^{-1}\partial_\lambda Q\right)\\
&= -i\tfrac{k}{12\pi}\int d^2x ds\ \epsilon_{\mu\nu\lambda}\ \mathrm{tr}\left[Q^{-1}\partial_\mu Q\partial_\nu Q^{-1}\partial_\lambda Q\right]\\
&= -i\tfrac{k}{12\pi}\int d^2x ds\ \epsilon_{\mu\nu\lambda}\ a_\alpha\partial_\mu a_\beta\partial_\nu a_\gamma\partial_\lambda a_\delta \mathrm{tr}\left[\tilde\sigma_\alpha^\dagger\tilde\sigma_\beta\tilde\sigma_\gamma^\dagger\tilde\sigma_\delta\right]\\
&= -i\tfrac{k}{6\pi}\int d^2x ds\ \epsilon_{\mu\nu\lambda}\ \{\ +\epsilon_{abc}\ a_a\partial_\mu a_b\partial_\nu a_c\partial_\lambda a_0\\
&\qquad\qquad -\epsilon_{abd}\ a_a\partial_\mu a_b\partial_\nu a_0\partial_\lambda a_d\\
&\qquad\qquad +\epsilon_{cda}\ a_a\partial_\mu a_0\partial_\nu a_c\partial_\lambda a_d\\
&\qquad\qquad -\epsilon_{cdb}\ a_0\partial_\mu a_b\partial_\nu a_c\partial_\lambda a_d\ \}\\
&\overset{\text{boundary cond.}}{=} -i\tfrac{2k}{3\pi}\int d^2x ds\ \epsilon_{\mu\nu\lambda}\ \epsilon_{abc}\ a_a\partial_\mu a_b\partial_\nu a_c\partial_\lambda a_0.
\end{aligned}$$

For a better reading, the coordinates are renamed $x_1 = x,\ x_2 = s,\ x_3 = y$. The Levi-Civita-Symbol acquires an extra minus sign. With this new convention, the instanton of size λ at position $\mathbf{x}_0$ is

$$\begin{aligned}
a_0 &= \frac{\|\mathbf{x}-\mathbf{x}_0\|^2-\lambda^2}{\|\mathbf{x}-\mathbf{x}_0\|^2+\lambda^2},\\
a_k &= \frac{2\lambda\left(x-x_0\right)_k}{\|\mathbf{x}-\mathbf{x}_0\|^2+\lambda^2}.
\end{aligned}$$

(Note, that $a_2 = 0$ on the physical space, in accordance to the boundary conditions.) Differentiating and inserting into the WZW-term,

$$\begin{aligned}
iS_{WZ} &= ik\frac{64\lambda^5}{3\pi}\int d^3x\ \frac{\left(x-x_0\right)_a\left(x-x_0\right)_\mu}{\left(\|\mathbf{x}-\mathbf{x}_0\|^2+\lambda^2\right)^5}\epsilon_{bc\lambda}\epsilon_{bca}\\
&= ik\frac{128\lambda^5}{3\pi}2\pi\int_0^\infty dr\ \frac{r^4}{\left(r^2+\lambda^2\right)^5}\\
&= ik\pi. \qquad\qquad (A.1)
\end{aligned}$$

For odd WZW-levels k, the newly obtained $\mathbb{Z}_2$ topological term indeed acquires the non-trivial value $i\pi \pmod{2\pi i}$.

B Fierz identities

In this section a list of Fierz identities useful for the present work will be given.

SU(N)

Let $\{it^a\}_{a=1}^{N^2-1}$ be a basis of the Lie algebra $\mathfrak{su}(N)$ [9] such that

$$\begin{aligned}
t^{a\dagger} &= t^a,\\
\mathrm{tr}t^a &= 0,\\
\mathrm{tr}t^a t^b &= \delta^{ab}.
\end{aligned}$$

Then

$$\sum_a t^a_{ij}t^a_{kl} = \delta_{il}\delta_{jk} - \frac{1}{N}\delta_{ij}\delta_{kl}. \qquad (B.1)$$

[9] the unconventional notation is due to the physicists' wish to consider hermitian rather than anti-hermitian generators and is kept throughout for consistency

Sp(2N)

Let $\{i\tau^a\}_{a=1}^{N(2N+1)}$ be a basis of the Lie algebra $\mathfrak{sp}(2N)$ such that

$$\begin{aligned} \tau^{a\dagger} &= \tau^a = -\hat{\sigma_y}\tau^{aT}\hat{\sigma_y}, \\ \mathrm{tr}\tau^a &= 0, \\ \mathrm{tr}\tau^a\tau^b &= \delta^{ab}. \end{aligned}$$

($\hat{\sigma_y} = \sigma_y \otimes \mathbb{I}_N$, σ_y is the usual second Pauli-Matrix). Then

$$\sum_a \tau^a_{ij}\tau^a_{kl} = \frac{1}{2}\left(\delta_{il}\delta_{jk} - (\hat{\sigma_y})_{ki}(\hat{\sigma_y})_{jl}\right). \tag{B.2}$$

O(N)

Let $\{i\tau^a\}_{a=1}^{\frac{N(N-1)}{2}}$ be a basis of the Lie algebra $\mathfrak{o}(N)$ such that

$$\begin{aligned} \tau^{a\dagger} &= \tau^a = -\tau^{aT}, \\ \mathrm{tr}\tau^a &= 0, \\ \mathrm{tr}\tau^a\tau^b &= \delta^{ab}. \end{aligned}$$

Then

$$\sum_a \tau^a_{ij}\tau^a_{kl} = \frac{1}{2}\left(\delta_{il}\delta_{jk} - \delta_{ki}\delta_{jl}\right). \tag{B.3}$$

$\frac{\mathbf{SU(2N)}}{\mathbf{Sp(2N)}}$

Let $\{it^a\}_{a=1}^{N(2N-1)-1}$ be a basis of the tangent space $\mathfrak{p}_{\frac{SU(2N)}{Sp(2N)}}$ such that

$$\begin{aligned} t^{a\dagger} &= t^a = \hat{\sigma_y}t^{aT}\hat{\sigma_y}, \\ \mathrm{tr}t^a &= 0, \\ \mathrm{tr}t^at^b &= \delta^{ab}. \end{aligned}$$

Then

$$\sum_a t^a_{ij}t^a_{kl} = \frac{1}{2}\left(\delta_{il}\delta_{jk} + (\hat{\sigma_y})_{ki}(\hat{\sigma_y})_{jl}\right) - \frac{1}{2N}\delta_{ij}\delta_{kl}. \tag{B.4}$$

$\frac{\mathbf{SU(N)}}{\mathbf{O(N)}}$

Let $\{it^a\}_{a=1}^{\frac{N(N+1)}{2}-1}$ be a basis of the tangent space $\mathfrak{p}_{\frac{SU(N)}{O(N)}}$ such that

$$\begin{aligned} t^{a\dagger} &= t^a = t^{aT}, \\ \mathrm{tr}t^a &= 0, \\ \mathrm{tr}t^at^b &= \delta^{ab}. \end{aligned}$$

Then

$$\sum_a t^a_{ij}t^a_{kl} = \frac{1}{2}\left(\delta_{il}\delta_{jk} + \delta_{ki}\delta_{jl}\right) - \frac{1}{N}\delta_{ij}\delta_{kl}. \tag{B.5}$$

C Derivation of renormalized coupling constants

C.1 Renormalized action

First divide the Q-field in the bare action,

$$S_0[Q] = \int d^2x \left\{ \frac{\sigma_0}{8\pi} tr\left[\nabla Q^{-1}\nabla Q\right] - \frac{c_0}{8\pi}\left[\mathrm{tr} Q^{-1}\nabla Q\right]^2 + \frac{\sigma_0}{8\pi}\frac{m^2}{4}\mathrm{tr}\left[Q - Q^{-1}\right]^2 \right\},$$

into fast and slow contributions:

$$Q \to U^{-1}QV,$$

where U, V describe slowly varying fields and Q is fast. Hence,

$$S_0[Q] \to S_0\left[\left(U^{-1}V\right)\right] + S_0[Q] + S_{IA}[Q,U,V]. \tag{C.1}$$

Now expand the exponential in S_{IA} to second order in gradients of slow fields and reexponentiate the Q-averaged terms to obtain the renormalized action:

$$\begin{aligned}
S'\left[\left(U^{-1}V\right)\right] &= S_0\left[\left(U^{-1}V\right)\right] \\
&+ \int d^2x\, \frac{\sigma_0}{4\pi}\left\langle \mathrm{tr}\left[Q^{-1}\left(U\nabla U^{-1}\right)Q\left(V\nabla V^{-1}\right) - \left(U\nabla U^{-1}\right)\left(V\nabla V^{-1}\right)\right]\right\rangle \\
&- \frac{1}{2}\int d^2x d^2x' \\
&\quad \langle\{\frac{\sigma_0}{4\pi}\mathrm{tr}\left[\left(Q\nabla Q^{-1}\right)\left(U\nabla U^{-1}\right) + \left(Q^{-1}\nabla Q\right)\left(V\nabla V^{-1}\right)\right] \\
&\qquad\qquad -\frac{c_0}{4\pi}\mathrm{tr}\left[Q^{-1}\nabla Q\right]\mathrm{tr}\left[\left(U^{-1}V\right)^{-1}\nabla\left(U^{-1}V\right)\right]\}_x \\
&\quad \{\frac{\sigma_0}{4\pi}\mathrm{tr}\left[\left(Q\nabla Q^{-1}\right)\left(U\nabla U^{-1}\right) + \left(Q^{-1}\nabla Q\right)\left(V\nabla V^{-1}\right)\right] \\
&\qquad\qquad -\frac{c_0}{4\pi}\mathrm{tr}\left[Q^{-1}\nabla Q\right]\mathrm{tr}\left[\left(U^{-1}V\right)^{-1}\nabla\left(U^{-1}V\right)\right]\}_{x'}\rangle.
\end{aligned}$$

Here $\langle ... \rangle = \int \mathcal{D}[Q] ... e^{-S_0[Q]}$ denotes the average over fast fields.

C.2 Background field formalism

In order to calculate the renormalized coupling constants σ and c, the background field formalism is employed (similar to [Pru87a]).

U(1)-Goldstone bosons

First consider, for all symmetry classes, the slow modes g_0 of U(1)-subgroup: $U^{-1} = V = e^{\frac{i}{2}g_0\mathbf{1}}$. These renormalize $\sigma + \mathrm{tr}\mathbf{1}c$. As the renormalization of σ is calculated below, the formula for c is given:

$$c = c_0 - \frac{\sigma - \sigma_0}{\mathrm{tr}\mathbf{1}} + \frac{1}{\mathrm{Vol}^2}\int d^2x d^2x' \frac{\left(\sigma_0 + \mathrm{tr}\mathbf{1}c_0\right)^2}{8\pi\left(\mathrm{tr}\mathbf{1}\right)^2}\left\langle \mathrm{tr}\left[\left(Q^{-1}\nabla Q\right)_x\right]\mathrm{tr}\left[\left(Q^{-1}\nabla Q\right)_{x'}\right]\right\rangle. \tag{C.2}$$

($\mathrm{Vol} := \int d^2x$).

Goldstone bosons of special submanifold

Now consider the slow Goldstone modes g_a, which live on the special submanifold $S\mathcal{M}$ of the σ-model manifold $\mathcal{M}$:

class	$S\mathcal{M}$	slow fields	generators
AIII	$SU(N)$	$U^{-1} = V = e^{\frac{i}{2} g_a t^a}$	$t^{a\dagger} = t^a$; $\mathrm{tr} t^a = 0$; $\mathrm{tr} t^a t^b = \delta^{ab}$
BDI	$SU(2N)/Sp(2N)$	$\sigma_y U^{-T} \sigma_y = V = e^{\frac{i}{2} g_a t^a}$	$t^{a\dagger} = t^a = \sigma_y t^{aT} \sigma_y$; $\mathrm{tr} t^a = 0$; $\mathrm{tr} t^a t^b = \delta^{ab}$
CII	$SU(N)/O(N)$	$U^{-T} = V = e^{\frac{i}{2} g_a t^a}$	$t^{a\dagger} = t^a = t^{aT}$; $\mathrm{tr} t^a = 0$; $\mathrm{tr} t^a t^b = \delta^{ab}$

Note that the Goldstone modes are considered one by one, hence within this paragraph $g_a t^a$ is not to be understood as a (Einstein-) sum.
This way one obtains

$$\begin{aligned}
\sigma \quad = \quad & \sigma_0 + \frac{1}{\mathrm{Vol}} \int d^2x \frac{1}{2} \left\langle \mathrm{tr}\left[Q^{-1} t^a Q t^a - t^{a2}\right]\right\rangle \\
& + \frac{1}{\mathrm{Vol}^2} \int d^2x d^2x' \frac{\sigma_0^2}{16\pi} \\
& \quad \left\langle \mathrm{tr}\left[\left(Q\nabla Q^{-1}\right)_x t^a\right] \mathrm{tr}\left[\left(Q\nabla Q^{-1}\right)_{x'} t^a\right] - \mathrm{tr}\left[\left(Q\nabla Q^{-1}\right)_x t^a\right] \mathrm{tr}\left[\left(Q^{-1}\nabla Q\right)_{x'} t^a\right]\right\rangle \\
\overset{\text{CII, BDI}}{=} \quad & \sigma_0 + \frac{1}{\mathrm{Vol}} \int d^2x \frac{1}{2} \left\langle \mathrm{tr}\left[Q^{-1} t^a Q t^a - t^{a2}\right]\right\rangle \\
& + \frac{1}{\mathrm{Vol}^2} \int d^2x d^2x' \frac{\sigma_0^2}{8\pi} \left\langle \mathrm{tr}\left[\left(Q^{-1}\nabla Q\right)_x t^a\right] \mathrm{tr}\left[\left(Q^{-1}\nabla Q\right)_{x'} t^a\right]\right\rangle . \qquad \text{(C.3)}
\end{aligned}$$

Stabilizer modes

Finally stabilizer modes s_a, which will not generate any translation on the manifold, are considered.

class	stabilizer	slow fields	generators
AIII	$SU(N)$	$U = V = e^{\frac{i}{2} s_a \tau^a}$	$\tau^{a\dagger} = \tau^a$; $\mathrm{tr}\tau^a = 0$; $\mathrm{tr}\tau^a\tau^b = \delta^{ab}$
BDI	$Sp(2N)$	$\sigma_y U^{-T} \sigma_y = V = e^{\frac{i}{2} s_a \tau^a}$	$\tau^{a\dagger} = \tau^a = -\sigma_y \tau^{aT} \sigma_y$; $\mathrm{tr}\tau^a = 0$; $\mathrm{tr}\tau^a\tau^b = \delta^{ab}$
CII	$O(N)$	$U^{-T} = V = e^{\frac{i}{2} s_a \tau^a}$	$\tau^{a\dagger} = \tau^a = -\tau^{aT}$; $\mathrm{tr}\tau^a = 0$; $\mathrm{tr}\tau^a\tau^b = \delta^{ab}$

This leads to the following Ward-identity:

$$\begin{aligned}
\int d^2x \left\langle \mathrm{tr}\left[Q^{-1}\tau^a Q t^a - \tau^{a2}\right]\right\rangle \quad = \quad & \frac{1}{\mathrm{Vol}} \int d^2x d^2x' \frac{\sigma_0}{8\pi} \langle \mathrm{tr}\left[\left(Q\nabla Q^{-1}\right)_x \tau^a\right] \mathrm{tr}\left[\left(Q\nabla Q^{-1}\right)_{x'} \tau^a\right] \\
& + \mathrm{tr}\left[\left(Q\nabla Q^{-1}\right)_x \tau^a\right] \mathrm{tr}\left[\left(Q^{-1}\nabla Q\right)_{x'} \tau^a\right]\rangle \\
\overset{\text{CII, BDI}}{=} \quad & \frac{1}{\mathrm{Vol}} \int d^2x d^2x' \frac{\sigma_0}{4\pi} \left\langle \mathrm{tr}\left[\left(Q^{-1}\nabla Q\right)_x \tau^a\right] \mathrm{tr}\left[\left(Q^{-1}\nabla Q\right)_{x'} \tau^a\right]\right\rangle . \qquad \text{(C.4)}
\end{aligned}$$

C.3 Renormalized coupling constants

Now, both the renormalization of σ (C.3) and the Ward identity (C.4) are averaged over generators using the Fierz identities (B.1) - (B.5). The second term in (C.3) becomes of the type $\mathrm{tr}Q^{-1}\mathrm{tr}Q + ...$ and is replaced using the Ward identity. Finally one obtains:

$$\sigma = \sigma_0 + \frac{1}{\mathrm{Vol}} \int d^2x d^2x' \, \frac{\sigma_0^2}{8\pi} \frac{1}{\mathrm{tr}\mathbf{1} \; dim\left[S\mathcal{M}\right]} \left\{ \mathrm{tr}\mathbf{1} \left\langle \mathrm{tr}\left[\left(Q^{-1}\nabla Q\right)_x \left(Q^{-1}\nabla Q\right)_{x'} \right] \right\rangle - \left\langle \mathrm{tr}\left[\left(Q^{-1}\nabla Q\right)_x \right] \mathrm{tr}\left[\left(Q^{-1}\nabla Q\right)_{x'} \right] \right\rangle \right\}, \tag{C.5}$$

$$c = c_0 + \frac{1}{\mathrm{Vol}} \int d^2x d^2x' \, \frac{\sigma_0^2}{8\pi} \frac{-1}{\mathrm{tr}\mathbf{1} \; dim\left[S\mathcal{M}\right]} \left\langle \mathrm{tr}\left[\left(Q^{-1}\nabla Q\right)_x \left(Q^{-1}\nabla Q\right)_{x'} \right] \right\rangle + \left[\frac{\sigma_0^2}{8\pi} \frac{dim\left[\mathcal{M}\right]}{\left(\mathrm{tr}\mathbf{1}\right)^2 \; dim\left[S\mathcal{M}\right]} + \frac{2\sigma_0 c_0}{\mathrm{tr}\mathbf{1} \; 8\pi} + \frac{c_0^2}{8\pi} \right] \left\langle \mathrm{tr}\left[\left(Q^{-1}\nabla Q\right)_x \right] \mathrm{tr}\left[\left(Q^{-1}\nabla Q\right)_{x'} \right] \right\rangle. \tag{C.6}$$

Hence for all three chiral symmetry classes the conductivity and the coupling constant of the Gade term are renormalized in an equivalent way by current-current correlation functions.
The dimensions of the corresponding manifolds are listed below ($dim\left[\mathcal{M}\right] = dim\left[S\mathcal{M}\right]+1$).

	$S\mathcal{M}$	$dim\left[S\mathcal{M}\right]$	$\mathrm{tr}\mathbf{1}$
AIII	$SU(N)$	N^2-1	N
BDI	$\frac{SU(2N)}{Sp(2N)}$	$2N^2-N-1$	$2N$
CII	$\frac{SU(N)}{O(N)}$	$\frac{N^2+N-2}{2}$	N

C.4 Kubo formula in terms of background fields

Here the connection between the Kubo formula and eq. (C.5) shall be made. To this end, the fermionic chiral action at the saddle point is considered

$$S = \int d^2x \; \bar{\Psi} \begin{pmatrix} i\gamma Q & \xi\left(\mathbf{p}\right) \\ \xi^*\left(\mathbf{p}\right) & i\gamma Q^{-1} \end{pmatrix} \Psi,$$

where $\xi\left(\mathbf{p}\right)$ is a function of momentum operators, which depends on the underlying microscopic theory. The substitution $Q \to U^{-1}QV$ is absorbed into a slow rotation of fermionic degrees of freedom [10]. This way, there arises an extra term in the action:

$$\delta S = \int d^2x \; \bar{\Psi} \begin{pmatrix} 0 & U\left[\xi\left(\mathbf{p}\right), U^{-1}\right] \\ V\left[\xi^*\left(\mathbf{p}\right), V^{-1}\right] & 0 \end{pmatrix} \Psi.$$

Goldstone modes

First, consider Goldstone bosons of the special submanifold $U^{-1} = V = e^{\frac{i}{2}g_a t^a}$ as in sec. C.2. Again the gradients of g_a are constant and the modes are considered one by one. Then,

$$\delta S = \int d^2x \; \bar{\Psi} \begin{pmatrix} 0 & \frac{i}{2}\left[\xi\left(\mathbf{p}\right), g_a\right] t^a \\ -\frac{i}{2}\left[\xi^*\left(\mathbf{p}\right), g_a\right] t^a & 0 \end{pmatrix} \Psi = -\frac{1}{2} \int d^2x \; \bar{\Psi}\left(\nabla g_a\right) \cdot \mathbf{j} \, \sigma_z t^a \Psi.$$

$\mathbf{j}$ is the current operator $\frac{\delta S}{\delta p}$.

[10] Even though the theory might display chiral anomaly, this rotation has unit Jacobian as it is slow.

Stabilizer modes

Next, the stabilizer modes $U = V = e^{\frac{i}{2}s_a\tau^a}$ are considered:

$$\delta S = \int d^2x\ \bar{\Psi}\begin{pmatrix} 0 & -\frac{i}{2}\left[\xi\left(\mathbf{p}\right), s_a\right]\tau^a \\ -\frac{i}{2}\left[\xi^*\left(\mathbf{p}\right), s_a\right]\tau^a & 0 \end{pmatrix}\Psi = -\frac{1}{2}\int d^2x\ \bar{\Psi}\left(\nabla s_a\right)\cdot\mathbf{j}\,\tau^a\Psi.$$

Kubo formula

Differentiating twice the partition function with respect to the gradients of Goldstone respectively stabilizer modes and averaging over generators yields the conductivity,

$$\begin{aligned}
\sigma \overset{\left\{\begin{smallmatrix}\text{AIII}\\ \text{BDI \& CII}\end{smallmatrix}\right\}}{=} & \frac{\left\{\begin{smallmatrix}4\\8\end{smallmatrix}\right\}}{\pi}\mathrm{Tr}\left\langle \left.\frac{\delta^2}{\delta\left(\partial_x s_a\right)^2}\right|_{(\partial_x s_a)=0}\mathcal{Z}\left[(\partial_\mu s_a)\right] - \left.\frac{\delta^2}{\delta\left(\partial_x g_a\right)^2}\right|_{(\partial_x g_a)=0}\mathcal{Z}\left[(\partial_\mu g_a)\right]\right\rangle_{\text{gen.}} \\
= & \frac{\left\{\begin{smallmatrix}1\\2\end{smallmatrix}\right\}}{\pi}\mathrm{Tr}\left\langle \overline{\bar{\Psi} j_x\,\tau^a\Psi\bar{\Psi} j_x\,\tau^a\Psi} - \overline{\bar{\Psi} j_x\,\sigma_z t^a\Psi\bar{\Psi} j_x\,\sigma_z t^a\Psi}\right\rangle_{\text{generators}} \\
\overset{SCBA}{=} & -\frac{1}{\pi}\mathbf{tr}\left[j_x\mathcal{G}^R j_x\mathcal{G}^R - j_x\mathcal{G}^R j_x\mathcal{G}^A\right].
\end{aligned} \tag{C.7}$$

'Tr' includes trace over flavours, replicas, spins and integration over space, whereas **tr** excludes replicas. Note that for classes BDI and CII, the τ-space (valley) degree of freedom is incorporated into the NLσM manifold [11]. To reobtain it after averaging over generators, the extra factor of 2 had to be included.
On the other hand, differentiating the renormalized NLσM action in the above way(s) yields

$$\sigma = \begin{cases} \frac{1}{\pi^2}\times(\text{eq. (C.5)}) = \frac{n}{\pi^2} + \ldots & \text{AIII,} \\ \frac{2}{\pi^2}\times(\text{eq. (C.5)}) = \frac{2n}{\pi^2} + \ldots & \text{BDI \& CII.} \end{cases}$$

(in units of $\left[\frac{e^2}{\hbar}\right]$.) This eventually motivates the slow (background) fields to have constant gradient and assigns eq.s (C.5) and (C.6) the correct physical meaning.

D Perturbative corrections

In order to calculate the average over fast fields in the given non-linear integration space, exponential coordinates will be chosen:

$$Q = e^{iW_a t^a} \approx \mathbf{1} + iW_a t^a - \frac{1}{2}W_a W_b t^a t^b.$$

The summation is to be understood. The generators t^a live on $\mathfrak{u}(N)$, $\mathfrak{p}_{\frac{U(2N)}{Sp(2N)}}$ and $\mathfrak{p}_{\frac{U(N)}{O(N)}}$ for classes AIII, BDI and CII respectively. Note that $t^0 = \frac{1}{\sqrt{\mathrm{tr}1}}$ is now explicitely included.

[11] Even though $\frac{U(N)}{O(N)}$ is used throughout, in the derivation of class CII NLσM (see ch. 4) it becomes apparent that for microscopic reason $\frac{U(2N)}{O(2N)}$ is necessary.

Fast propagators

Expanding the bare action (5.1) for fast fields to order $\mathcal{O}\left(W^2\right)$, the propagators for the W_a fields follow:

$$\left\langle W_a\left(\mathbf{p}\right)W_b\left(\mathbf{q}\right)\right\rangle = \Pi_a\left(\mathbf{q}\right)\delta^{ab}\left(2\pi\right)^2\delta\left(\mathbf{p}+\mathbf{q}\right), \tag{D.1}$$

where

$$\Pi_a\left(\mathbf{q}\right) = \begin{cases} \frac{8\pi}{2(\sigma_0(\mathbf{q}^2+m^2)+\mathrm{tr}\mathbf{1}c_0\mathbf{q}^2)}, & \text{if } a=0, \\ \frac{8\pi}{2\sigma_0(\mathbf{q}^2+m^2)}, & \text{else.} \end{cases} \tag{D.2}$$

Expectation value of single trace term

$$\begin{aligned} \int d^2x d^2x' \quad & \left\langle \mathrm{tr}\left[\left(Q^{-1}\nabla Q\right)_x\left(Q^{-1}\nabla Q\right)_{x'}\right]\right\rangle \\ \doteq \quad & \int\left(\mathbf{dp}\right)\left(\mathbf{dp}'\right)\frac{-\mathbf{p}\cdot\mathbf{p}'}{4}\left\langle W_a^{-\mathbf{p}}W_b^{\mathbf{p}}W_c^{-\mathbf{p}'}W_d^{\mathbf{p}'}\right\rangle \mathrm{tr}\left[\left[t^a,t^b\right]\left[t^c,t^d\right]\right] \\ = \quad & \mathrm{Vol}\frac{8\pi}{\sigma_0^2}\ln\frac{\Lambda}{m}\sum_{S\mathcal{M}}\mathrm{tr}\left[t^at^bt^at^b - t^{a2}t^{b2}\right] \\ = \quad & -\mathrm{Vol}\,\ln\frac{\Lambda}{m}\frac{8\pi}{\sigma_0^2}\mathrm{tr}\mathbf{1}dim\left[S\mathcal{M}\right]\begin{cases} 1 & \text{AIII}, \\ \frac{1}{2} & \text{BDI}, \\ \frac{1}{2} & \text{CII}. \end{cases} \end{aligned} \tag{D.3}$$

The dot above first equals sign indicates that terms with less than four W-fields are zero (integral over one fast and one slow field).

Expectation value of term with two traces

$$\begin{aligned} \int d^2x d^2x' \quad & \left\langle \mathrm{tr}\left[\left(Q^{-1}\nabla Q\right)_x\right]\mathrm{tr}\left[\left(Q^{-1}\nabla Q\right)_{x'}\right]\right\rangle \\ \doteq \quad & \int\left(\mathbf{dp}\right)\left(\mathbf{dp}'\right)\frac{-\mathbf{p}\cdot\mathbf{p}'}{4}\left\langle W_a^{-\mathbf{p}}W_b^{\mathbf{p}}W_c^{-\mathbf{p}'}W_d^{\mathbf{p}'}\right\rangle \mathrm{tr}\left[t^a,t^b\right]\mathrm{tr}\left[t^c,t^d\right] \\ = \quad & 0. \end{aligned} \tag{D.4}$$

Perturbative corrections to coupling constants

$$\Delta\sigma^{pert} = -\mathrm{tr}\mathbf{1}\ln\frac{\Lambda}{m}\begin{cases} 1 & \text{AIII}, \\ \frac{1}{2} & \text{BDI}, \\ \frac{1}{2} & \text{CII}. \end{cases} \tag{D.5}$$

$$\Delta c^{pert} = \ln\frac{\Lambda}{m}\begin{cases} 1 & \text{AIII}, \\ \frac{1}{2} & \text{BDI}, \\ \frac{1}{2} & \text{CII}. \end{cases} \tag{D.6}$$

E Supersymmetric calculation of the perturbative corrections in AIII

It shall be demonstrated that one-loop perturbation theory is exact for the AIII-NLσM. Consider the supersymmetric version of the bare action (5.1)

$$S_0[Q] = \int d^2x \left\{ -\frac{\sigma_0}{8\pi} \mathrm{Str}\left[\nabla Q^{-1} \nabla Q\right] - \frac{c_0}{8\pi} \left[\mathrm{Str} Q^{-1} \nabla Q\right]^2 \right\}.$$

The following parametrization of the field $Q \in U(1|1)$ will be used:

$$Q = \begin{pmatrix} 1 & 0 \\ \nu & 1 \end{pmatrix} \begin{pmatrix} 1 & \mu \\ 0 & 1 \end{pmatrix} \begin{pmatrix} e^a & 0 \\ 0 & e^{ib} \end{pmatrix} = \begin{pmatrix} 1 & 0 \\ \nu & 1 \end{pmatrix} \begin{pmatrix} e^a & 0 \\ 0 & e^{ib} \end{pmatrix} \begin{pmatrix} 1 & \mu' \\ 0 & 1 \end{pmatrix}.$$

($\mu' = e^{-(a-ib)}\mu$. $a \in \mathbb{R}$, $b \in [0, 2\pi)$, μ, ν, μ' Grassmannians).
Direct computation yields

$$\begin{aligned} \mathrm{Str}\left[dQ dQ^{-1}\right] &= -\left[(da)^2 + (db)^2 + 2e^{a-ib} d\mu' d\nu\right] \\ &= -\begin{pmatrix} da & db & d\mu & d\nu \end{pmatrix} \begin{pmatrix} 1 & 0 & 0 & -\mu \\ 0 & 1 & 0 & i\mu \\ 0 & 0 & 0 & 1 \\ \mu & -i\mu & -1 & 0 \end{pmatrix} \begin{pmatrix} da \\ db \\ d\mu \\ d\nu \end{pmatrix}. \end{aligned}$$

Therefore, this parametrization has a trivial Jacobian. Defining $\psi := a - ib$, the action is

$$S = \int d^2x \, \frac{\sigma_0}{8\pi} \left[|\nabla\psi|^2 + 2\nabla\mu\nabla\nu - 2\nabla\psi\mu\nabla\nu\right] - \frac{c}{8\pi} (\nabla\psi)^2. \tag{E.1}$$

This implies the Feynman rules depicted in fig. E.1 (for consistency, mass-term regularization is used again). In particular, there exists only a single possible Feynman graph (fig. E.2) to correct any of the two coupling constants σ_0, c_0.
The graph corrects c in the following way (the approximation of slow external momenta is denoted by "$\approx$"):

$$\begin{aligned} \frac{1}{2}\langle S_{IA}\rangle &= \frac{1}{2}\left(\frac{\sigma}{4\pi}\right)^2 \int d^2x d^2x' \, (\partial_\alpha\psi)_{\mathbf{x}} \, (\partial_\beta\psi)_{\mathbf{x}'} \left\langle (\mu\partial_\alpha\nu)_{\mathbf{x}} \, (\mu\partial_\beta\nu)_{\mathbf{x}'} \right\rangle \\ &\approx \frac{1}{2} \int (\mathbf{dp}) \, \frac{p_\alpha p_\beta}{(\mathbf{p}^2 + m^2)} \int d^2x \; (\partial_\alpha\psi)\,(\partial_\beta\psi) \\ &\approx \int dp \, \frac{p}{p^2 + m^2} \int d^2x \, \frac{(\nabla\psi)^2}{8\pi} \\ &= \ln\frac{\Lambda}{m} \int d^2x \, \frac{(\nabla\psi)^2}{8\pi}. \end{aligned}$$

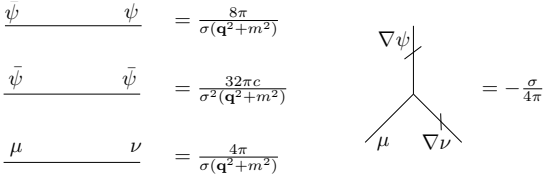

Figure E.1: Feynman rules for the action (E.1)

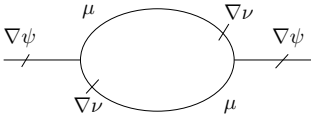

Figure E.2: The only possible Feynman diagram.

Eventually, the *exact* RG-equations are [12]

$$\begin{aligned} -\tfrac{d\sigma}{d\ln m} &= 0, \\ -\tfrac{dc}{d\ln m} &= 1. \end{aligned}$$

F $\mathbb{Z}_2$-Instanton in class CII

First replace the topologically trivial saddle point $Q = \mathbf{1}$ by an instanton solution: Here a simple rotation of the generalized $O(3)$-instanton (skyrmion) used by Pruisken [Pru87a] will be considered:

$$Q_{\mathbb{Z}_2} = \begin{pmatrix} \tilde{Q}_{\mathbb{Z}_2} & \vec{0}^T \\ \vec{0} & \mathbf{1}_{(2N-2)\times(2N-2)} \end{pmatrix},$$

where

$$\begin{aligned} \tilde{Q}_{\mathbb{Z}_2} &= \frac{1}{\lambda^2 + \|\mathbf{x}-\mathbf{x}_0\|} \begin{pmatrix} \|\mathbf{x}-\mathbf{x}_0\|^2 - \lambda^2 + i2\lambda\,(x-x_0) & i2\lambda\,(y-y_0) \\ i2\lambda\,(y-y_0) & \|\mathbf{x}-\mathbf{x}_0\|^2 - \lambda^2 - i2\lambda\,(x-x_0) \end{pmatrix} \\ &= a_3\mathbf{1}_2 + ia_2\sigma_x + ia_1\sigma_z, \end{aligned}$$

and $\mathbf{a} = \frac{1}{\lambda^2+\|\mathbf{x}-\mathbf{x}_0\|}\left(2\lambda\,(x-x_0)\,, 2\lambda\,(y-y_0)\,, \|\mathbf{x}-\mathbf{x}_0\|^2 - \lambda^2\right)^T$ represents the $O(3)$-instanton of size λ and at position $\mathbf{x}_0$.
The solution chosen precisely corresponds to Pruisken's version of the instantons for the QHE, only the boundary condition here is different: $Q_{\mathbb{Z}_2} \xrightarrow{\mathbf{r}\to\infty} \mathbf{1}$ for chiral systems, as there is no advanced/retarded space. Therefore, the version given above is simply

$$Q_{\mathbb{Z}_2} = U^{-1}\sigma_3 Q_{QHE} U \text{ where } U = \frac{1}{\sqrt{2}}\left(\mathbf{1} - i\sigma_x\right).$$

Action with instanton configuration

As $Q_{\mathbb{Z}_2} \in SU(N)$ the Gade-term does not contribute to the instanton action:

$$\operatorname{tr}\left[Q^{-1}\partial_\mu Q\right] = \mathbf{a}\cdot\partial_\mu\mathbf{a} = 0 \text{ as } \|\mathbf{a}\| = 1. \tag{F.1}$$

Hence, only the kinetic term contributes to the action

$$S_{\mathbb{Z}_2} = 2\sigma_0 + i\pi,$$

consistent with [Pru87b].

Volume of space of possible projections

As with vortices, the instanton can be inserted equivalently in any other pair of replicas. Rotating the instanton by all $O(N)$ yields an overcounting of same configurations. To understand the space of projections write

$$\begin{aligned} Q_{\mathbb{Z}_2} &= a_3 \begin{pmatrix} \mathbf{1}_2 & \vec{0}^T \\ \vec{0} & \mathbf{0}_{(2N-2)\times(2N-2)} \end{pmatrix} \\ &+ ia_2 \begin{pmatrix} \sigma_x & \vec{0}^T \\ \vec{0} & \mathbf{0}_{(2N-2)\times(2N-2)} \end{pmatrix} \\ &+ ia_1 \begin{pmatrix} \sigma_z & \vec{0}^T \\ \vec{0} & \mathbf{0}_{(2N-2)\times(2N-2)} \end{pmatrix} \\ &+ \begin{pmatrix} \mathbf{0}_{2\times2} & \vec{0}^T \\ \vec{0} & \mathbf{1}_{(2N-2)\times(2N-2)} \end{pmatrix}. \end{aligned}$$

[12] This matches eq.s (5.5).

In order to determine the stabilizer look for the subgroup of $O(N)$ of matrices commuting with $Q_{\mathbb{Z}_2}$. Because of the first and the last term, the stabilizer has to be a subgroup of $O(2) \times O(N-2)$. Among the $O(2)$-matrices, all except $\{\pm\mathbf{1}\}$ do not commute with σ_x and σ_y.
Therefore the volume of the space covered by projections of the instanton is

$$\mathrm{Vol}_{\hat{P}_{inst}} = \mathrm{Vol}\frac{O(N)}{\mathbb{Z}_2 \times O(N-2)} = \mathrm{Vol}\frac{O(N)}{\mathbb{Z}_2 \times O(N-1)}\frac{O(N-1)}{O(N-2)} = 2\frac{\pi^{N-\frac{1}{2}}}{\Gamma\left(\frac{N}{2}\right)\Gamma\left(\frac{N-1}{2}\right)}.$$

Other degrees of freedom of the instanton

The instanton can further be shifted in space and turned around its center without changing the value of the action. As the corrections to the coupling constants are also invariant under these transformations (see (F.2)), they will be *multiplied* by $2\pi\mathrm{Vol}$. Note that the non-vanishing expectation value is not λ-independent, it will hence be *integrated* using the following measure:

$$\int \frac{d\lambda}{\lambda^3} \langle ... \rangle .$$

For a derivation, see [Pru87b].

Expectation values with instanton configuration

As stated above (F.1), only the single trace term has a non-vanishing expectation value. As the instanton is precisely the same as Pruisken's, here his result [Pru87a] p.77 formula (6.10a) is copied

$$\int d^2x d^2x' \left\langle \mathrm{tr}\left[\left(Q^{-1}\nabla Q\right)_x \left(Q^{-1}\nabla Q\right)_{x'}\right]\right\rangle_{\mathbb{Z}_2} = -16\pi^2\lambda^2. \tag{F.2}$$

Instanton induced corrections

Collecting the results from above and of equations (C.5) and (C.6) the corrections to the coupling constants are:

$$\Delta\sigma^{\mathbb{Z}_2} = N4\pi^2\sigma_0^2 e^{-2\sigma_0}\frac{Vol_{\hat{P}}}{N\dim\frac{SU(N)}{O(N)}}\ln\frac{\Lambda}{m}, \tag{F.3}$$

$$\Delta c^{\mathbb{Z}_2} = -4\pi^2\sigma_0^2 e^{-2\sigma_0}\frac{Vol_{\hat{P}}}{N\dim\frac{SU(N)}{O(N)}}\ln\frac{\Lambda}{m}, \tag{F.4}$$

where $\frac{Vol_{\hat{P}}}{N\dim\frac{SU(N)}{O(N)}} = \frac{4\pi^N}{\sqrt{\pi}N(N+2)(N-1)\Gamma\left(\frac{N}{2}\right)\Gamma\left(\frac{N-1}{2}\right)} = \frac{\pi^N}{\sqrt{\pi}(N+2)\Gamma\left(\frac{N}{2}+1\right)\Gamma\left(\frac{N+1}{2}\right)} \to \frac{1}{2\pi}$. The arrow indicates replica limit

G Estimate of the core energy of a vortex

The core energy is defined

$$S_{\mathrm{core}} = V_{\mathrm{inside}}\left(s_{inside} - s_{outside}\right), \tag{G.1}$$

where s indicates the action per unit volume. For the AIII-model considered in sec. 7.2.2 the difference of action per unit volume is

$$\begin{aligned}
s_{inside} - s_{outside} &= \frac{n\gamma^2}{\pi\alpha}(N-1) - n(N-1)\int (\mathbf{dp})\, ln\left(\mathbf{p}^2+\gamma^2\right) - n\int (\mathbf{dp})\, ln\left(\mathbf{p}^2\right) \\
&\quad -\frac{n\gamma^2}{\pi\alpha}N + nN\int (\mathbf{dp})\, ln\left(\mathbf{p}^2+\gamma^2\right) \\
&\overset{SCBA}{=} -n\int (\mathbf{dp})\,\frac{\gamma^2}{\mathbf{p}^2+\gamma^2} + ln\left(1-\frac{\gamma^2}{\mathbf{p}^2+\gamma^2}\right) \\
&\overset{\frac{\gamma^2}{\mathbf{p}^2+\gamma^2}\in(0,1]}{=} n\int (\mathbf{dp})\sum_{n=2}^{\infty}\frac{1}{n}\left(\frac{\gamma^2}{\mathbf{p}^2+\gamma^2}\right)^n \\
&\overset{k:=\frac{\mathbf{p}^2+\gamma^2}{\gamma^2}}{=} \frac{n\gamma^2}{4\pi}\sum_{n=2}^{\infty}\frac{1}{n(n-1)}\, k^{-n+1}\big|_{k=1}^{\infty} \\
&= \frac{n\gamma^2}{4\pi}\left(\sum_{n=2}^{\infty}-\frac{1}{n}+\frac{1}{n-1}\right) = \frac{n\gamma^2}{4\pi}.
\end{aligned} \tag{G.2}$$

Multiplying this result with the volume of the vortex core yields

$$S_{\text{core}} = \frac{n}{4}. \tag{G.3}$$

H Vortex-induced corrections

In order to calculate the effect of the vortices, the ordinary saddle point $Q_{SP} = \mathbf{1}$ will be replaced by a field configuration including one vortex-antivortex pair. This corresponds to the situation of a dilute gas of vortex dipoles, which are of small extension.

$$Q_{SP} = Q_{V-AV} = e^{i\left[\phi_{\mathbf{x}_1}(\mathbf{x})-\phi_{\mathbf{x}_2}(\mathbf{x})\right]}\hat{P} + \left(\mathbf{1}-\hat{P}\right). \tag{H.1}$$

The fact that the function $\phi_{\mathbf{x}_i}(\mathbf{x})$ describes a vortex at position $\mathbf{x} = \mathbf{x}_i$ is encoded in its (analytical) property

$$\nabla_\mu \phi_{\mathbf{x}_i}(\mathbf{x}) = \text{rot}_\mu \ln\frac{\|\mathbf{x}-\mathbf{x}_i\|}{\gamma^{-1}}$$

(γ^{-1} is the vortex core diameter).

The projection operator $\hat{P}$ maps onto a single-replica subspace, for example

$$\hat{P} = \begin{cases} \begin{pmatrix} 1 & \vec{0}^T \\ \vec{0} & \mathbf{0}_{N-1} \end{pmatrix} & \text{for classes AIII and CII,} \\ \begin{pmatrix} \mathbf{1}_2 & \vec{0}^T \\ \vec{0} & \mathbf{0}_{2N-2} \end{pmatrix} & \text{for class BDI.} \end{cases}$$

Below, the integration over all possible projections will be performed.

Action for vortex-antivortex pair

Introducing the vortex-dipole (H.1) into the bare action (3.3) one obtains

$$S_{V-AV} = 2S_{core} + \text{tr}\hat{P}\frac{\sigma_0 + \text{tr}\hat{P}c_0}{2}\ln\frac{\|\mathbf{x}_1-\mathbf{x}_2\|}{\gamma^{-1}} + S_m. \tag{H.2}$$

The mass term provides the regularization (see section 5.1.2) for dividing fast and slow fields. For simplicity it will have the following approximate effect: $e^{-S_m} \approx \theta\left(m^{-1} - \|x_1 - x_2\|\right)$.

Expectation value of current-current-correlators considering vortices

$$
\begin{aligned}
\tfrac{1}{\mathrm{tr}\hat{P}} \quad & \int d^2x d^2x' \left\langle \mathrm{tr}\left[\left(Q^{-1}\nabla Q\right)_x \left(Q^{-1}\nabla Q\right)_{x'} \right] \right\rangle = \\
\tfrac{1}{\left(\mathrm{tr}\hat{P}\right)^2} \quad & \int d^2x d^2x' \left\langle \mathrm{tr}\left[\left(Q^{-1}\nabla Q\right)_x \right] \mathrm{tr}\left[\left(Q^{-1}\nabla Q\right)_{x'} \right] \right\rangle \sim \\
- \quad \mathrm{Vol}_{\hat{P}} \quad & \int d^2x d^2x' \int \frac{d^2x_1 d^2x_2}{\gamma^{-4}} \mathrm{rot}_\mu \left(\ln \frac{\|\mathbf{x}-\mathbf{x}_1\|}{\gamma^{-1}} - \ln \frac{\|\mathbf{x}-\mathbf{x}_2\|}{\gamma^{-1}} \right) \\
& \qquad \mathrm{rot}'_\mu \left(\frac{\ln\|\mathbf{x}'-\mathbf{x}_1\|}{\gamma^{-1}} - \ln \frac{\|\mathbf{x}'-\mathbf{x}_2\|}{\gamma^{-1}} \right) e^{-S_{V-AV}} = \\
\mathrm{Vol}_{\hat{P}} \quad & \gamma^4 \int d^2x d^2x' \int_{\frac{1}{\gamma}} d^2\xi \left[2\ln \frac{\|\mathbf{x}'-\mathbf{x}\|}{\gamma^{-1}} - \ln \frac{\|\mathbf{x}'-\mathbf{x}-\boldsymbol{\xi}\|}{\gamma^{-1}} - \ln \frac{\|\mathbf{x}'-\mathbf{x}+\boldsymbol{\xi}\|}{\gamma^{-1}} \right] \\
& \qquad \times y_0^2 \pi e^{-\mathrm{tr}\hat{P}\frac{\sigma_0+\mathrm{tr}\hat{P}c_0}{2}\ln\frac{\|\xi\|}{\gamma^{-1}}} \approx \\
- \quad \mathrm{Vol}_{\hat{P}} \quad & \mathrm{Vol}\, \frac{\gamma^4\pi^2 y_0^2}{2}\, \mathrm{I}_\xi .
\end{aligned}
\tag{H.3}
$$

$\Delta ln\left(\mathbf{x}\right) = 2\pi\delta\left(\mathbf{x}\right)$ has been used both in the third and fourth line. "$\sim$" hints that the volume of zero modes also includes a factor of order one. Furthermore, the relative position vector $\boldsymbol{\xi} = \mathbf{x}_1 - \mathbf{x}_2$ was introduced in the fourth row and "$\approx$" indicates expansion in small $\|\xi\|$.
I_ξ ($\xi = \|\boldsymbol{\xi}\|$) denotes the following integral (which is divergent for small $\mathrm{tr}\hat{P}\frac{\sigma_0+\mathrm{tr}\hat{P}c_0}{2}$)

$$
\mathrm{I}_\xi = 2\pi \int_{\frac{1}{\gamma}} d\xi\, \xi^3 e^{-\mathrm{tr}\hat{P}\frac{\sigma_0+\mathrm{tr}\hat{P}c_0}{2}\ln\frac{\xi}{\gamma^{-1}}}.
$$

However, during this RG-step, only little (fast) dipoles $\xi < \frac{1}{m}$ are integrated out (in order to cure the divergence):

$$
\begin{aligned}
\mathrm{I}_\xi^{\mathrm{fast}} &= 2\pi \int_{\frac{1}{\gamma}}^{\frac{1}{m}} d\xi\, \xi^3 e^{-\mathrm{tr}\hat{P}\frac{\sigma_0+\mathrm{tr}\hat{P}c_0}{2}\ln\frac{\xi}{\gamma^{-1}}} \\
&= \frac{2\pi}{\gamma^4\left(4-\mathrm{tr}\hat{P}\frac{\sigma_0+\mathrm{tr}\hat{P}c_0}{2}\right)} \left[\left(\frac{\gamma}{m}\right)^{4-\mathrm{tr}\hat{P}\frac{\sigma_0+\mathrm{tr}\hat{P}c_0}{2}} - 1 \right] \\
&\approx \frac{2\pi}{\gamma^4}\ln\frac{\gamma}{m} + \mathcal{O}\left(\left(\ln\frac{\gamma}{m}\right)^2 \right).
\end{aligned}
\tag{H.4}
$$

Larger dipoles are still present (during this RG-step). Their influence is incorporated in

$$
\begin{aligned}
\mathrm{I}_\xi^{\mathrm{slow}} &= 2\pi \int_{\frac{1}{m}} d\xi\, \xi^3 e^{-\mathrm{tr}\hat{P}\frac{\sigma_0+\mathrm{tr}\hat{P}c_0}{2}\ln\frac{\xi}{\gamma^{-1}}} \\
&= \left(\frac{\gamma}{m}\right)^{4-\mathrm{tr}\hat{P}\frac{\sigma_0+\mathrm{tr}\hat{P}c_0}{2}} \mathrm{I}_\xi .
\end{aligned}
\tag{H.5}
$$

Via rescaling, the initial lower bound for the integral is reobtained. The prefactor will be incorporated into the rescaled fugacity y^2 [JKKN77].

Volume of space of possible projections

The action with one vortex-antivortex pair (H.2) is invariant, if one rotates the projector $\hat{P}$ to another projector ($\mathrm{tr}\hat{P}$ invariant), shifts the dipole center or rotates the dipole in the

two-dimensional plane.
The precise way to rotate $\hat{P}$ depends on the symmetry class: The requirement

$$Q_{V-AV}(x) \xrightarrow{x\to\infty} \mathbf{1}$$

constricts the rotating matrices to subsets of $U(N)$, $Sp(2N)$ and $O(N)$ for AIII, BDI and CII respectively:

$$\left\{\hat{P}\right\} = \begin{cases} \left\{V^{-1}\hat{P}V\right\}_{V\in U(N)} & = \frac{U(N)}{U(1)\times U(N-1)} & = CP^{N-1} & \text{AIII,} \\ \left\{V^{-1}\hat{P}V\right\}_{V\in Sp(2N)} & = \frac{Sp(2N)}{Sp(2)\times Sp(2N-2)} & = HP^{N-1} & \text{BDI,} \\ \left\{V^{-1}\hat{P}V\right\}_{V\in O(N)} & = \frac{O(N)}{O(1)\times O(N-1)} & = RP^{N-1} & \text{CII.} \end{cases}$$

Here $\left\{\hat{P}\right\}$ stands for the space covered by projectors to be considered, the stabilizer reflects, that in Q_{V-AV} both $\hat{p}$ and $\mathbf{1}-\hat{P}$ are rotated.
Vortices are hence introduced on the complex, quaternionic and real projective space respectively. The volume of the manifold covered can be calculated explicitly (by rotating $\hat{P} = \mathbf{p}\otimes\mathbf{p}^*$, $\mathbf{p}^*\mathbf{p} = 1$, $\mathbf{p}$ lives on $\mathbb{C}^N$, $\mathbb{H}^N$ or $\mathbb{R}^N$ and $\mathbf{p}^*$ on the corresponding dual space):

$$\mathrm{Vol}_{\hat{P}} = \begin{cases} \frac{\mathbb{S}^{2N-1}}{\mathbb{S}^1} & = \frac{\pi^N}{\pi\Gamma(N)} & \text{AIII,} \\ \frac{\mathbb{S}^{4N-1}}{\mathbb{S}^3} & = \frac{\pi^{2N}}{\pi^2\Gamma(2N)} & \text{BDI,} \\ \frac{\mathbb{S}^{N-1}}{\mathbb{S}^0} & = \frac{\pi^{\frac{N}{2}}}{\Gamma\left(\frac{N}{2}\right)} & \text{CII.} \end{cases} \tag{H.6}$$

Vortex-induced corrections to coupling constants

The equations (C.5), (C.6), (H.3) - (H.6) describe the correction to the coupling constants due to dipoles. Summing and multiplying up, the vortex induced corrections (also given in the main text, sec. 7.3.4) are obtained.

$$\begin{array}{c|l} \text{AIII} & \begin{cases} \Delta\sigma^V &= -\frac{\pi^N}{\Gamma(N+2)}\sigma_0^2 y_0^2 \ln\frac{\gamma}{m} + \mathcal{O}\left(\left(\ln\frac{\gamma}{m}\right)^2\right), \\ \Delta c^V &= -\left[\sigma_0^2\frac{\pi^N}{\Gamma(N+2)} + 2\sigma_0 c_0\frac{\pi^N}{\Gamma(N+1)} + c_0^2\frac{\pi^N}{\Gamma(N)}\right] y_0^2\ln\frac{\gamma}{m} + \mathcal{O}\left(\left(\ln\frac{\gamma}{m}\right)^2\right), \\ y &= y_0\left(\frac{\gamma}{m}\right)^{2-\mathrm{tr}\hat{P}\frac{\sigma_0+\mathrm{tr}\hat{P}c_0}{4}}, \end{cases} \\ \hline \text{BDI} & \begin{cases} \Delta\sigma^V &= -\frac{\pi^{2N}}{\Gamma(2N+2)}\sigma_0^2 y_0^2 \ln\frac{\gamma}{m} + \mathcal{O}\left(\left(\ln\frac{\gamma}{m}\right)^2\right), \\ \Delta c^V &= -\left[\sigma_0^2\frac{\pi^{2N}}{\Gamma(2N+2)} + 2\sigma_0 c_0\frac{\pi^{2N}}{\Gamma(2N+1)} + c_0^2\frac{\pi^{2N}}{\Gamma(2N)}\right] y_0^2\ln\frac{\gamma}{m} + \mathcal{O}\left(\left(\ln\frac{\gamma}{m}\right)^2\right), \\ y &= y_0\left(\frac{\gamma}{m}\right)^{2-\mathrm{tr}\hat{P}\frac{\sigma_0+\mathrm{tr}\hat{P}c_0}{4}}, \end{cases} \\ \hline \text{CII} & \begin{cases} \Delta\sigma^V &= -\frac{2\pi^{\frac{N}{2}}}{(N+2)\Gamma\left(\frac{N}{2}+1\right)}\sigma_0^2 y_0^2 \ln\frac{\gamma}{m} + \mathcal{O}\left(\left(\ln\frac{\gamma}{m}\right)^2\right), \\ \Delta c^V &= -\left[\sigma_0^2\frac{\pi^{\frac{N}{2}}}{(N+2)\Gamma\left(\frac{N}{2}+1\right)} + 2\sigma_0 c_0\frac{\pi^{\frac{N}{2}}}{\Gamma\left(\frac{N}{2}+1\right)} + 2c_0^2\frac{\pi^{\frac{N}{2}}}{\Gamma\left(\frac{N}{2}\right)}\right] y_0^2\ln\frac{\gamma}{m} + \mathcal{O}\left(\left(\ln\frac{\gamma}{m}\right)^2\right), \\ y &= y_0\left(\frac{\gamma}{m}\right)^{2-\mathrm{tr}\hat{P}\frac{\sigma_0+\mathrm{tr}\hat{P}c_0}{4}}. \end{cases} \end{array} \tag{H.7}$$

For the different symmetry classes, different prefactors have been incorporated into y_0:

AIII	$y_0 \to y_0\frac{\sqrt{2\pi}}{4}$
BDI	$y_0 \to y_0\frac{1}{\sqrt{2}}$
CII	$y_0 \to y_0\frac{\pi}{4}$

I Symmetry classification of disordered systems

		time reversal T^2	chiral C	particle-hole $(CT)^2$	compact symmetric space	compact NLσM manifold $(\mathcal{M}_\sigma)$	$\pi_1(\mathcal{M}_\sigma)$	$\pi_2(\mathcal{M}_\sigma)$	$\pi_3(\mathcal{M}_\sigma)$	perturbative corrections 1 loop (2 loops)
Wigner-Dyson	A	0	0	0	$U(N)$	$\frac{U(2N)}{U(N)\times U(N)}$	0	$\mathbb{Z}$	0	0 (WL)
	AI	1	0	0	$\frac{U(N)}{O(N)}$	$\frac{Sp(4N)}{Sp(2N)\times Sp(2N)}$	0	0	0	WL
	AII	-1	0	0	$\frac{U(2N)}{Sp(2N)}$	$\frac{O(2N)}{O(N)\times O(N)}$	$\mathbb{Z}_2$	$\mathbb{Z}_2$	0	WAL
Chiral	AIII	0	1	0	$\frac{U(p+q)}{U(p)\times U(q)}$	$U(N)$	$\mathbb{Z}$	0	$\mathbb{Z}$	$\equiv 0$
	BDI	1	1	1	$\frac{SO(p+q)}{SO(p)\times SO(q)}$	$\frac{U(2N)}{Sp(2N)}$	$\mathbb{Z}$	0	0	$\equiv 0$
	CII	-1	1	-1	$\frac{Sp(2p+2q)}{Sp(2p)\times Sp(2q)}$	$\frac{U(N)}{O(N)}$	$\mathbb{Z}$	$\mathbb{Z}_2$	$\mathbb{Z}_2$	$\equiv 0$
Bogoliubov-deGennes	D	0	0	1	$SO(N)$	$\frac{O(2N)}{U(N)}$	0	$\mathbb{Z}$	0	WAL
	C	0	0	-1	$Sp(2N)$	$\frac{Sp(2N)}{U(N)}$	0	$\mathbb{Z}$	$\mathbb{Z}_2$	WL
	DIII	-1	1	1	$\frac{SO(2N)}{U(N)}$	$O(N)$	$\mathbb{Z}_2$	0	$\mathbb{Z}$	WAL
	CI	1	1	-1	$\frac{Sp(2N)}{U(N)}$	$Sp(2N)$	0	0	$\mathbb{Z}$	WL

Table of symmetry classes of disordered systems. First column: Cartan symbols denoting the ten symmetry classes of Hamiltonians. The corresponding symmetric spaces are given in the fifth column. Second, third and fourth column: absence (0) or presence (± 1) of time-reversal, chiral and particle hole symmetry respectively. As explained in 1.4 the operator realizing time-reversal, T, and charge conjugation, CT, might square to either $+1$ or -1. Sixth column: the symmetric spaces onto which the effective field theory (NLσM) maps. Their first, second and third homotopy group are given in the following three columns, see 1.7.1. Last column: perturbative one-loop renormalization group correction to conductivity. If the one loop correction vanishes, the two loop correction is given in brackets. WL denotes weak localization, WAL weak anti-localization. Adapted from [EM08] [MEGO10] and [SRFL08].